bushfire CRC


# BUSHFIRES EXTENDING INTO THE RURAL/URBAN INTERFACE

## FINAL REPORT FOR THE OPERATIONAL READINESS OF RURAL FIREFIGHTERS (AIR TOXINS) PROJECT

Michael S. Borgas and Fabienne Reisen

CSIRO

Publisher: Bushfire Cooperative Research Centre, East Melbourne, Victoria

ISBN: 978-0-9875218-3-5

Cover:
Left – Firefighters tackling a grass fire. Photo by CFA Communities and Communication.
Right – Firefighters at work in smoky conditions. Photo by CFS Promotions Unit.

Citation:

Borgas MS and Reisen F (2013) Bushfires extending into the rural/urban interface: Assessment of fire and emergency service workers' exposures to the complex mixture of toxic air pollutants at the rural urban interface and the likely health risks. Bushfire CRC, Australia.

# Contents

# Figures

# Tables

# Acknowledgments

This is a CSIRO co-investment project funded by the Bushfire CRC.

We acknowledge the contributions of the CSIRO project team: Kate Boast, Mahendra Bhujel and Paul Selleck for the analyses and assistance during the experimental burns. We also acknowledge the help of Justin Leonard in setting up the cone calorimeter and providing assistance with its operation.

# Abbreviations

| | |
|---|---|
| CDF | Cumulative distribution function |
| CO | Carbon monoxide |
| $CO_2$ | Carbon dioixe |
| HCl | Hydrogen chloride |
| HCN | Hydrogen cyanide |
| IARC | International Agency for Research on Cancer |
| MDF | Medium-density fibreboard |
| OES | Occupational exposure standard |
| PAHs | Polycyclic aromatic hydrocarbons |
| PE | Polyethylene |
| PIR | Polyisocyanurate |
| PM | Particulate matter |
| $PM_{2.5}$ | Particulate Matter less than 2.5 micrometers in diameter |
| PP | Polypropylene |
| PS | Polystyrene |
| PUR | Polyurethane |
| PVC | Polyvinyl chloride |
| RUI | Rural-urban interface |
| STEL | Short-term exposure limit |
| TWA | Time-weighted average |
| VOCs | Volatile organic compounds |

# Executive summary

Bushfires extending into the rural urban interface (RUI) will release a variety of pollutants into the atmosphere, some of which could potentially harm fire and emergency service workers and residents in the vicinity of the fire. At present, extensive research on exposures to air toxics has been conducted at bushfires and prescribed burns within Australia. Exposure studies have also focused on toxicity of fire effluents in the context of structural fires. However the findings cannot be easily extrapolated to the rural-urban context.

Exposures at fires in the RUI differ due to the presence of a more complex mixture of fuels, more complex fire behaviour and smoke plume dispersion and different firefighting tactics including minimal respiratory protection and working under extreme weather conditions. These aspects add complexity to predicting firefighters' exposures to toxic chemicals and make it difficult to extrapolate from existing research findings on exposures at bushfires, prescribed burns and structural fires.

Research has also been conducted on emissions from a range of burning materials under well-controlled conditions. While these studies provide important information on types of air pollutants released during combustion of materials, the data are presented as emission yields and are not necessarily representative of personal exposures.

Currently, fire and land management agencies do not have scientific evidence to quantify the exposure to air toxics faced by workers at the RUI. There is a need to better understand the environment of the interface to assess exposure risks to firefighters, emergency service workers and residents during and after fires.

The objective of the research project is to improve our understanding of potentially toxic emissions and their exposure concentrations at the RUI by creating a scenario-based exposure assessment that will define exposure risks to firefighters. The emphasis is on inhalation exposures resulting from burning structures at the RUI at varying distances from the emission source and the smoke plume.

## Research results

Smoke emissions from burning structures

In the first instance the project identified the types and amount of major combustible materials in structure and contents of houses as well as in other objects commonly present around a house. The findings showed that wood and wood-based products made up the majority of the fuel load (80%) with the remaining fuel load being composed of polymeric materials, textile and paper.

A desktop study was also undertaken to determine the type of information that was available on emission products released from burning materials. Based on those findings, experimental burns were conducted at well-ventilated conditions using a cone calorimeter to investigate the combustion products and yields of 11 commonly used materials in structures, house contents and furnishings for which limited information on their combustion products was available. The materials included five wood-based materials and six polymeric materials. The experimental tests were carried out to enhance our understanding on emissions of speciated volatile organic compounds (VOCs), carbonyls and particles. A number of these compounds are strong irritants and probable carcinogens and may add to the toxic effects of other toxic gases present in the smoke such as hydrogen cyanide (HCN) and ammonia.

The experimental tests revealed that among the 11 materials that were tested, the most pollution resulted from the combustion of polyester insulation, polystyrene, polyurethane (PUR) foam and a wool/nylon blend carpet. These materials ranked high in emissions of carbon monoxide (CO), particles, carbonyls and VOCs (e.g., benzene, toluene, naphthalene). Among wood-based materials, medium-density fibreboard and

particle board with melamine surface ranked highest in emissions, with pine ranking lowest. Since wood-based products make up the majority of mass in building structures, emissions from wood-based products may contribute more significantly to total emissions and hence to exposures than emissions from the polymeric materials. Nevertheless for acute exposures over short-time periods, the more hazardous emissions from polymeric materials may dominate.

Smoke dispersion

A new dispersion technique was developed to translate emissions derived from literature data and/or experimental data into exposure concentrations downwind. Current dispersion models typically use long averaging times (usually one hour or longer) which potentially smoothes over short-term episodes. As a result they are not able to examine exposure events at high concentration levels over short duration. These events are however highly likely to occur in emergency situations such as fires in the RUI and are a major focus of this research study.

The new dispersion model takes into account puffs released over short time periods. Each puff is emitted into a wind with known speed and direction at the source and at the specific time of release. This new technique provides a high resolution plume modelling and estimated exposure concentrations over short exposure times (1-15 min). The short-time fluctuations of concentrations are important to determine the hazard to particularly highly toxic chemicals in plumes.

A simple rural-urban environment has been modelled for a 3 hour slow burn of a brick veneer house in winds at 10 km $hr^{-1}$, 20 km $hr^{-1}$ and 30 km $hr^{-1}$ and conditions similar to the Canberra bushfires of 18$^{th}$ January 2003. The modelling was conducted for 15-minute periods to determine the mean concentrations. The peak maximum exposure was established from the top four peak concentrations in each 15-minute period. The dispersion model was run with and without lateral offsets.

The results are presented either as time series of absolute concentrations or normalised by the mean concentration. Probability distributions are also presented to determine how likely and often it is that the exposure will exceed safe levels.

The results from the dispersion model runs show a number of trends:

- A decrease in absolute concentrations with downwind distance and when moving away from the centreline of the plume;
- An increase in absolute concentrations with increased wind speed. The plume is dispersed much quicker and less clean air is entrained within the smoke plume, resulting in higher concentrations;
- A reduction in fluctuations further downwind, with mean concentrations being broadly representative of any sampled concentration;
- Higher peak-to-mean ratios closer to the source, which may lead to situations where short-term exposure limits are satisfied, but peak maximum limits for toxic gases are exceeded;
- Higher fluctuations at higher wind speed;
- Higher fluctuations in concentrations at the plume edge. This means that although mean concentrations are smaller at the edge of the plume, peak concentrations can be significant. The peak levels are however more intermittent so that clean air spaces are observed between episodic peaks. These episodes of clean air spaces are limited when moving towards the plume centreline.
- Highly intermittent peak concentrations that can be two to five times the mean concentration. Both magnitude and frequency depend on distance downwind and lateral offset from the plume centre line.

Exposure and health risks

The results of the modelled scenario indicate that within 50 m of the burning house exposures are on average constantly exceeding peak and short-term exposure limits and there is no safe approach without protection.

At a distance of 100 m downwind, exposures are still exceeding peak limits, but mean concentrations are within safe exposure limits. In that case, it is essential to understand how often high concentrations occur to minimise exposure risks. The frequency of peak exposures can be estimated from the cumulative distribution functions provided by the model.

Further downwind (150 m), peak concentrations can still be close to their respective peak limits, primarily at high wind speeds. However, the frequency of high concentrations is generally lower. An informed strategy for unprotected operations could be considered in that case.

At close proximity (up to 100 m), exposures to CO and HCN can reach hazardous levels and present a significant health risk. This risk is reduced when positioned further than 150 m from the source of the fire. At 150 m from the source, peak limits for CO and HCN are not exceeded. However CO and HCN are both asphyxiants and present a health hazard when taking into account additive health effects.

Irritation to eyes and respiratory tract is a common health risk, as a large number of pollutants in the smoke are irritants and present at elevated concentrations. Fine particles are a major issue even at 150 m away from the source of the fire.

Impact on the central nervous system which leads to fatigue, dizziness and impaired vigilance is also a potential significant health & safety risk. Pollutants such as toluene, xylene, ethylbenzene, styrene and phenol have been measured in smoke. Due to the additive effects, exposure to smoke plume can pose a significant health risk.

Simulated room burns

Ambient air sampling was conducted during a training exercise at the CFA Training Centre in Fiskville to study the concentrations of a range of air pollutants in smoke plumes from simulated room burns and provide some validation of the model.

Three rooms were burnt sequentially, with each room set up to simulate a living room, a kid's bedroom and an office. Sampling boxes containing a range of air monitoring equipment were set up at the back of the building within the smoke plume.

The air pollutants measured reflected what was observed during combustion of individual materials under controlled conditions. However while the modelled scenario resulted in high concentrations in plumes 50 m to 150 m downwind, these high levels were not observed in the ambient measurements. The difference could be explained by the lower mass loading of combustible materials during the room burns and the difficulty in capturing the densest part of the smoke during the room burns.

## Research contribution and application

The research has improved our understanding of exposure risks to personnel and communities during bushfires that extend into the RUI. Research provided estimates of exposure to toxic chemicals downwind of a typical burning house and in meteorological weather typical of bushfire conditions.

The emphasis for assessing this exposure risk has been on inhalation exposures that occur outside of burning structures at varying distances from the emission source and the smoke plume and on acute exposures to high concentrations of toxic gases and particles.

The new dispersion model allows accurate estimates of emissions and is more highly resolved in time than traditional diffusion models allow. Past practice does not give reliable assessment of acute short term exposure, and the new model gives a better understanding and more precise estimates of the potential exposure risks. It also provides a reliable estimate of the probability distribution for how likely and often exposures exceed safe levels.

The models of both wind and dispersion are simple but flexible enough to be useful for wide assessment of exposure scenarios and for application in emergency response. Exposure estimates from seconds to minutes can be developed with local inputs of mean and varying wind, and source characteristics on site during an incident.

The outcomes from the research can be used to inform training, work practices and appropriate use of personal respiratory protective equipment, as well as to provide advice on firefighter and community safety.

While this study provided important information on exposures during fires at the RUI, we acknowledge the uncertainties and limitations surrounding the modelled exposure estimates. Major uncertainties include the type and amount of combustible materials consumed during fires in the RUI, the rate of consumption and the emission rates of pollutants. There is a significant variability in the type, amount, composition and spatial distribution of materials present at the RUI. Emission rates can also be highly variable as they are dependent on fire conditions (e.g. ventilation, temperature) and fire geometry.

In the current model, emissions data focused on well-ventilated conditions and combustion of individual materials. In real life, fire undergoes various stages from well-ventilated flaming conditions to low-oxygenated smouldering conditions. Modelling exposure estimates for smouldering conditions would allow gaining a better understanding of exposures during mop-up situations.

The dispersion model can be also be adjusted to include multiple burning houses, multiple node complex fires and/or more realistic node based fires.

The modelled exposure estimates would also benefit from a more rigorous validation of the data. This could potentially be achieved by comparing modelled CO and HCN concentrations to those measured by fire agencies at structural fires.

# 1 Background

The impacts of large bushfires on air quality and health have been studied in a number of research studies worldwide (Emmanuel 2000; DeBell et al. 2004; Frankenberg et al. 2005; Phuleria et al. 2005; Kunzli et al. 2006; Vedal and Dutton 2006; Wu et al. 2006; Wegesser et al. 2009; Dutkiewicz et al. 2011). The impact on air quality from bushfires into urbanised areas has received less attention. Wildfires at the rural urban interface (RUI) continue to impact on communities in bushfire-prone areas such as south-eastern Australia, California and southern Europe and can result in losses of life and property (Beringer 2000; Gill and Stephens 2009; Blanchi et al. 2010). Climate change is predicted to increase both fire severity and fire season duration, while a forecasted population growth in the peri-urban areas will expose more residents and homes to an increased bushfire risk. As a result fighting bushfires at the RUI is likely to become more frequent, but currently little is known about air toxics species emitted and exposure concentrations inhaled by fire and emergency workers during firefighting at bushfires that extend into the RUI.

At present, extensive research on occupational exposures has been conducted at prescribed burns and bushfires within Australia. The research has shown that during prescribed burning and bushfire operations firefighters are exposed to a range of hazardous pollutants particularly fine particles, carbon monoxide (CO), formaldehyde and volatile organic compounds (VOCs) such as benzene, toluene, xylenes and phenol (Reisen and Brown 2009; Reisen and Meyer 2009; Reisen et al. 2011).

The outcomes are not readily applicable to fires at the RUI as burning structures are likely to change both the composition and concentration of emissions. Some air toxics will be the same as those emitted from bushfires; however their yields are likely to differ. Also, composition and hence toxicological properties of smoke from fires at the RUI will differ. The presence of nitrogen-rich materials such as wool, nylon, polyurethane (PUR) release hydrogen cyanide (HCN), an asphyxiant, ammonia, nitriles and other nitrogenated organic compounds, while combustion of polyvinylchloride (PVC) releases hydrogen chloride (HCl), a severe irritant and other chlorinated organic compounds.

Previous studies have also investigated exposures at structural fires (Brandt-Rauf et al. 1988; Jankovic et al. 1991; Bolstad-Johnson et al. 2000; Austin et al. 2001b), which have found air pollutants of concern to be CO, formaldehyde, acrolein, HCl, HCN, hydrogen sulphide, hydrogen fluoride, benzene, nitrogen dioxide, sulphur dioxide and polycyclic aromatic hydrocarbons (PAHs). A recent study has assessed firefighters personal exposures during vehicle fire suppression (World Health Organization (WHO) 1999). In this particular case, formaldehyde was the only air pollutant measured at concentrations exceeding occupational exposure standards (OES). The predominant contributors to the hazard index for respiratory effects were formaldehyde, acrolein, CO, benzene and isocyanates. The development of protective equipment (e.g. self-contained breathing apparatus) and its use in structural firefighting has resulted in reduced incidents from smoke exposure.

During bushfires that extend into urbanised areas, firefighters commonly do not use self-contained breathing apparatus. It is unclear whether the respiratory protection currently used for fighting fires at the RUI is adequate to protect fire and emergency service workers against toxic pollutants in the smoke plume. Furthermore unlike structural fires, RUI fires are fought outdoors under extreme weather conditions which can influence intensity and duration of exposure.

Further research is required to better define the composition of emissions and their concentrations in smoke plumes. This will then enable an assessment of any potential exposure risk and whether current

personal protective equipment is adequate to protect fire and emergency service workers from the toxic combustion products.

# 2 Research Approach

The objective of the research project is to identify major toxic components in emissions from bushfires extending into the RUI and assess whether concentrations of air toxics in the smoke could potentially impact firefighter's health or safety.

At prescribed burns and bushfires, monitoring of major air toxics in bushfire smoke was conducted within the breathing zone of firefighters actively working at or near burns or fire line (Reisen and Brown 2009; Reisen and Meyer 2009; Reisen et al. 2011). The monitoring program was designed to ensure that as many influencing factors as possible were accounted for to improve the validity of the results. Factors investigated included vegetation class, fire class (specifically fuel reduction burns in both regional native forest and urban interface and slash burns) and fire ground work activity. The exposures and their ability to impair health and well-being were then evaluated in relation to established OES.

Collecting personal exposure data at bushfire incidents extending into the RUI poses a difficult challenge. Fires at the RUI are unpredictable and it is much more difficult to monitor firefighters on the fire ground, as their primary focus is on protection of people and property. Therefore, the research plan was set up to ensure that it could deliver results without fire events.

The research approach adopted was to model smoke plume dispersion in RUI fires, where a burning house or houses emit a range of toxic chemicals to which firefighters and nearby residents are exposed. The approach is focussed on determining acute exposure to toxic chemicals that may limit safe first-responder approach to the burning house without protective equipment, or may present a health hazard to nearby residents in adjacent houses. The short-term high concentrations of the main toxic emissions are estimated with dispersion models for typical house-fire emissions.

The RUI is characterised by a wide range of fuel classes including vegetation, house structure, house contents, vehicles, items surrounding the house (e.g. fences, decking, outdoor furniture), as well as garages and/or sheds and any items contained within them. If these materials burn they can release significant quantities of various toxic chemicals into the air.

The exposure and health risks of fire fighters or nearby residents in the urban environment depend on

(1) Smoke emissions from the burning house(s)
(2) Wind flow conditions downwind of the house(s)
(3) Positions downwind for likely exposure

## 2.1 Smoke emissions

Burnt buildings or structures in the RUI are a complex source of emitted combustion products into the atmosphere from a wide variety of building and furnishing materials and personal items.

An estimation of the amount of combustible materials in a house structure and house contents is presented in Tables 1 and 2. The masses of materials for house structure were adapted from Robbins (Robbins et al. 2010).

**Table 1 House structure components and estimated amount of materials**

| Structure component | Combustible Materials | Estimated amount (kg) |
|---|---|---|
| Foundation | Timber<br>Polyvinyl chloride (PVC) | 1600<br>94 |
| Wall cladding | Weatherboard sheets, Plywood sheets<br>Plasterboard<br>Polystyrene (PS), PVC | 2650<br>4500<br>2000 |
| Frame | Timber | 11000 |
| Roofing | PVC or Polypropylene (PP) roofing membrane | |
| Insulation | Polyester, PS, PUR, polyisocynurate (PIR) | 300 |
| Flooring (130 $m^2$) | Wood, particleboard, medium-density fibreboard (MDF)<br>Carpet (wool, nylon) | 9000<br>650 |
| Window frame | Wood<br>PVC | 140 |

**Table 2 Estimated amount of materials in house contents**

| Material | Total estimated mass (kg) | Mass fraction (%) | Mass fraction (%) (Persson and Simonson 1998) | Mass fraction (%) (Robbins et al. 2010) |
|---|---|---|---|---|
| Wood | 1520 | 29.5 | 58 | 36 |
| Wood-based products | 1240 | 24 | | 17.5 |
| Textile | 700 | 13 | 15 | 16 |
| PS | 325 | 7 | | 1.5 |
| PUR | 190 | 3.5 | 5 | 4 |
| PVC | 245 | 5 | 5 | 6.5 |
| PP/PE | 580 | 11 | 2.1 (PE) | 8.5 |
| Paper | 400 | 8 | 15 | 10 |

Emissions are strongly influenced by the nature of the burning material and the physical conditions of the fire (e.g. fire intensity, ventilation and geometry). A reliable method to characterise combustion product yields of major combustible materials present at the RUI is to conduct small bench-scale well-controlled experiments. They can be set up to better understand the role that a number of factors such as temperature and ventilation play on the yield of combustion products. Even though they provide crucial information on combustion products and yields, they are conducted under well-defined fire intensity and ventilation conditions and usually on pure materials. Therefore they do not necessarily represent real fire scenarios where fires undergo various fire stages ranging from pyrolysis to well-ventilated and under-ventilated flaming combustion and where a mixture of materials burn which may change the fire conditions and emission rates or composition.

Emissions data used as input into the dispersion model were derived either from existing literature data and/or from additional experimental testing that was conducted using a cone calorimeter on selected structural and furnishing materials. A summary of the emissions data for key air toxics and selected structural and furnishing materials is provided in Table 3. These values are for flaming conditions and more detailed information on emissions is provided in Appendix B.

**Table 3 Emission yields of major air toxics for selected structural and furnishing materials**

| | Emission yields in (g $kg^{-1}$)[a] | | | | | | |
|---|---|---|---|---|---|---|---|
| **Toxic chemical** | **Wood** | **Wood-based products** | **PUR foam** | **Polyester** | **Carpet** | **Polystyrene** | **PVC** |
| CO | 7-9 | 4-48 | 11-40 | 20-40 | 13-20 | 10-50 | 20-200 |
| HCN | | <1 | 1.5-4.0 | ~1 | 1.5-12 | | |
| HCl | | | | | | | 130-500 |
| Particles | 2-13 | 3.2-5.5 | 13-26 | 58 | 35-38 | 40-126 | 1 |
| Benzene | 0.01-0.15 | 0.02-0.2 | 0.1-13 | 1.2-3.3 | 1.2-10.5 | 1-10 | |
| Styrene | | | | 0.02-0.06 | 0.01-0.13 | 19-24 | |
| Formaldehyde | 0.03-0.2 | 0.1-0.25 | 0.2-1.4 | 0.8-1.2 | 0.25 | 0.4-1.5 | |
| Naphthalene | 0.03-0.1 | 0.003-0.1 | 0.02-0.4 | 0.04-0.16 | 0.04-1.1 | 0.1-0.5 | |
| Isocyanates | 0.004-0.025 | 0.75 | 0.9-1.6 | | ~1 | | |

[a] The emission yields are derived from a number of small-scale laboratory testing studies reviewed in Reisen (Reisen 2011a) and from cone calorimeter tests (Reisen and Borgas 2012). Also refer to Appendix B.

## 2.2 The nature of plumes and winds

The two key characteristic of winds are the mean wind that blows in a fixed general direction downwind and the turbulent (rapid time varying) winds that fluctuate around the mean wind. The turbulent winds are responsible for both spreading out plumes and generating fine structure in the plumes as clean air is entrained into the plume and diluting the concentrations.

Figure 1 shows a simulation of turbulent winds in the atmospheric boundary layer, with $(u, v, w)$ for downwind, lateral and vertical winds respectively. Winds are recorded at two sample points 10 m apart; they are highly correlated and overlapping for atmospheric winds with length scale greater than 20 m. The time scale of the winds is T=50 seconds.

The mean wind in the x direction (velocity U) is 6 m $s^{-1}$ with fluctuations of 0.5 m $s^{-1}$, and similar fluctuations in the lateral and vertical directions. The fluctuating winds help transport the material transversely and spread out the plume in the atmosphere in a well known diffusive manner on average (Weil et al. 1992). The highly fluctuating nature of the atmosphere makes the plume characteristics on short time scales complex and difficult to model.

A new technique is employed in this work to give highly resolved stochastic models of plume behaviour allowing short-term resolution of fluctuating concentrations, merging of multiple plumes from multiple sources and the development of spatial characteristics downwind.

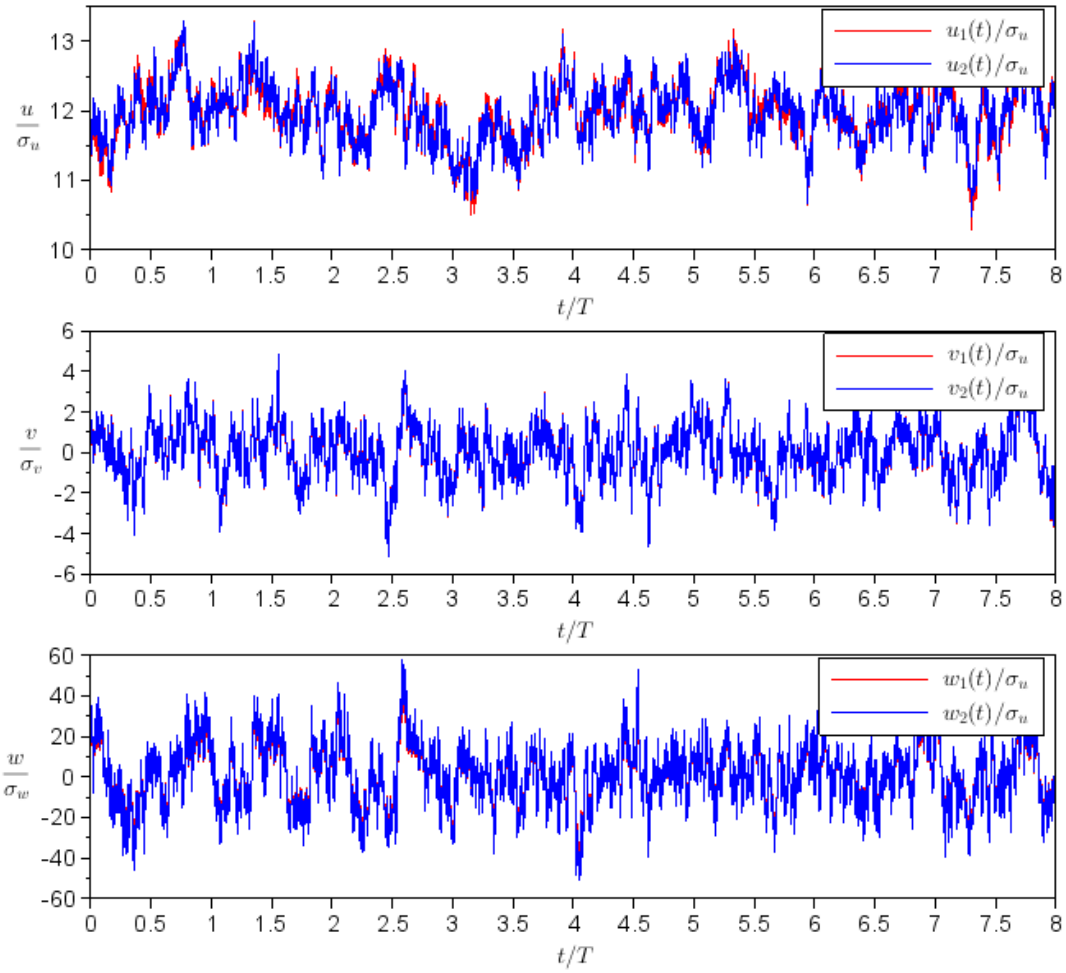


**Figure 1 Turbulent atmospheric winds as functions of time at two spatial points.**

For bushfire conditions, mean wind speeds are high and for distances of up to 200 m downwind, the travel time from source to sample point is less than a minute making it a near-source phenomenon. Because the plume travel times are less than the time scale of the major atmospheric eddies, the traditional diffusion models of atmospheric mixing are not useful and special Lagrangian techniques like those adopted in this work are needed.

A smoke plume is usually buoyant and tends to rise in the atmosphere, but for slow fires in windy conditions the plumes are bent over and spread rapidly downwind and more slowly vertically and laterally across the wind. The spreading plume is controlled by the turbulence in the atmosphere which is influenced by the surface properties (buildings, trees, roughness, terrain and moisture).

## 2.3 How does the nature of the smoke and wind influence the exposure to toxic chemicals?

The material composition of a house and surrounding combustible items defines what is emitted in the smoke. The emission rate depends on how fast the house and materials burns, which can depend on the wind but mostly is material and building-properties dependent.

Smoke plumes can contain toxic gases like CO, HCl and HCN, irritants like carbonyls and other VOCs or chemicals with known carcinogenic properties including benzene, formaldehyde and particulate matter (PM).

The impact of a toxic material depends on the exposure of the chemical on a human subject exposed to the plume. The exposure depends on the concentration of a chemical in the plume. Higher concentrations are generally observed near to the source of the plume compared to further downwind.

The wind carries the smoke plume downwind. The longer the smoke is carried, the more the turbulent spreading dilutes the smoke in the atmosphere and lowers the concentration of gases and particles. The exposure risk increases as we go closer to the source of the smoke where the concentrations are the highest. The exposure risk also increases when approaching the centreline of the plume, making wind direction a critical factor.

## 2.4 How do we determine what and where it is dangerous?

The hazard from toxic chemicals can occur from acute exposure for even just a few seconds at very high concentrations or chronic exposure of lower concentrations for longer times. Most common regulations are for longer term exposures for planned activity like safe workplace exposure or safe community standards for everyday life. Emergency situations like fires and accidents can lead to acute exposures at uncommonly high concentrations and it is important to examine exposure events at high concentration levels but possibly short duration to design safe operations in a smoke plume environment.

### 2.4.1 EMISSION MODELLING

Estimates of emissions are possible for typical houses if we know common materials for houses, emission factors for toxic chemicals of interest for each material and a prescribed burning pattern of the materials as the house is consumed by fire. The typical-house smoke emission is a merged set of plumes from a localised footprint in the house at any instant and emerging at some height above the house.

### 2.4.2 DISPERSION MODELLING

Dispersion modelling converts the plume emissions into concentrations averaged over long times which will serve as exposure estimates downwind of smoke plume events. The modelled surface concentrations are compared against existing OES and/or air quality guidelines to assess the potential health hazard of a smoke plume. Further downwind and laterally at the edge of the plume average concentrations can fall to low levels, but short term peak concentrations of a few seconds duration can still be large. Complex models of puffs of chemicals emitted at the source with complex turbulent winds, undertaken in this work, allow more detailed plume modelling with estimates of concentrations averaged over short exposure times obtained and probability distributions estimated for how likely and often it is that the exposure will exceed safe levels.

# 3 Dispersion scenario of a suburban area

## 3.1 Description

The dispersion domain and scenario we consider in this study corresponds to the Canberra bushfires of 18th January 2003. Figure 2 shows an image of pre-burned housing estate in Canberra.

**Figure 2 Housing estate prior to exposure to a bushfire front on the 18th January 2003.**

On January 18th 2003 a wind direction change and increase in wind strength occurred from the hours of 0900 to 1800. The wind bore down from 340 degrees early in the day, turning gradually through the day to 310 degrees. The wind speed increased from 10 km $hr^{-1}$ to 30 km $hr^{-1}$, peaking at 48 km $hr^{-1}$ before dropping back to 30 km $hr^{-1}$. These gradual changes occurred over a 9 hour time span, so that minimal changes in wind speed would be observed over any fifteen minute period. Even at the lowest wind speed, wind conditions are strong enough to disperse smoke emitted from any burning house.

Our prime interest is to determine possible safe buffer zones for scenarios where one or two houses may be burning and a plan for safe access and approach is required.

The calculations of dispersion we consider will be based on a selection of mean wind speeds U, and wind speed fluctuations $\sigma$. The wind speed fluctuations are typical values for atmospheric conditions and determine the turbulence of the winds

1. Low winds $U = 3\ m\ s^{-1}$ $\sigma = 0.15\ m\ s^{-1}$
2. Medium winds $U = 6\ m\ s^{-1}$ $\sigma = 0.25\ m\ s^{-1}$
3. High winds $U = 9\ m\ s^{-1}$ $\sigma = 0.3\ m\ s^{-1}$
4. Very high winds $U = 12\ m\ s^{-1}$ $\sigma = 0.5\ m\ s^{-1}$

The direction of the wind for the case we consider varies slowly from 310 degrees to 340 degrees over a 9 hour period, so for any given 15 minute period the wind direction shifts on average by less than a degree.

The values chosen for wind-speed fluctuations are modest and related to the length scale L of turbulent correlations which we take as 50 m for these flows. This suggests that the plume time scale (a Lagrangian time scale) is

1. Low winds $t_L = 55\ s$ $U \cdot t_L = 165\ m$
2. Medium winds $t_L = 33\ s$ $U \cdot t_L = 198\ m$
3. High winds $t_L = 28\ s$ $U \cdot t_L = 252\ m$
4. Very high winds $t_L = 16\ s$ $U \cdot t_L = 192\ m$

Within the range of exposure zones of interest the plumes are highly turbulent. The turbulent conditions may persist to distances exceeding 200 m. Beyond the near-field turbulent dispersion, exposure still persists, but the plume dispersion is better described by the mean flow characteristics.

The post burn impact on the Canberra suburban scene shows a significant fraction of houses and many trees destroyed. Figure 3 shows a recovery scene with numerous houses missing compared to prior to the fire shown in Figure 2.

**Figure 3 Image of post-fire Canberra. A house fire is modelled at the upper left and arrows indicates the prevailing wind directions spanned during the fire event, and the length of the arrow is 150 m buffer-zone length. The ellipse is an example of no-go buffer zone.**

## 3.2 Emissions

Given a typical house fire at the point illustrated in Figure 3 and known wind conditions, we need to know emission rates of target chemicals from the fire to calculate dispersion. The emission rates are dependent on the specific material that is burning at a nominal seat of the fire and generating a specific emission.

For the following example the nominal footprint of the fire at any given 15 minute emission period is of the order of $1m^2$. For example, emissions could be coming from a window exit with ventilation of the house from other non-emitting openings. Modelling of the mixing inside the house is not attempted in this work. More complex multiple node sources can be considered and are possibly more realistic but are not considered in this study.

### 3.2.1 A HOUSE FIRE SCENARIO

A house fire is a very complex process, and may have a rich variety of behaviour over the duration of the burning period, which may last from minutes to hours.

For longer house burns (e.g., one to three hours), the emission source of a particular burning material at any instant is a localised fire spot which may move over time in the footprint of the house. This is particularly the case if we consider a single chemical emission, for example emissions of HCl from burning patches of PVC.

In this study we consider a slow burn. The heat release is sufficiently low that in strong wind conditions we can account for plume rise with a nominal source height at the fire and neglect the buoyant rise downwind.

Situations of fast and intense fires lead to plumes that rise significantly and cause impacts further downwind. Therefore they are less of a concern to people on the ground near the source of the fire.

The characteristics of the scenario to model are as follows:

1. A burn time of 3 hours to consume the combustible materials of the house
2. A constant rate of emissions over the burn time
3. The nodes of emission are localised and in different positions, but nominally chosen at a single point for modelling purposes.
4. The lateral offset from the plume centreline can account for the uncertainty in determining exactly which part of the house is burning at any particular time.
5. Modelling will nominally be for 15-minute time periods and peak exposures in each 15-minute period are used to define exposure risks.

### 3.2.2 A BOX MODEL OF INTERNAL MIXING

The model for house emissions depends on ventilation rate, $v$, of the house (Shelter-in-Place Report 2011). At least for the initial phase of a burning building this is a characteristic of the building and wind speed outside. Typical values of room ventilation are 5 room volumes per hour. When structural damage occurs and buoyant exchange enhancement occurs this may increase. For low exchange rates, the combustion may be controlled by the oxygen supply. For typical rooms mixing occurs internally over time scales of minutes, with overall ventilation in tens of minutes. The concentration of gases (or particles) for emission rate $q$, is just $q/v$ when equilibrium has been reached (after a few minutes).

### 3.2.3 TYPICAL BUILDING MATERIALS AND EMISSIONS

The Canberra housing stock is typically brick veneer. Indicative materials of a typical house are shown in Appendix A. Emission rates were derived from Reisen (Reisen 2011) and Table 3 shows the emissions for a small selection of toxic chemicals. A summary of the net mass of material and emissions is shown in Table 4. The emission rates were calculated on the basis of knowing the net mass of material, the emission factors for specific toxic gases, and finally the time over which the house burns which converts the net emission into an emission rate.

**Table 4 Typical House with net mass and estimated emission rates ($q$) for key toxic emissions**

| Material | Mass (kg) | CO (g $kg^{-1}$) | HCN (g $kg^{-1}$) | Benzene (g $kg^{-1}$) | HCl (g $kg^{-1}$) |
|---|---|---|---|---|---|
| Wood | 15000 | 20 | 1 | 0.15 | 0 |
| Polyester | 300 | 40 | 1 | 3 | 0 |
| Carpet | 300 | 20 | 12 | 10 | 0 |
| PVC | 100 | 200 | 0 | 0 | 150 |
| Plastics | 1000 | 40 | 2 | 10 | 0 |
| **Net emissions (g)** | | **378000** | **20900** | **16150** | **15000** |
| $q$ (g $s^{-1}$) | 1 hr | 105 | 5.81 | 4.49 | 4.17 |
| $q$ (g $s^{-1}$) | 2 hr | 52.5 | 2.90 | 2.24 | 2.08 |
| $q$ (g $s^{-1}$)[1] | 3 hr | 35 | 1.94 | 1.50 | 1.39 |

The emission rates are based on either a one, two or three hour burn, assuming that all combustible materials within the house are burnt during that time period. Longer burns will spread the same net emissions evenly over the longer time span resulting in lower emission rates. Shorter burns in more intense fires potentially give higher exposures, although this may be mitigated by greater plume rise which is not studied in detail in this current work.

At any given time period as short as 15 minutes or less we will suppose that the key toxic emissions are emitted from a small footprint within the overall footprint of the house. It is possible to model multiple nodes emitting simultaneously (see section 5) but for simplicity we consider single node emissions at this point.

Similarly, it is possible that multiple houses or adjacent out buildings or vehicles may be burning simultaneously giving multiple emission sources. However, unless the sources are within metres of each other they may be regarded as independent and assessments can be based on single source properties. This will be discussed below.

### 3.2.4 EMISSIONS FROM A BURNING CAR

Other infrastructure may burn in a complex urban environment, shown in Figure 2. To illustrate multisource plumes interacting we will consider a house plume and a plume from a nearby burning car. First of all, the emissions factors for a car are estimated.

Combustible materials in a car are comprised of 120 kg of plastics and foam and 60 kg of rubber-like compounds ("Automobile". The World Book Encyclopedia 1996). Emissions from these materials generate

toxic compounds, particularly CO and HCN. Combustion that is limited by oxygen availability and at temperatures of 900 degrees, typically generates the following emissions (Simonson et al. 2000):

- 800 g $kg^{-1}$ of CO
- 11 g $kg^{-1}$ of HCN

The emission factors were chosen to differentiate from the house materials scenarios. For materials like foam, synthetic rubber and melamine, emission factors are typically like those in Table 3 (e.g., 1-3 mg $kg^{-1}$ HCN). However, for the car emissions a high emissions scenario was chosen based on burning of particular plastics and also a shorter consumption time for the duration of the car burn.

For a fire consuming materials in 30 minutes gives emission rates of

- 52.8 g $s^{-1}$ of CO
- 0.8 g $s^{-1}$ of HCN.

For ventilation rates of 0.3 $m^3s^{-1}$, the near source plume concentrations are large (and dangerous):

- 150 g $m^{-3}$ of CO
- 2400 mg $m^{-3}$ of HCN.

These concentrations near the emission point at the source are hazardously high and dilutions by factors of 200 or more are required to reach levels below short-term exposure limits downwind (see below).

These emission factors are used in section 5 to estimate exposures to plumes from multiple sources in the burning RUI.

## 3.3 High time-resolution dispersion model

Modelling a plume from a point source is a classic problem in atmospheric science, but it is usually only possible to determine concentrations averaged over 15 minutes or longer. In this study a new technique is used that adds turbulent wind velocities at the source of emissions, takes into account puffs released with these initial winds and follows their Lagrangian paths downwind. The process is approximated with Gaussian puffs for simple models of turbulence in the surface layer and for approximately uniform wind.

The complexity of urban-rural canopy is simply to create the appropriate roughness and generate significant turbulent eddies in the surface layer. The scale of the surface layer eddies is a lumped parameter including the canopy, and surface roughness effects. The Gaussian puff is mass conserving by reflecting the plume in the nominal surface where we assume zero flux conditions.

Details of the model are given in Appendix C.

The advantage of this new model is that it automatically generates concentration time series with turbulent fluctuations which are accurate to the extent that an implicit time filtering occurs by the model Eulerian-Lagrangian interaction. However, it turns out that the time filtering of concentrations is of the duration of seconds or less for the near field plumes that we consider and we arrive at least-biased estimates of short-times scale concentration fluctuations that are available even with vastly more complicated modelling systems.

Short time fluctuations of concentrations are important for determining the hazard to particular highly toxic chemicals in plumes and lead to many situations where estimates of risk based on mean concentrations alone are invalid and often low mean concentrations are accompanied by high peak concentrations and unsafe environments.

## 3.4 Health-effect time scales

The calculations we focus on are 15-minute simulations of concentration time series at selected points downwind (mainly 50 m, 100 m and 150 m) of the burning house to assess acute effects from exposure to high concentrations of toxic gases or particles. For 15-minute exposures we mainly consider positions directly downwind of the fire. The Canberra bushfire meteorology suggests systematic variability of wind direction and speed over the time scales of hours, but for the purposes of short-term exposure calculations the mean wind direction and speed can be assumed constant.

The estimated peak concentrations from the dispersion model are resolved down to time-average fidelity of about 5 seconds.

# 4 Dispersion Results

Dispersion models for complex turbulent winds are described in Borgas (Borgas 2012; Borgas 2013) and Appendix C.

The output of the models at a fixed exposure point downwind is a time series of concentrations

$$\{C(t); t \in [0, T]\} \quad (1)$$

for T=15 minutes = 900 seconds. The calculations are for unit mass per second emission rates ($q_1$ = 1 g $s^{-1}$), and all relevant quantities for actual emission rates shown in Table 4 are obtained by simple multiplication of concentrations by the emission rate.

In addition to time series we calculate the time averaged concentration as follows

$$\bar{C} = \frac{1}{T-T_s}\int_{T_s}^{T} C(t)dt \quad (2)$$

Where $T_s$ is the finite time it takes to transport the smoke plume from the source point to the exposure point for a finite wind speed, $T$ is the total sample time (sufficiently large to include many peak episodes) and $C(t)$ is the instantaneous signal at time $t$. The over bar indicates a time averaged quantity.

Finally, we calculate the cumulative probability density function (CDF) for the sample $\{C(t); t \in [T_s, T]\}$

$$P(C) = \text{probability sample } c \leq C \quad (3)$$

On the CDF plots we also show for comparison the exponential distribution

$$P(C) = \exp(-C/\bar{C}) \quad (4)$$

The CDF shown are all normalised by the mean value of the time series, so effectively peak-to-mean ratios are plotted. These are commonly used for description of fluctuations.

As mentioned above for actual emission rates $q$ in Table 4, the appropriate mean is simply

$$\bar{C}_q = q\bar{C} \quad (5)$$

This allows the single time series to be used for multiple species on the understanding that they are all emitted from the same point at that time in the house fire.

Dispersion results are shown at a variety of distances downwind, typically 50 m, 100 m and 150 m. For the higher wind speeds we also considered 200 m and 300 m.

Cases of lateral offsets (from the direct centreline) were also considered. This displacement from the plume centreline, where the likelihood of encountering the plume is high, often had a dramatic impact on the shape of the CDF, giving much higher peak-to-mean ratios. This is primarily about the smaller mean concentrations at the edge of the plume, where peak concentrations can be significant, making a large lateral excursion. As a result peak concentrations are similar to the peak concentrations measured on the centreline, but are less frequent.

The other tendency we see is the reduction in fluctuations further downwind. Peak-to-mean ratios cluster around a value of 1 meaning that the mean concentration is broadly representative of any sampled concentration. However, for positions approaching the source of emission, the peak-to-mean ratios can be much larger, leading to situations where short-term exposure limits are satisfied, but peak maximum limits

for toxic gases are exceeded. Clearly, when the mean values exceed the peak maximum limits at close proximity to the source, the exposure is dangerous.

In the following Figures, concentrations are either plotted normalised by the mean concentration of the time series, or shown as absolute concentrations for a unit-rate emission factor. The concentrations in absolute concentrations show decreases in absolute scale with downwind distance, and with lateral offset from the centreline of the plumes. These differences are also shown in the probability distributions of the fluctuations (normalised by the mean), but in complex spatially distributed patterns, generally with larger fluctuations near the source, but also with larger fluctuations further from the centreline. However, because the mean concentration is smaller with distance from the centreline, large fluctuations at the edge of the plumes can still correspond to small absolute concentrations.

## 4.1 Estimates of peak behaviour

The results shown below typically consist of 15-minute sampling time series at a point downwind of source emissions. The 15-minute mean concentration is clearly the most basic measure of exposure. However, peak concentrations are characteristic of the plumes, which are highly intermittent. The sampling is simulated with sub-second time resolution, typically for 800 seconds. The peaks reported in Table 6 are selected at the threshold with 4 highest peaks in the given time series of 5 minute duration, which is a more robust estimate than the maximum concentration recorded. Comparison with typical probability distributions (which are plotted below for each time series) gives an exceedance probability of roughly 0.05 for high concentration exposures.

By sampling for longer periods more extreme mixing and short-term exposure behaviour can be encountered, but our metric is essentially the extreme exposures that are likely to occur 5% of the time during a typical 15-minute exposure. The peak-to-mean ratios typically turn out to be multiples of between two and five, that is the short term exposures are estimated to be between two and five times the mean concentration depending on distance downwind and lateral offset from the plume centreline. No simple parameterisations, as functions of the spatial distribution, are provided, but tabulated results are given. In general peak-to-mean ratios decrease downwind, but increase with offsets away from the plume centreline.

## 4.2 Low wind speed (U=3 m $s^{-1}$)

### 4.2.1 DOWNWIND DISPLACEMENT 50 M

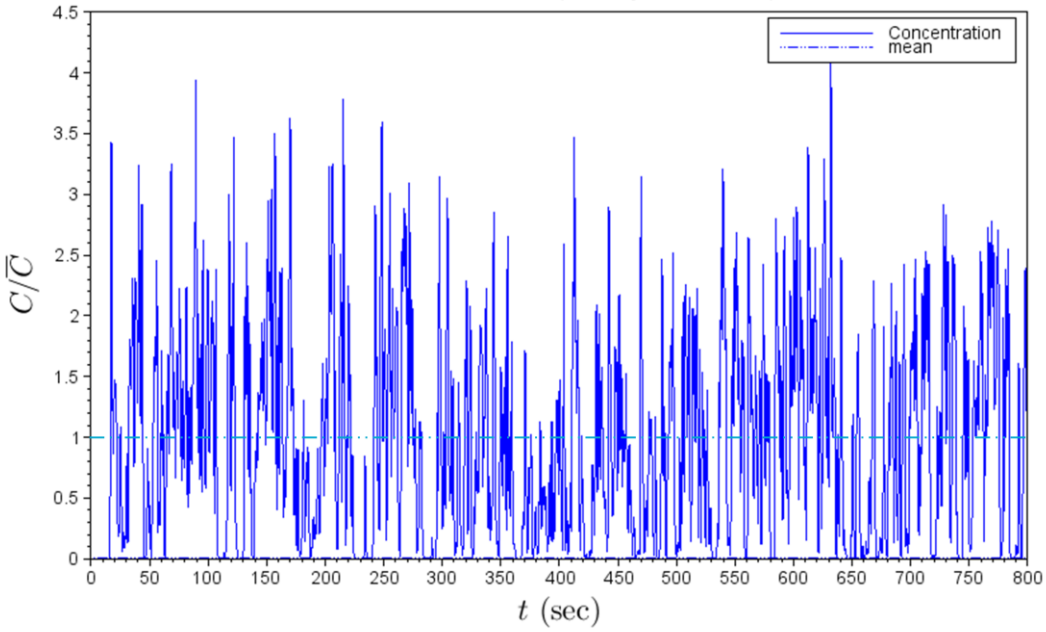


**Figure 4 Time series of normalised concentration, x=50 m U= 3 m $s^{-1}$**

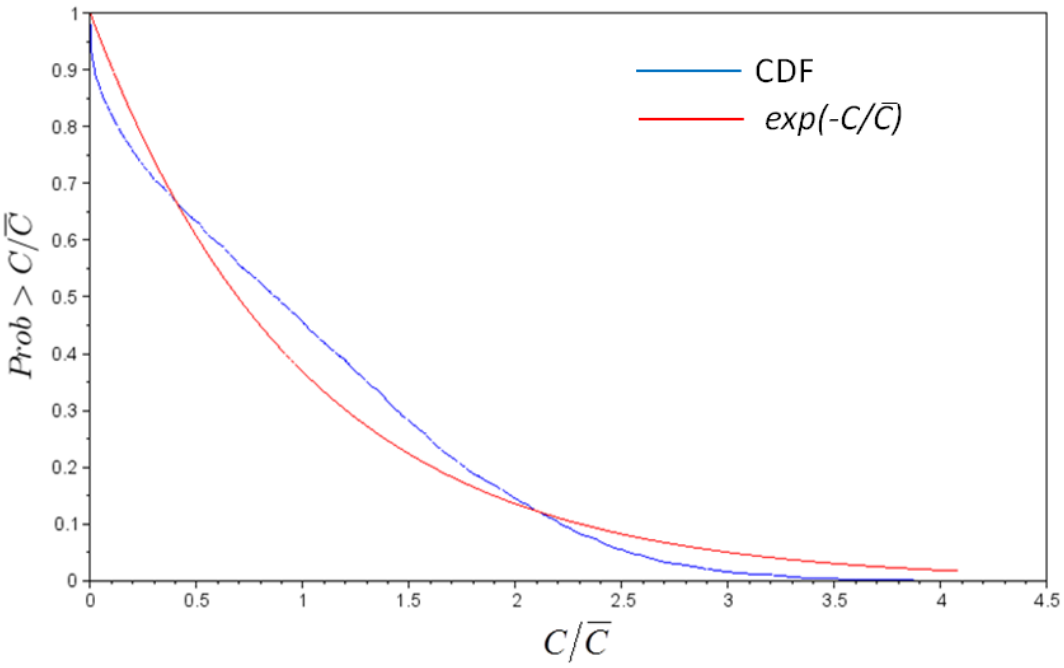


**Figure 5 Cumulative probability function of time series (blue) in Figure 4; exponential distribution (red)**

*Comments:* This scenario shows modest fluctuations, with excursions approximately 3 to 4 times higher than the mean concentration (Figure 4). The excursions occur frequently resulting in limited clean air exposure. The sampling is done at the plume centreline, with an almost constant exposure to the transported contaminant. The isolated peaks of high concentration may last less than a few seconds this close to the source. The probability distribution shows an almost linear decrease from unity at zero concentration and is less than the exponential distribution beyond a peak-to-mean ratio of 2 (Figure 5).

## Lateral Offset 5m

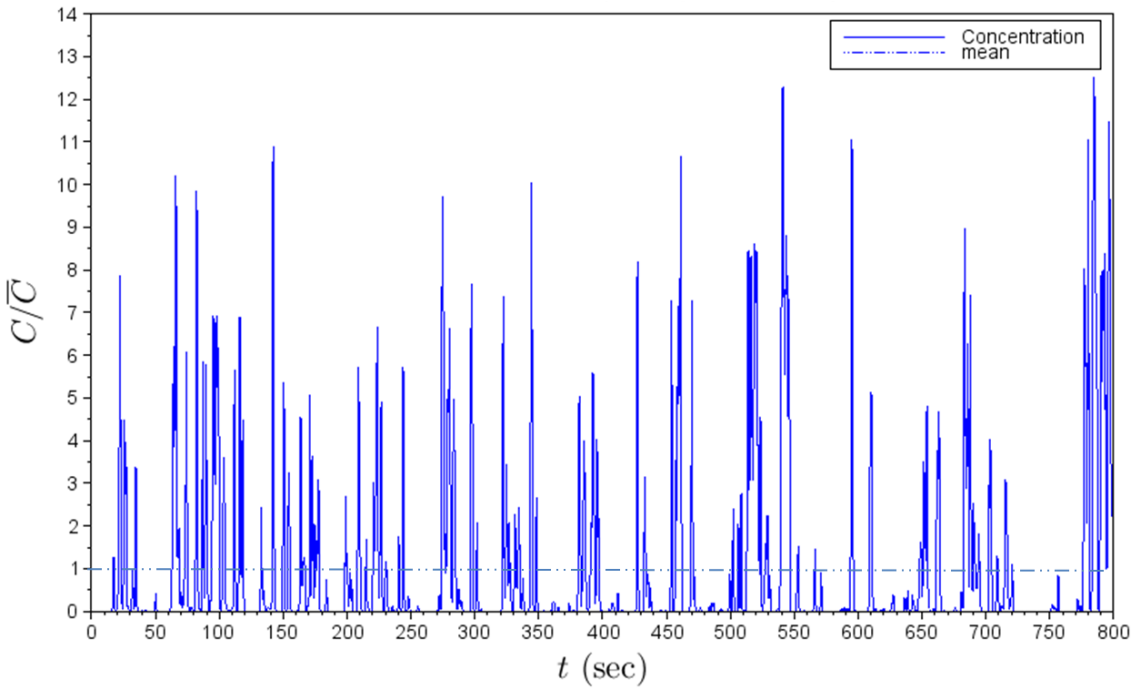


**Figure 6 Time series of normalised concentration for lateral offset 5 m**

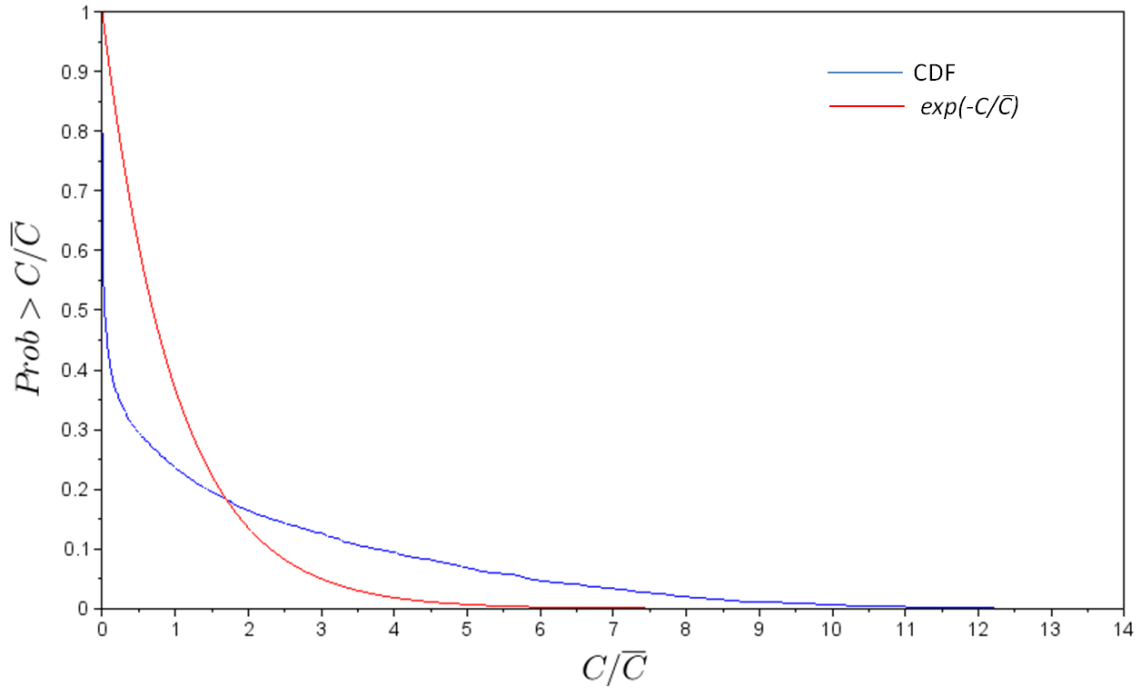


**Figure 7 Cumulative probability function of time series (blue) in Figure 6; exponential distribution (red)**

*Comments:* Figure 6 shows that the fluctuations relative to the mean are higher but more intermittent with a lateral offset away from the centreline (e.g. at the edge of the plume). This results in more clean air spaces between episodic peaks. The episodic peak excursions can be more than 10 times higher than the mean concentrations. When the plume is displaced laterally by the wind, high peaks occur. The concentrations cumulative probability in Figure 7 shows a rapid drop from unity at effectively zero concentrations with a probability of about 0.5 of detecting above zero exposure. There is a 10% probability of exceeding 4 times the mean concentration, much in excess of an exponential tail.

### 4.2.2 DOWNWIND DISPLACEMENT 100 M

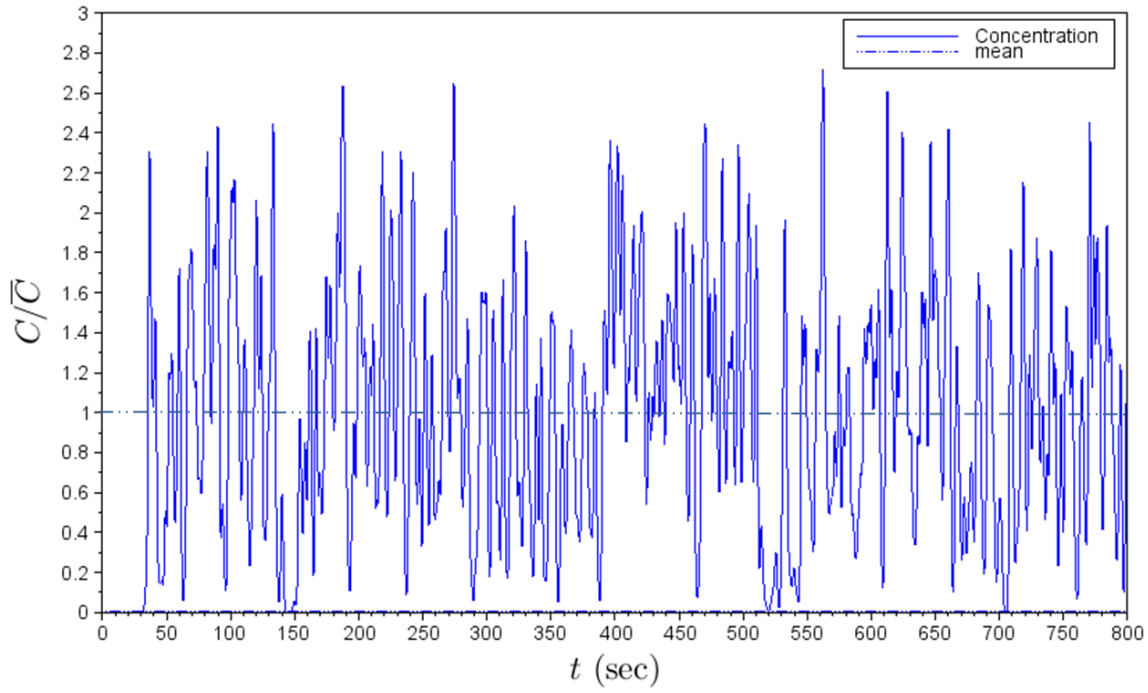


**Figure 8 Time series of normalised concentration, x=100 m U= 3 m $s^{-1}$**

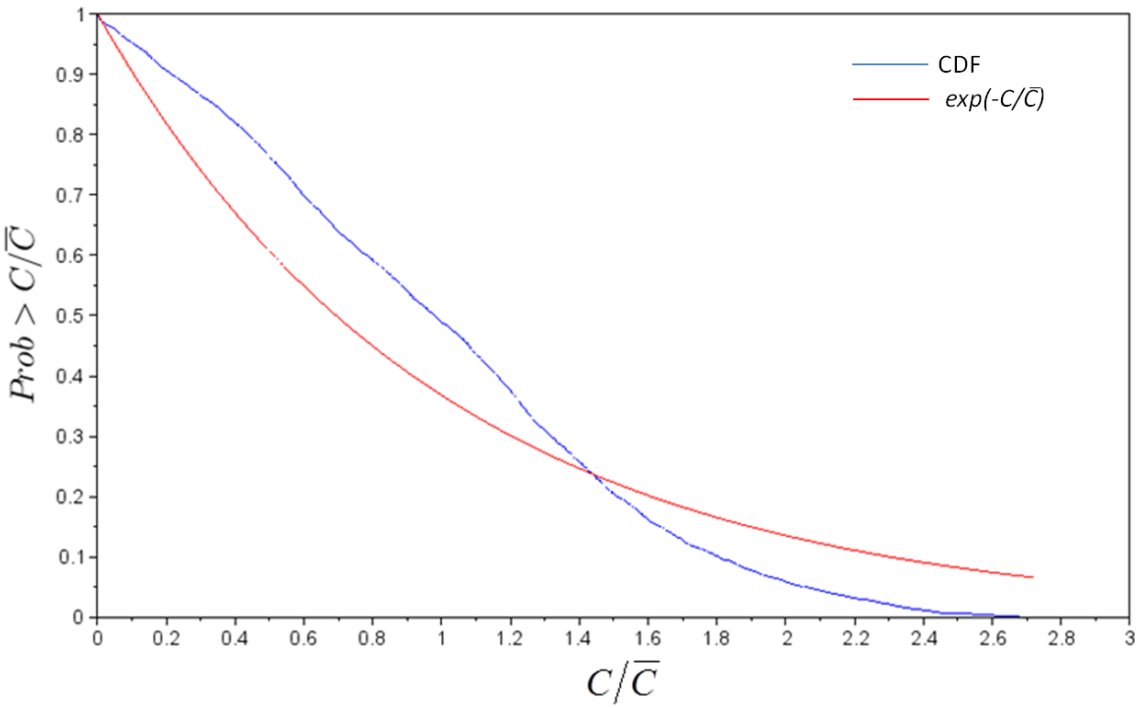


**Figure 9 Cumulative probability function of time series (blue) in Figure 8; exponential distribution (red)**

*Comments:* At 100 m downwind, directly on the centreline, modest peak-to-mean fluctuations occur, with limited clean air exposure (Figure 8). Peak excursions occur frequently. The peaks appear to be bounded above zero concentration as turbulent diffusion spreads the contaminant over all the air in the plume. The greater degree of mixing occurs further downwind. Even at 100 m and with more mixing, the peaks still

have typical durations of several seconds. The probability distributions become sub exponential tails at a peak-to-mean ratio of only 1.4 (Figure 9).

## Lateral Offset 10 m

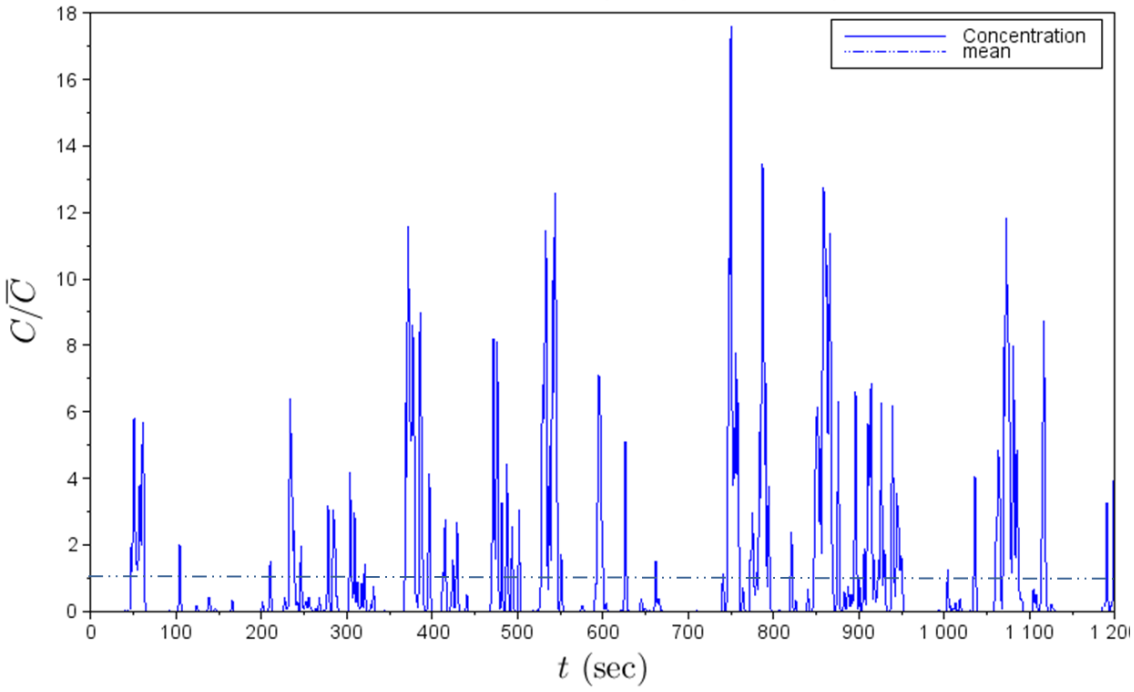


**Figure 10 Time series of normalised concentration for lateral offset of 10 m**

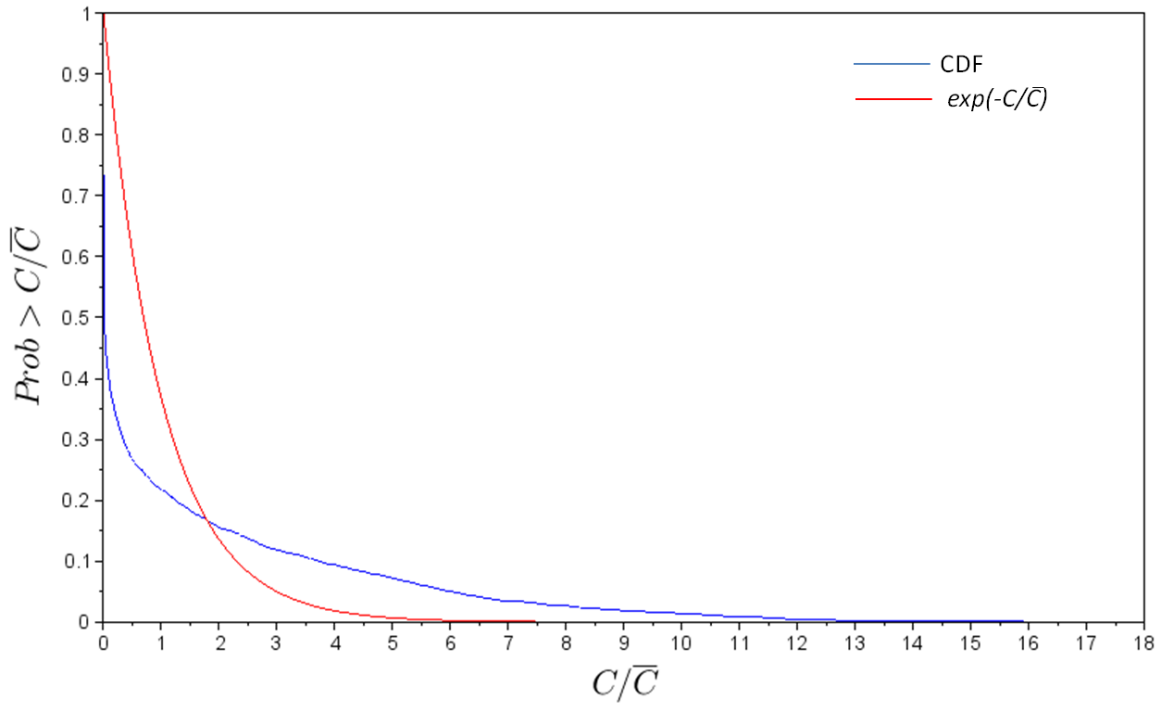


**Figure 11 Cumulative probability function of time series (blue) in Figure 10; exponential distribution (red)**

*Comments:* At 100 m downwind but offset laterally by 10 m from the source, high peak-to-mean fluctuations occur (ratios above 10) and more clean air intermittency is present, i.e zero concentrations patches of duration of up to 60 seconds (Figure 10). The nature of sampling at the edge of the plume is also

clear in the probability distribution in Figure 11 with a dramatic drop down at zero concentration to about a probability of 0.47 and a super exponential tail beyond peak-to-mean ratios of 2.

### 4.2.3 DOWNWIND DISPLACEMENT 150 M

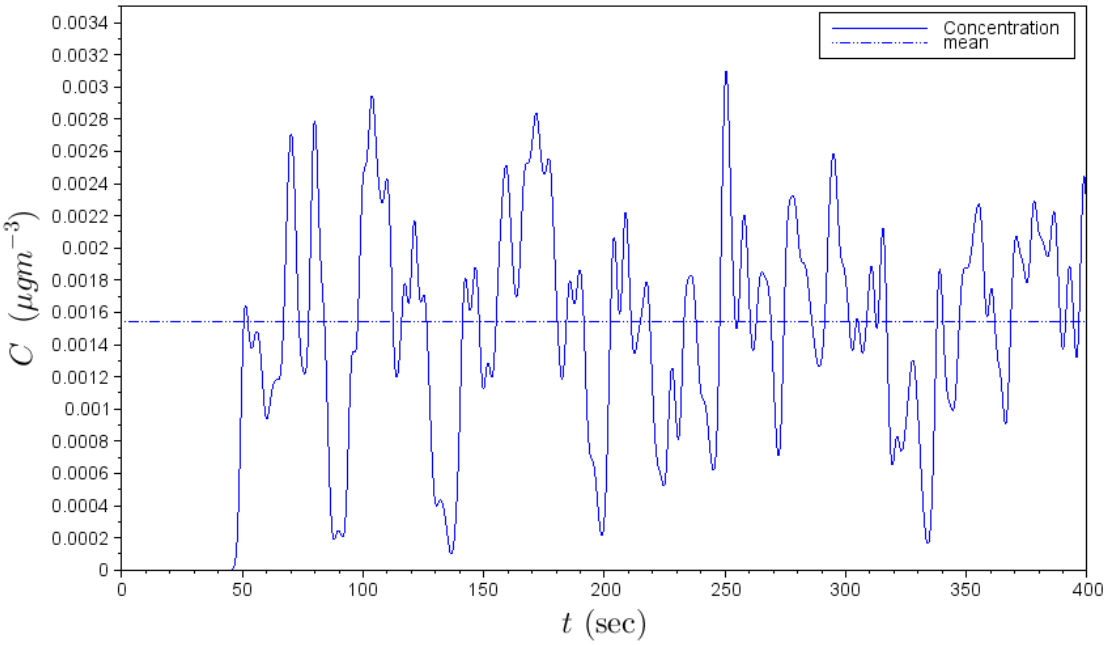


**Figure 12 Time series of absolute concentration for a 1 g $s^{-1}$ emission source, x=150 m U= 3 m $s^{-1}$**

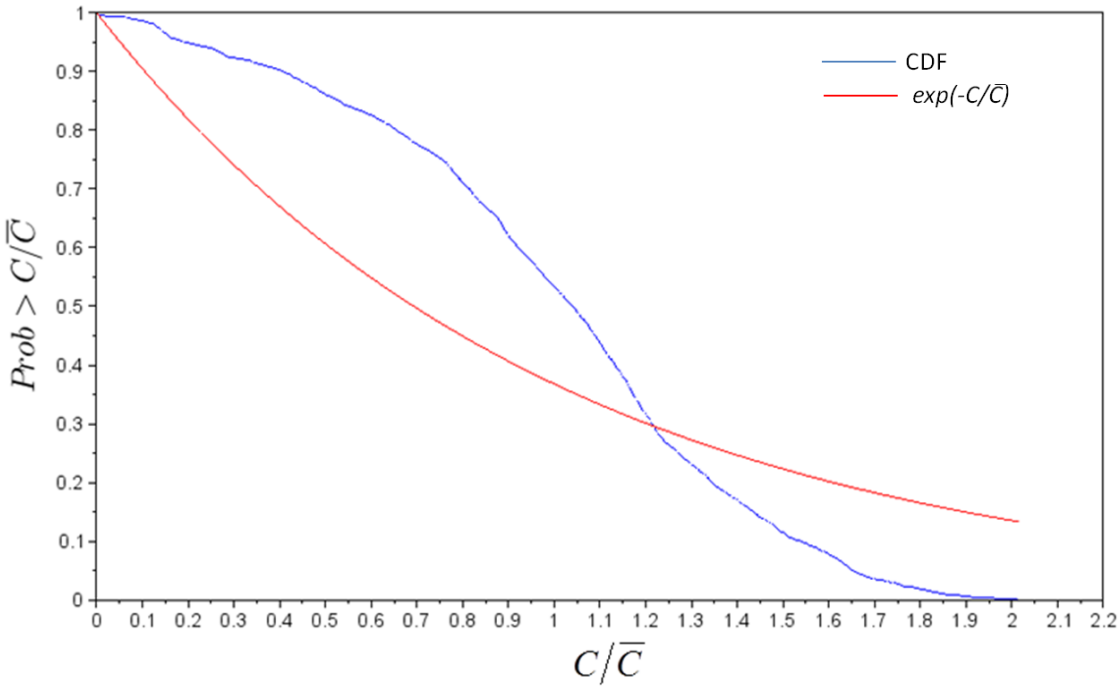


**Figure 13 Cumulative probability function of time series (blue) in Figure 12; exponential distribution (red)**

*Comments:* At 150 m downwind the fluctuations are even more modest (peak-to-mean fluctuation no more than 2) and strongly bounded above zero on the centreline, i.e. effectively no likelihood of clean air exposure. Figure 12 shows the finite advection time it takes the plume to reach the sampling point 150 m downwind (approximately 44 seconds at a wind speed of 3 m $s^{-1}$). Figure 12 shows absolute concentrations

to be used for reference in plots below to show variations in absolute concentration with wind speed and distance from the source. The slope of the CDF at zero concentrations is flat, so it is almost certain that the concentrations are bounded away from zero. The CDF also becomes sub-exponential at peak-to-mean ratio of about 1.2 (Figure 13).

## 4.3 Mid wind speed (U=6 m $s^{-1}$)

### 4.3.1 DOWNWIND DISPLACEMENT 50 M

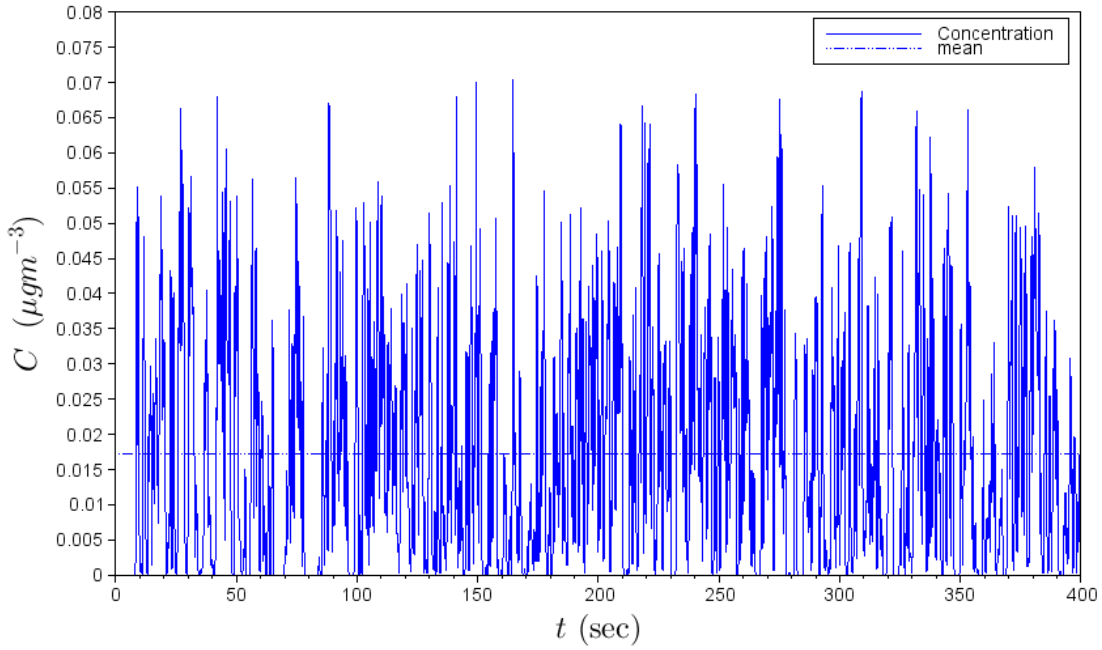


**Figure 14 Time series of absolute concentration for a 1 g $s^{-1}$ emission source, x=50 m U= 6 m $s^{-1}$.**

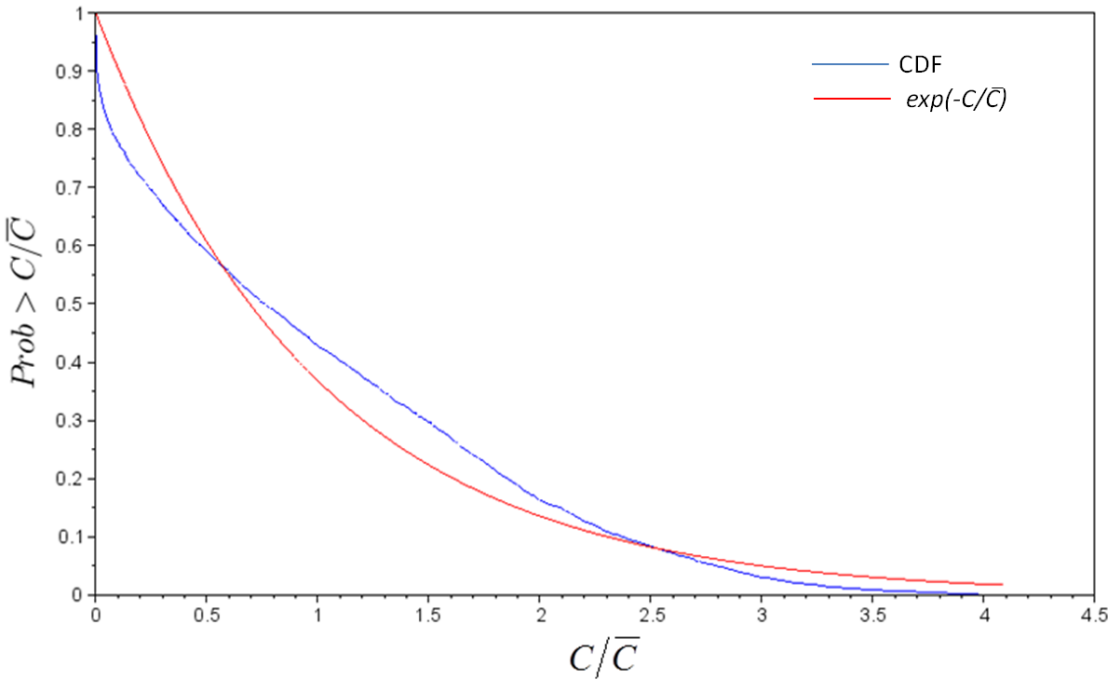


**Figure 15 Cumulative probability function of time series (blue) in Figure 14; exponential distribution (red)**

*Comments:* At higher wind speeds the peak-to-mean fluctuations at 50 m downwind are modest with isolated peaks of around 3 to 4 times the mean concentrations. There is also a very rapid recurrence of lesser episodic peaks giving limited clean air exposure, with a maximum of a few seconds of zero sampling at the plume centreline. The probability distribution in Figure 15 shows a short step down (with a 90%

chance of finite concentration exposure at any instant), and with the tail going sub exponential at a ratio of 2.5. The CDF is super exponential in a range of ratios from 0.5 to 2.5.

### Offset 5 m

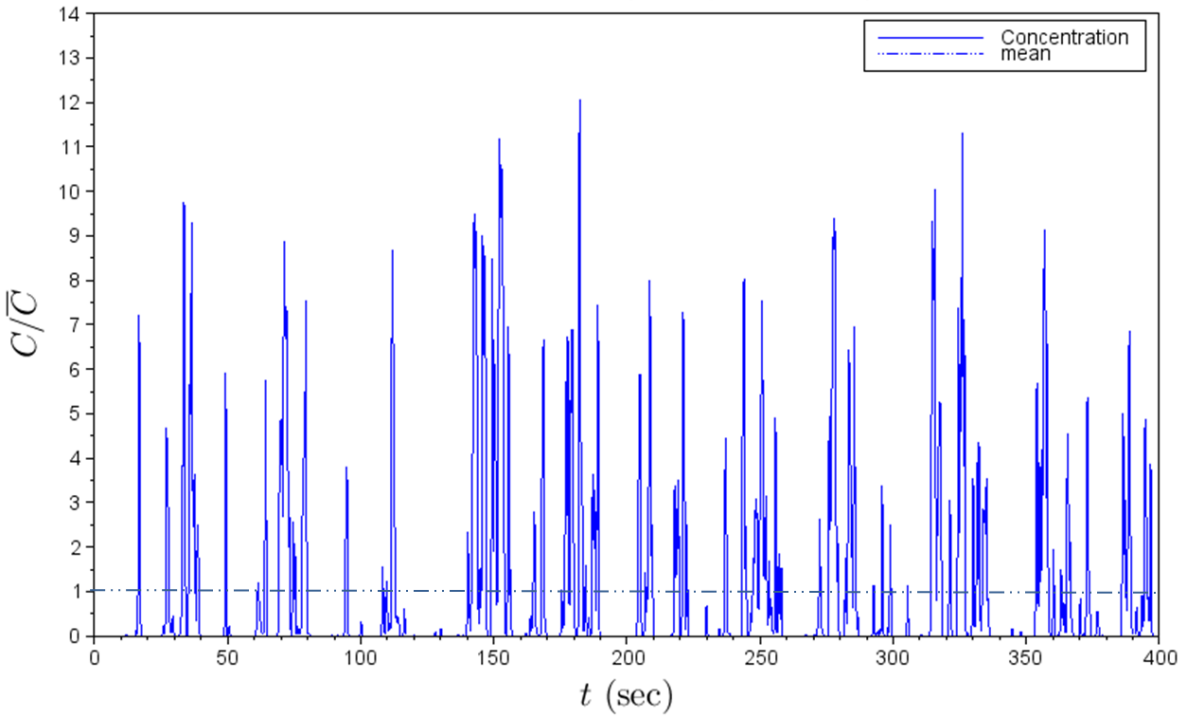


**Figure 16 Time series of normalised concentration for a lateral offset of 5 m**

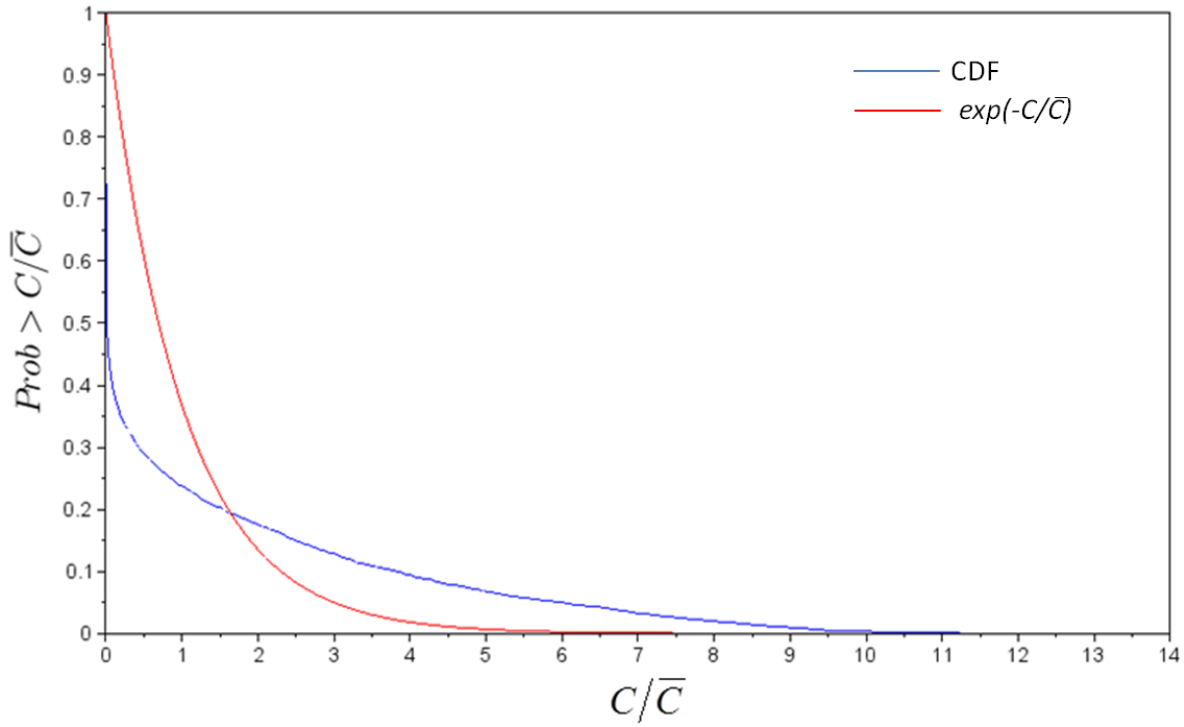


**Figure 17 Cumulative probability function of time series (blue) in Figure 16; exponential distribution (red)**

*Comments:* When sampling laterally offset from the centreline at higher speed, high fluctuation ratios in excess of 10 to 1 occur along with many zero-concentration intermittency gaps, i.e. clean air spaces between episodic peaks of duration around 10 seconds (Figure 16). This behaviour is observed because the

sampling is at the edge of the narrower plume at higher speed. The CDF shows the dramatic intermittency (zero-concentration) drop down with a probability of about 0.5 of finite concentration at any instant, and with super-exponential tails beyond ratios of 1.7 (Figure 17).

### 4.3.2 DOWNWIND DISPLACEMENT 100 M

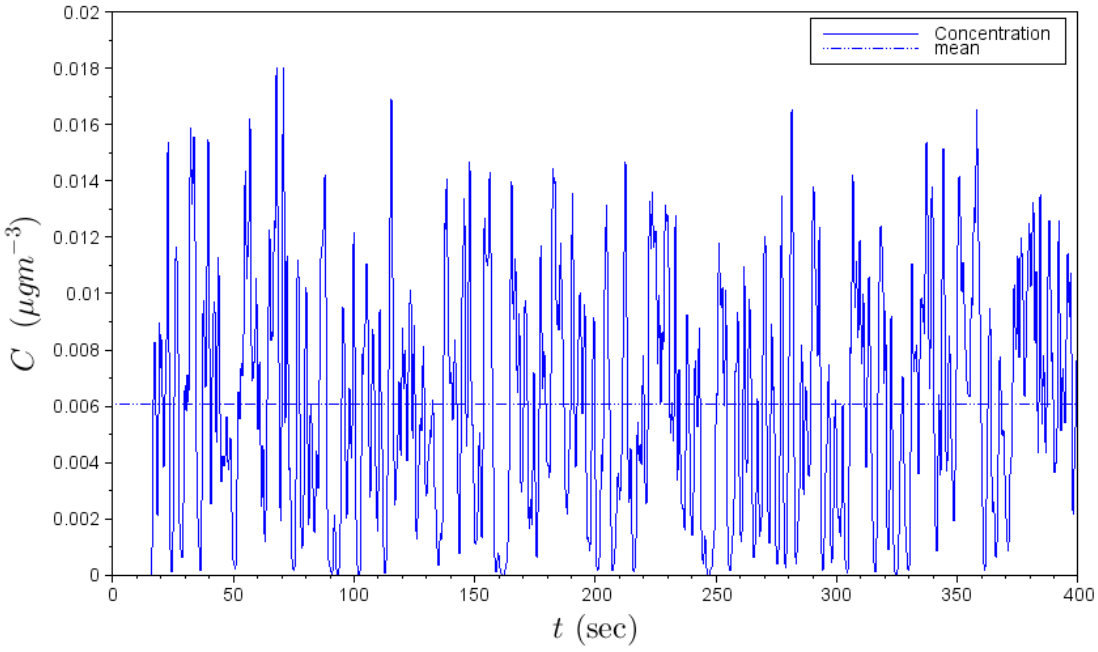


**Figure 18 Time series of absolute concentration for a 1 g $s^{-1}$ emission source, x=100 m U= 6 m $s^{-1}$**

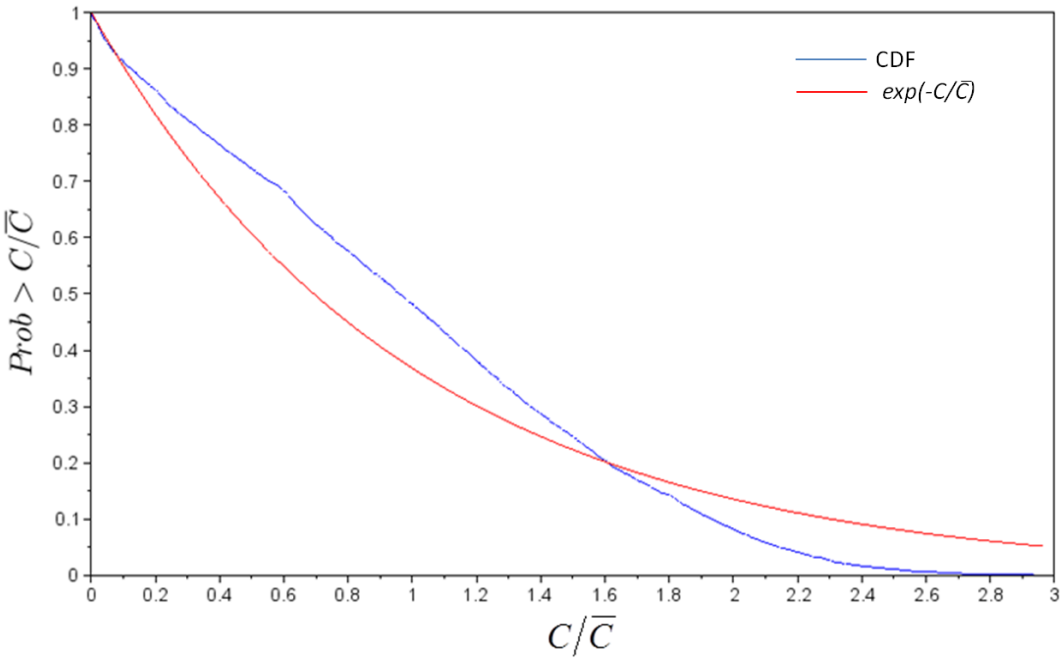


**Figure 19 Cumulative probability function of time series (blue) in Figure 18; exponential distribution (red)**

*Comments:* At higher wind speeds and further downwind similar patterns to those presented above emerge. Reduced peak-to-mean ratios on the centreline with typical episodic excursion of 2 to 2.5 are observed, and most fluctuations are bounded away from zero as plume diffusion more completely fills the centreline of the plume. The CDF shows no definite baseline shift with finite slope of the CDF at zero

concentration and approximately linear decline to sub exponential tails at a ratio of about 1.6 (Figure 19). Absolute concentrations are shown to decrease with downwind distance at a fixed wind speed (Figures 14 and 18).

### 4.3.3 DOWNWIND DISPLACEMENT 150 M

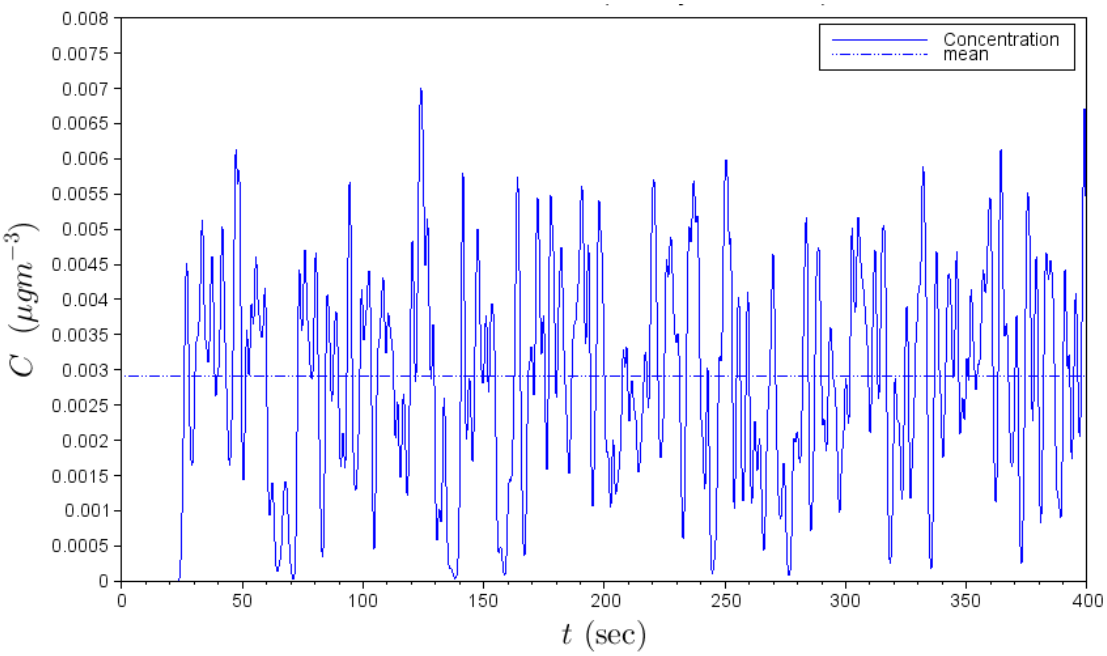


**Figure 20 Time series of absolute concentration for a 1 g $s^{-1}$ emission source, x=150 m U= 6 m $s^{-1}$**

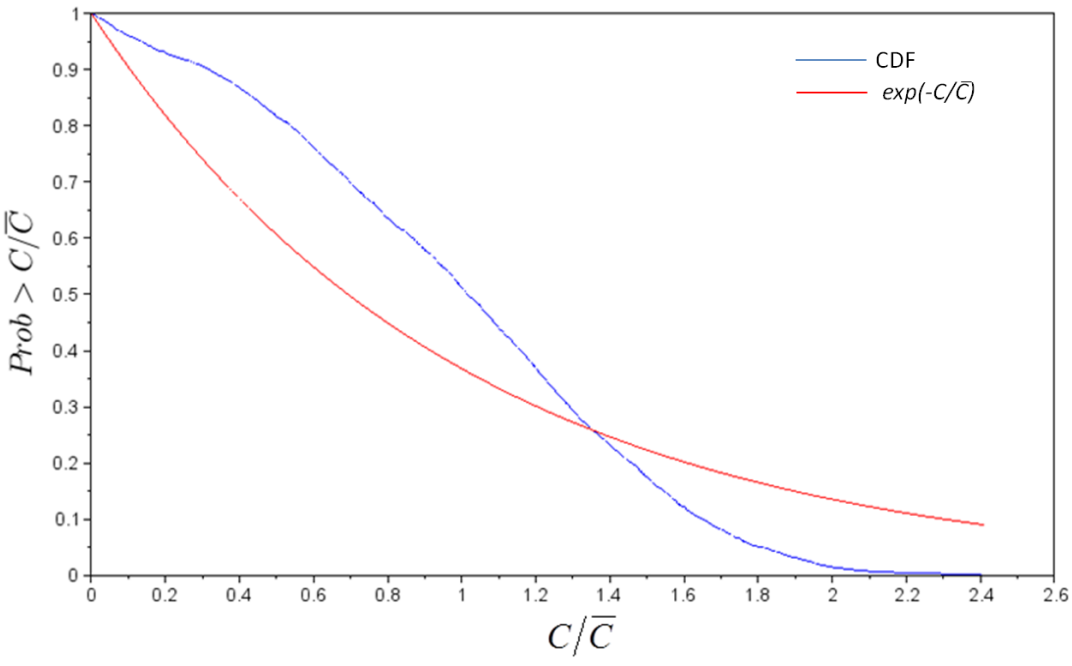


**Figure 21 Cumulative probability function of time series (blue) in Figure 20; exponential distribution (red)**

*Comments:* Even further downwind at higher wind speed, the moderation of fluctuations continues with relatively few peak-to-mean ratios above 2. The clean air exposure is even more limited as shown by the flattening of the CDF at zero concentration (Figure 21). Sub exponential tails occur at ratios beyond 1.3.

## 4.4 High wind speed (U=9 m $s^{-1}$)

### 4.4.1 DOWNWIND DISPLACEMENT 50 M

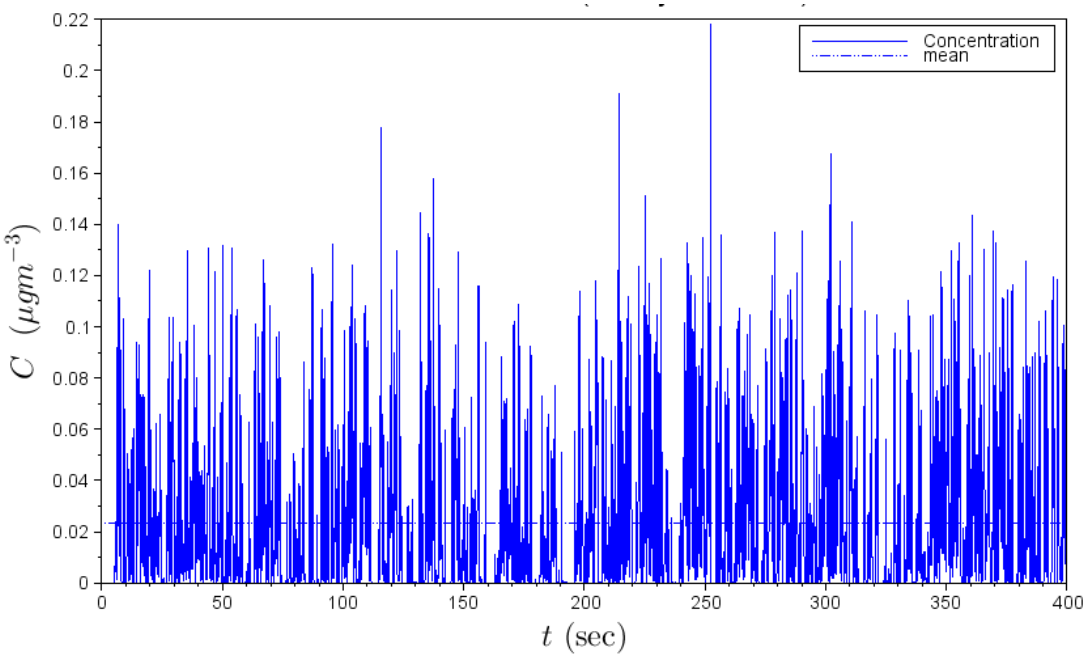


**Figure 22 Time series of absolute concentration for a 1 g $s^{-1}$ emission source, x=50 m U= 9 m $s^{-1}$**

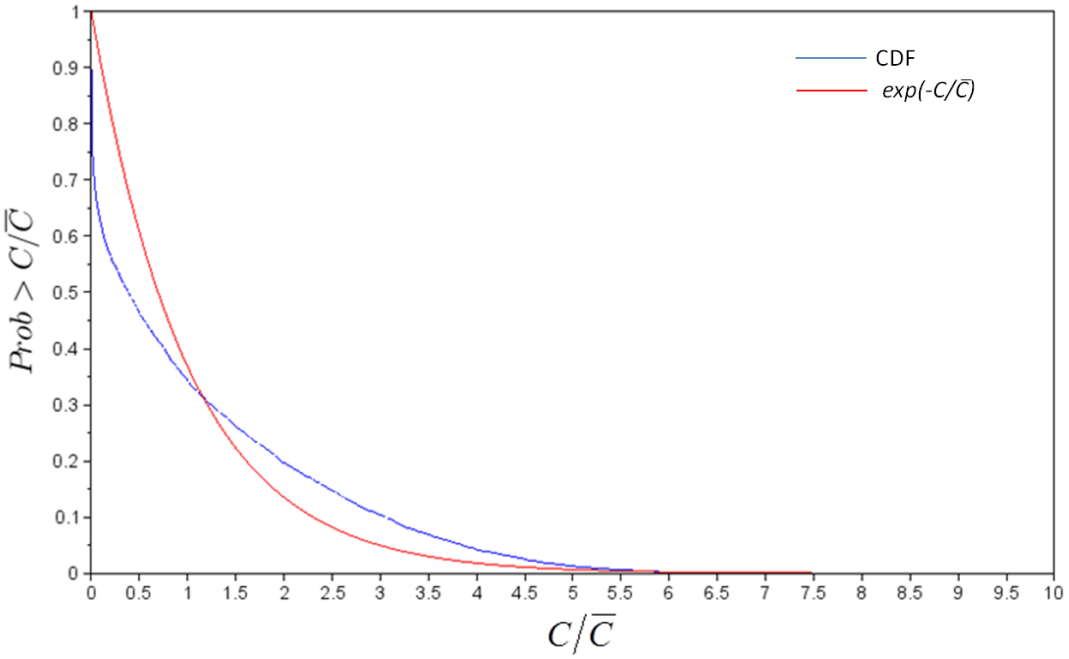


**Figure 23 Cumulative probability function of time series (blue) in Figure 22; exponential distribution (red)**

*Comments:* At an even higher wind speed there is a slight intensification of the fluctuation process with ratios of nearly 8 on the centreline. This intensification is also indicated by super exponential tails in the CDF beyond ratios of about 1 and an increase in the clean air exposure even on the centreline. The CDF indicated a 25% probability of zero concentration. At higher wind speed the absolute concentration of peak fluctuations is larger than at lower wind speed (Figures 14 and 22) because little mixing occurs in the short

elapsed time from source to receptor. Generally overall the mean concentration is lower because more zero concentration clean air is sampled in a high fluctuation plume.

### 4.4.2 DOWNWIND DISPLACEMENT 100 M

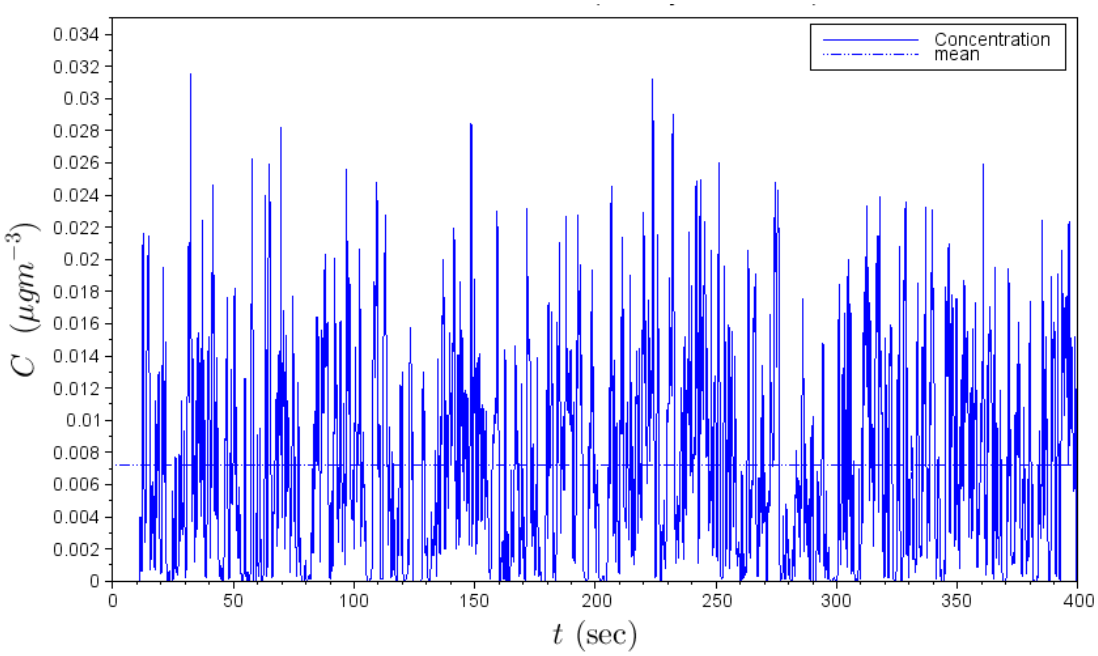


**Figure 24 Time series of absolute concentration for a 1 g $s^{-1}$ emission source, x=100 m U= 9 m $s^{-1}$**

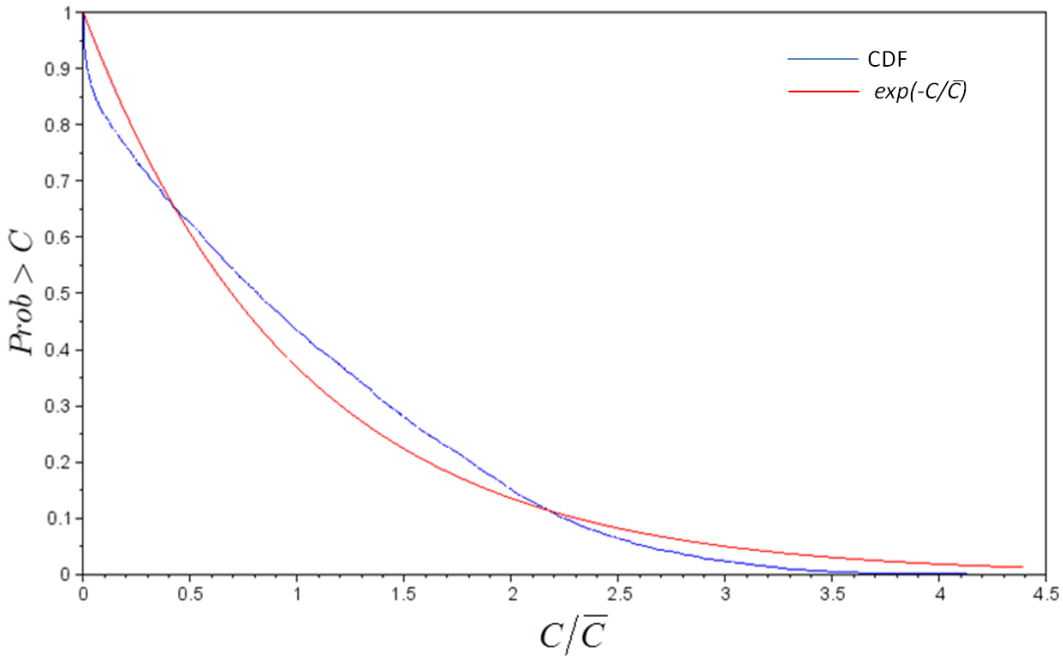


**Figure 25 Cumulative probability function of time series (blue) in Figure 24; exponential distribution (red)**

*Comments:* At higher wind speed, but further downwind, the intensification of fluctuations is moderated with episodic peaks of 3.5 and more limited clean air exposure as more turbulent mixing has occurred near the centreline. No above-zero-concentration baseline development is yet manifest and an observable fraction of zero concentrations occurs 7% of the time. Overall absolute concentration values, both peak and

mean, decrease with further distance downwind (Figures 22 and 24) . The CDF is sub exponential both at the low concentration end, but also for the tail with ratios beyond 2.1 (Figure 25).

### 4.4.3 DOWNWIND DISPLACEMENT 150 M

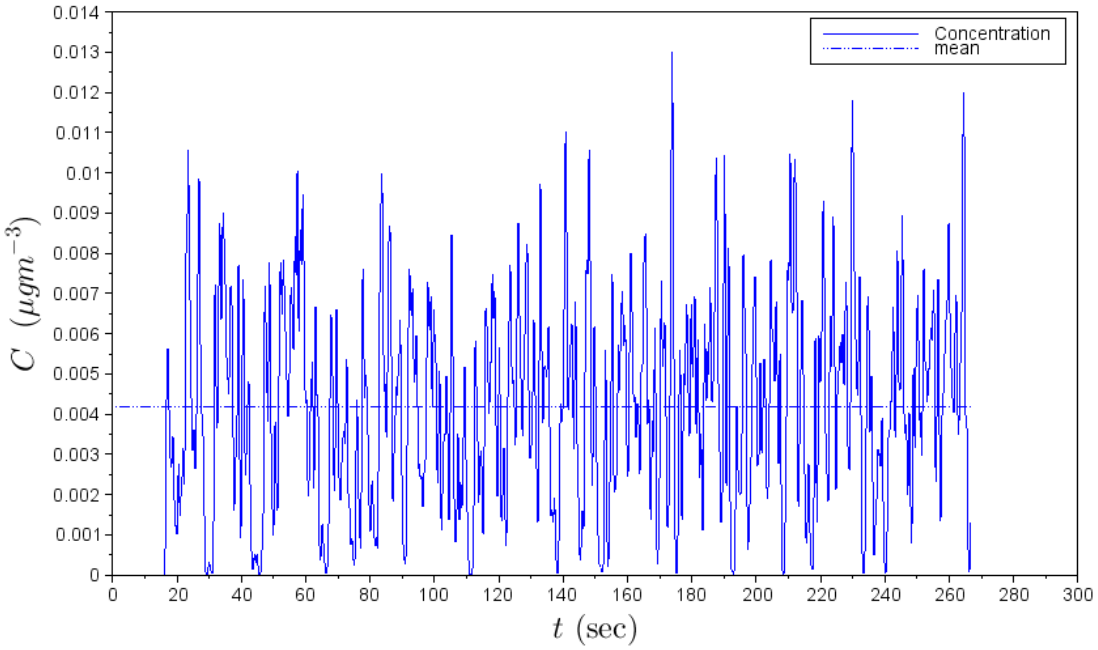


**Figure 26 Time series of absolute concentration for a 1 g $s^{-1}$ emission source, x=150 m U= 9 m $s^{-1}$**

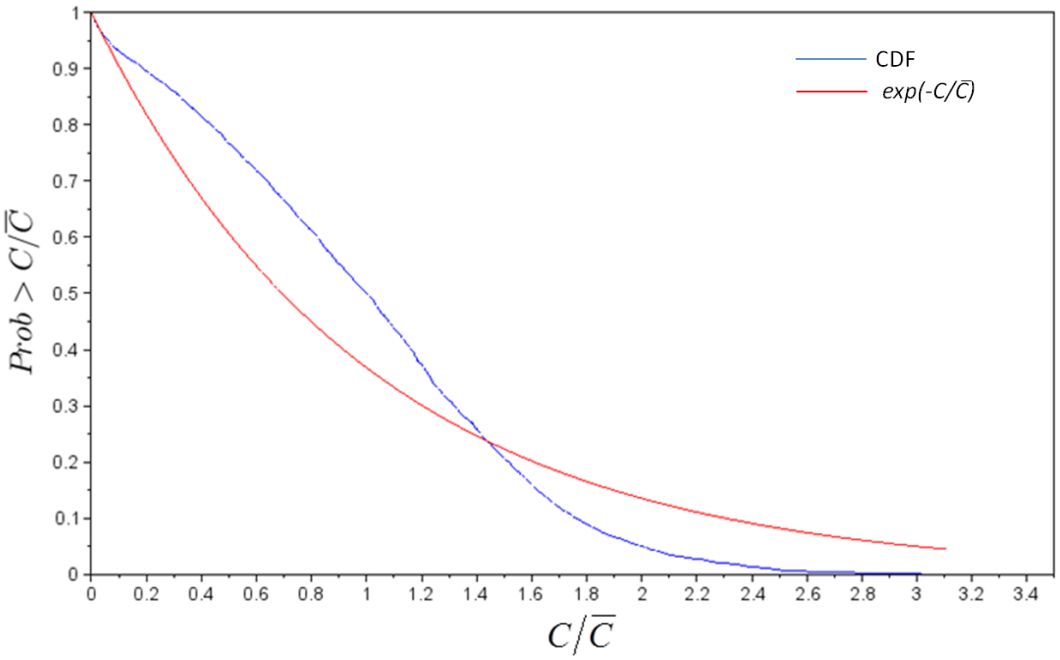


**Figure 27 Cumulative probability function of time series (blue) in Figure 26; exponential distribution (red)**

*Comments:* At higher wind speed, but increasingly further downwind on the plume centreline the fluctuations are moderated even further (ratios of about 2) and clean air exposure is very nearly approaching zero probability (the CDF shows almost a non-singular linear approach to zero) (Figure 27). The CDF is sub exponential beyond ratios of 1.4.

### 4.4.4 DOWNWIND DISPLACEMENT 300 M

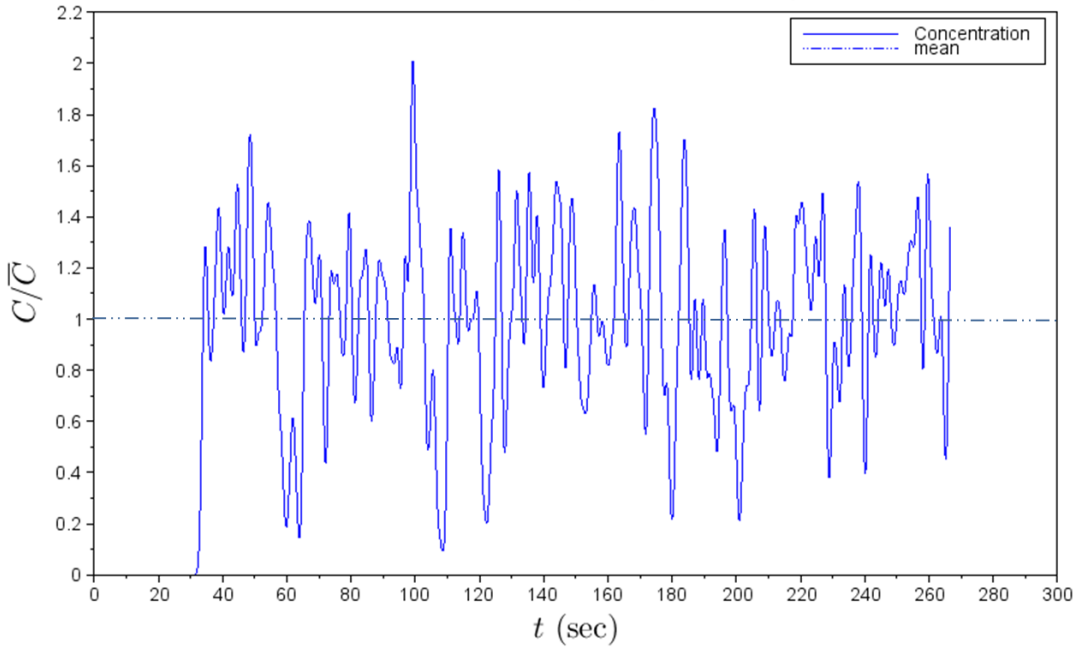


**Figure 28 Time series of normalised concentration, x=300 m U= 9 m $s^{-1}$**

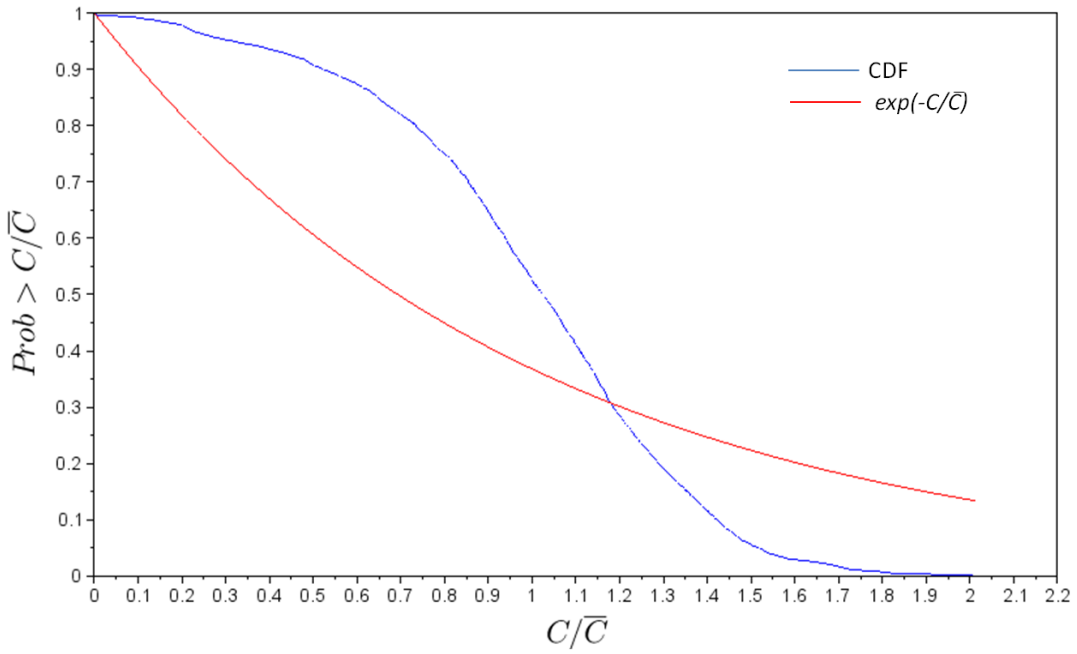


**Figure 29 Cumulative probability function of time series (blue) in Figure 28; exponential distribution (red)**

*Comments:* The downwind trends on the centreline are continued at 300 m from the source, with relatively small fluctuations of ratios 1.8 (Figure 28), and with the slope of the CDF at zero concentration flat and sub exponential tails beyond a ratio of 1.15 (Figure 29). Turbulent mixing has significantly smoothed the fluctuation field and in addition gives episodic peaks of duration of about 5 seconds. Beyond this distance the mean concentration becomes increasingly representative of the instantaneous value of the concentration field.

## 4.5 Very high wind speed (U=12 m $s^{-1}$)

### 4.5.1 DOWNWIND DISPLACEMENT 50 M

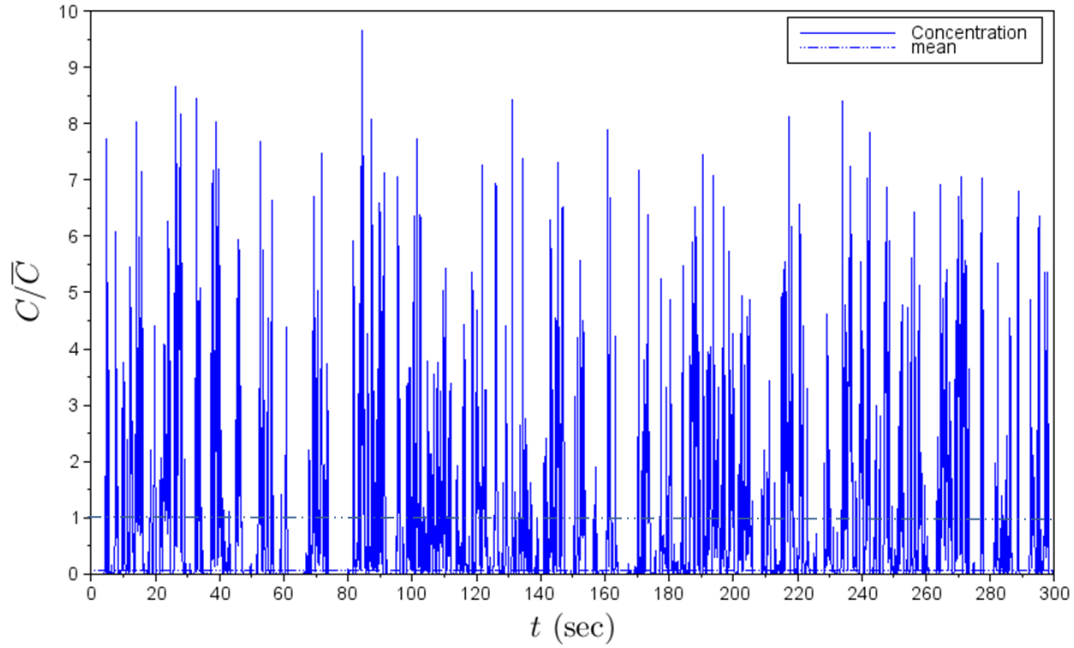


**Figure 30 Time series of normalised concentration, x=50 m U= 12 m $s^{-1}$**

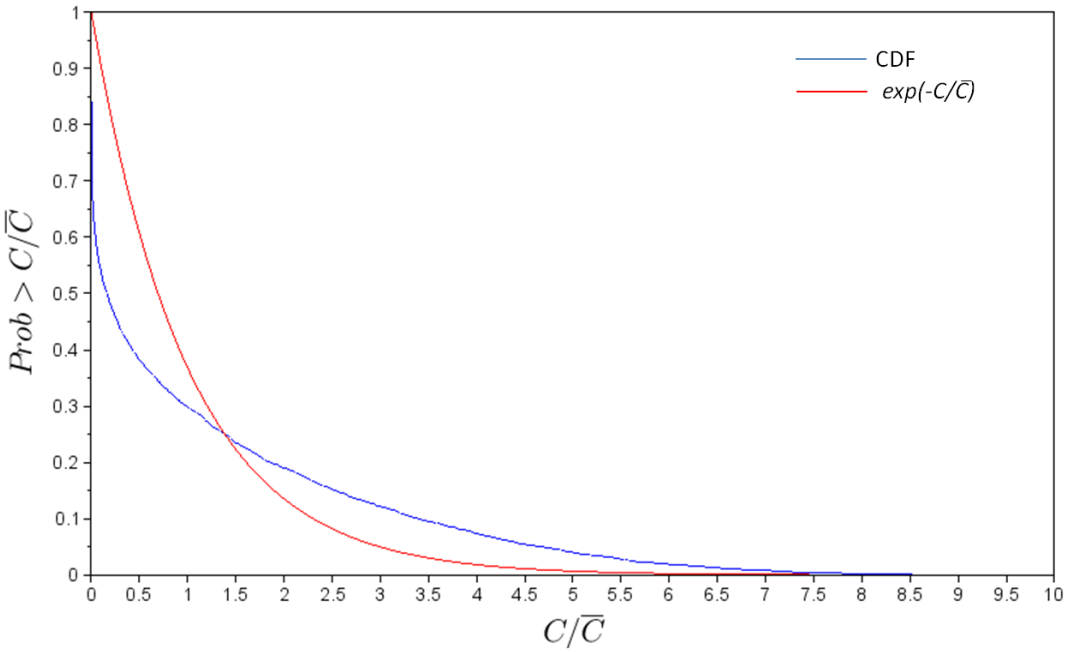


**Figure 31 Cumulative probability function of time series (blue) in Figure 30; exponential distribution (red)**

*Comments:* The highest wind speed considered in this study shows a continuation of the observed trends, with an intensification of fluctuations at 50 m from the source (about 4 seconds time-of-flight advection time) and with more clean air exposure manifest a frequent short zero concentration patches of clean air (Figures 4 and 30). At high wind speed the near source intermittency dominates and the plume is very thin allowing for clean air incursions in the short time for mixing from source to sampling point. The intensification is indicated by peak-to-mean ratios on the centreline in excess of 4, and with a 33% chance of exposure to zero concentration. The super exponential tail occurs beyond ratios of 1.4 (Figure 31).

### 4.5.2 DOWNWIND DISPLACEMENT 100 M

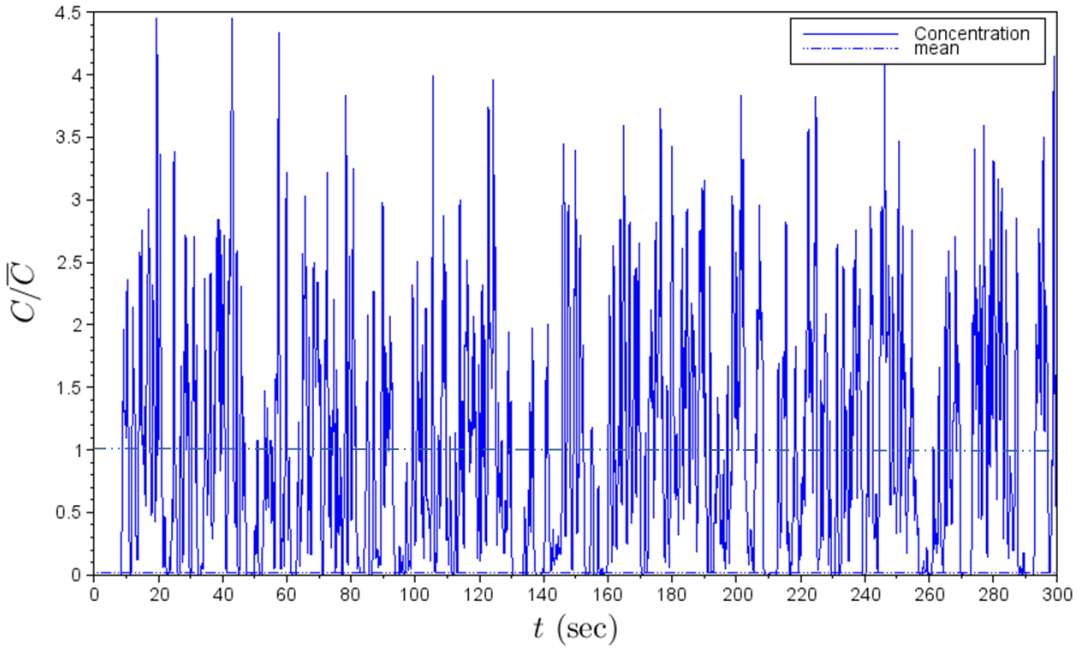


**Figure 32 Time series of normalised concentration, x=100 m U= 12 m $s^{-1}$**

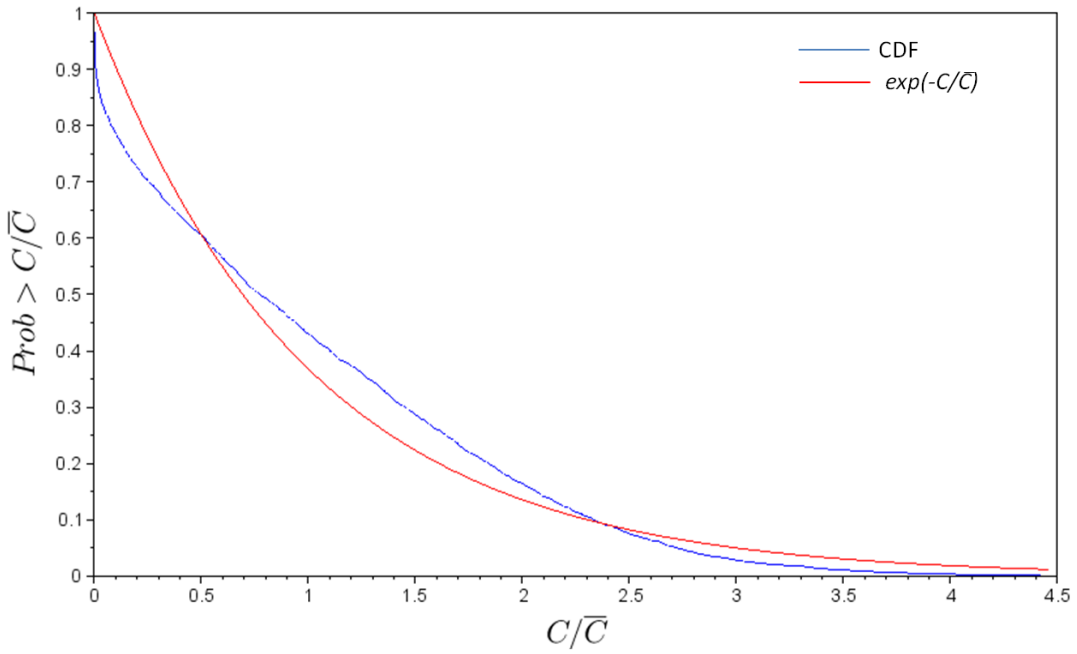


**Figure 33 Cumulative probability function of time series (blue) in Figure 32; exponential distribution (red)**

*Comments:* At the highest wind speed but further downwind, the fluctuations are again moderated, with lesser clean air exposure (Figure 32). Peak-to-mean episodic values are generally less than 3.5 and the probability of zero concentration less than 10%. At high wind speed the near source intermittency still dominates at 100 m although mixing of clean air to the centreline is reduced, a finite fraction of zero concentrations is observed. The CDF tail is sub exponential beyond ratios of 2.4 (Figure 33).

### 4.5.3 DOWNWIND DISPLACEMENT 150 M

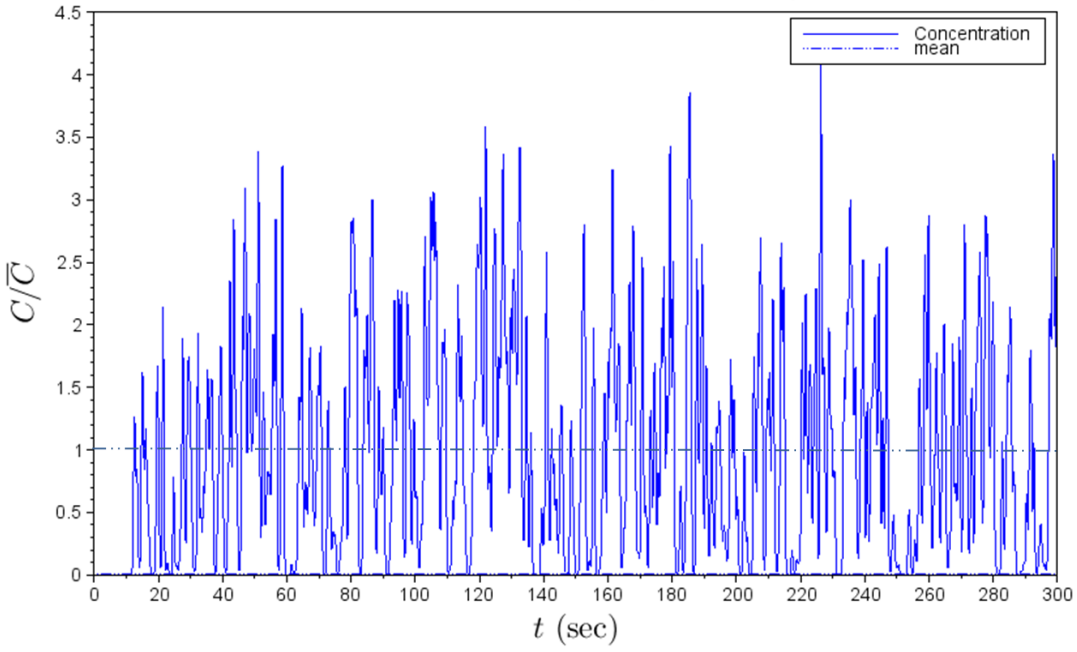


**Figure 34 Time series of normalised concentration, x=150 m U= 12 m $s^{-1}$**

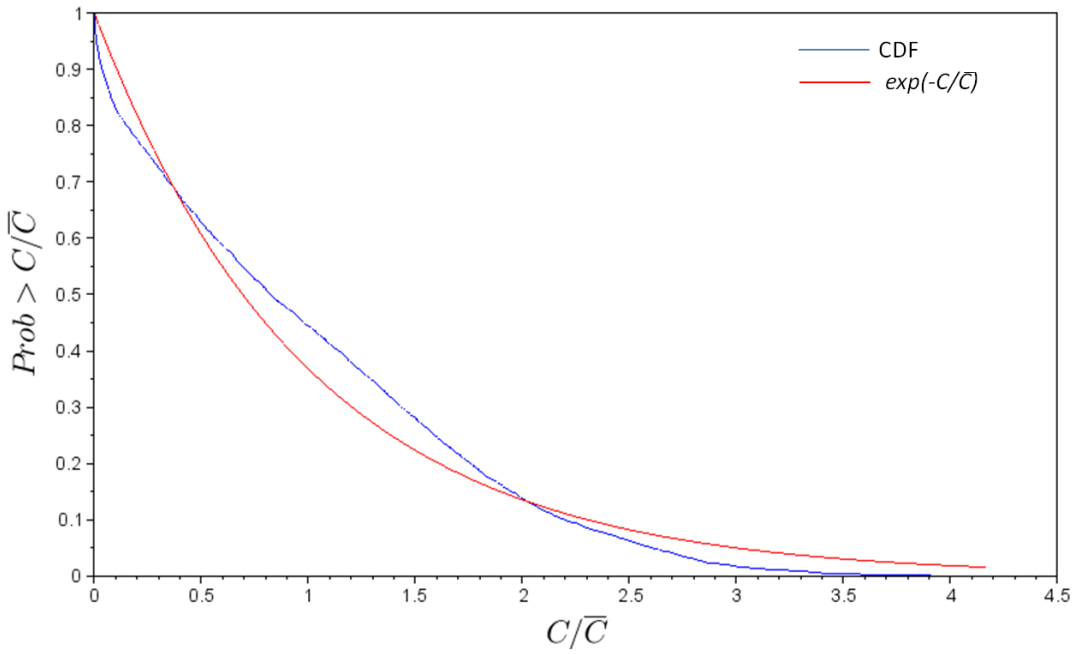


**Figure 35 Cumulative probability function of time series (blue) in Figure 34; exponential distribution (red)**

*Comments:* The trend is for further reduction in fluctuations further distance downwind. Even at 150 m from the source there is still detectable clean air exposure about 5% of the time. Fluctuation ratios continue to diminish to about 3.5 (Figure 34), with sub exponential tails in the CDF beyond ratios of 2 (Figure 35).

### 4.5.4 DOWNWIND DISPLACEMENT 200 M

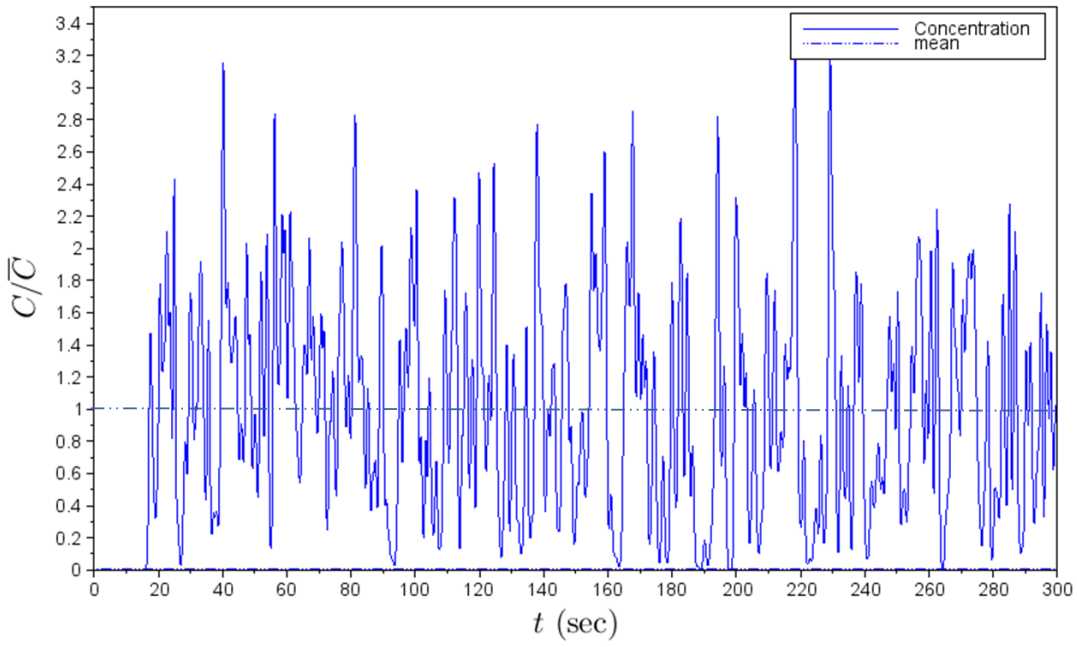


**Figure 36 Time series of normalised concentration, x=200 m U= 12 m $s^{-1}$**

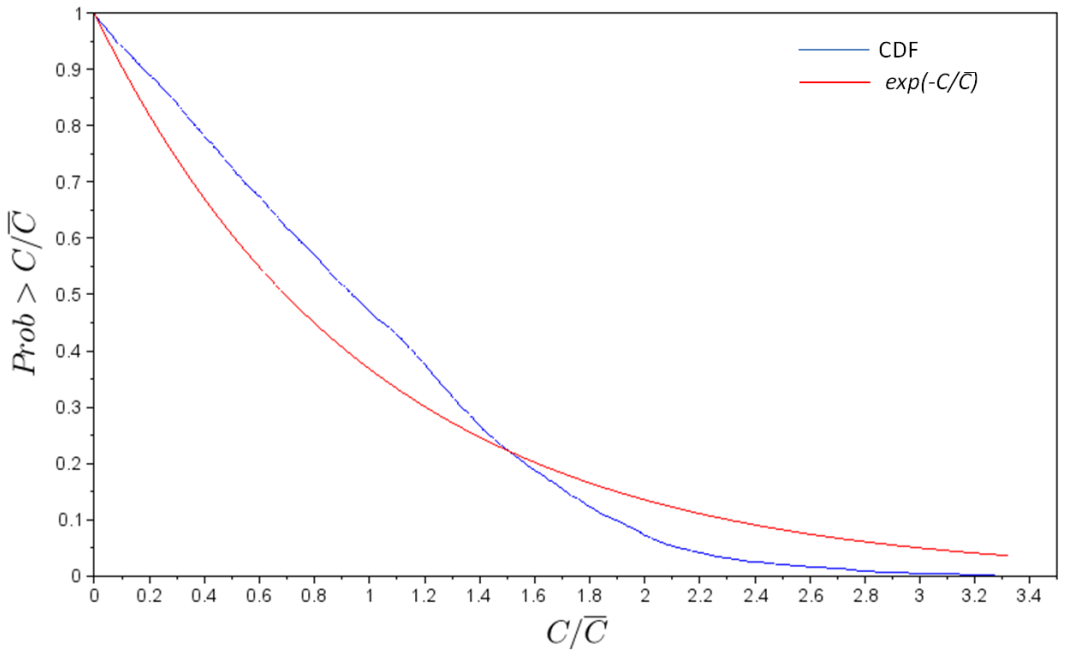


**Figure 37 Cumulative probability function of time series (blue) in Figure 36; exponential distribution (red)**

*Comments:* At the highest wind speed, and the furthest sampling point considered at this speed (200 m downwind on the centreline) further reduction in fluctuations intensity occurs with few episodic peaks above ratios of 3 (Figure 36). Finite above-zero baseline is beginning to emerge, although the CDF is not yet flat at zero concentration (Figure 37). The CDF tail becomes sub exponential beyond ratios of 1.4. At this distance downwind the individual episodic peaks are spanning a duration of about 5 seconds and turbulent diffusion smoothes out the plume structures.

### 4.5.5 THE OVERALL TRENDS

The figures above show a number of consistent trends.

Near the source an increase in wind speed increases the intensity of fluctuations with higher peaks and frequent patches of clean air exposures.

At a fixed wind speed, the intensity of fluctuation decreases with increasing distance from the source, with both lower episodic peaks and less chance of clean air exposure.

As we sample laterally from the plume centreline, the intensification of the fluctuations dramatically increases, with the emergence of high peak-to-mean ratios episodically and long duration and increasingly likely zero-concentration patches. However, the lateral variation of the mean concentration means that absolute exposure at the edges of plumes is not necessarily more dangerous, but rather that we are still likely to experience equivalent exposure as with centreline sampling, but increasingly mixed with clean air from the edges of the plume.

The variation of the CDF plots of ratios of peak-to-mean values shows clear transitions from steep singular zero concentration jumps, to flat baseline jumps with sampling bounded away from zero. The comparison with exponential distribution shows both sub and super exponential tails for large ratios depending on whether the process has weak or intense fluctuations respectively.

The results also show that even at 200 to 300 m downwind, the role of short-term fluctuations can be significant for describing the exposure characteristics of concentration plumes.

# 5 Multiple Sources – Burning Clusters

A common scenario is multiple burning houses where the plumes interact downwind and exposure to emissions from all sources is possible.

**Figure 38 Schematic of multiple plumes from several sources combining downwind.**

The specific example we consider is a two-source plume, separate plumes from a burning car and from a nearby house. The house emissions and car emissions are as defined in sections 3.2.3 and 3.2.4. The calculations are for positions directly downwind of the car, with the house source laterally offset by 10 m from the car. The source of the car fire emissions is at a height of 1 m, so vertically offset from the house. The winds at the sources are significantly correlated, for a mean wind speed of 6 m $s^{-1}$ and wind fluctuation of order 0.25 m $s^{-1}$ with a length scale of turbulent winds of 50 m.

The results are shown in Figures 38-40. For this particular example we consider the main tracer from the house fire as CO, and the main tracer from the burning car as HCN.

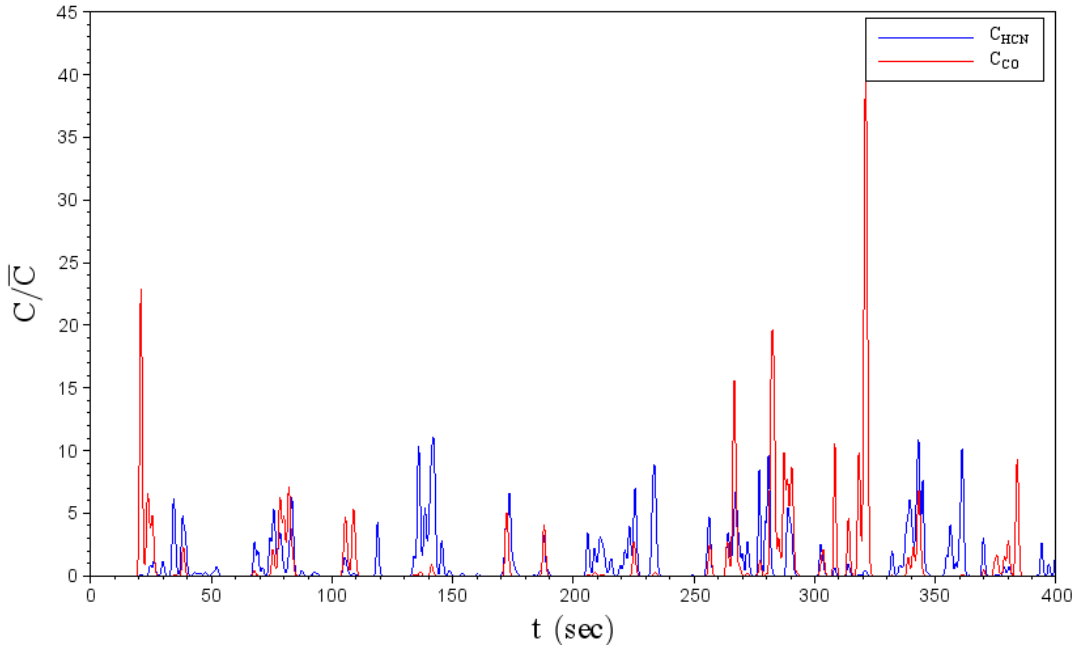


**Figure 39 Normalised Concentrations from two sources (burning house and car) at 100 m downwind.**

Figure 39 shows familiar spiky behaviour of intermittent concentrations in the contaminant plumes downwind. The red curve for the plume from the house-fire emissions has higher peak-to-mean excursions because the sample site is laterally offset by 10 m so the exposure is at the edge of the plume. The blue curve for the plume from the burning car is sampled closer to the plume centreline.

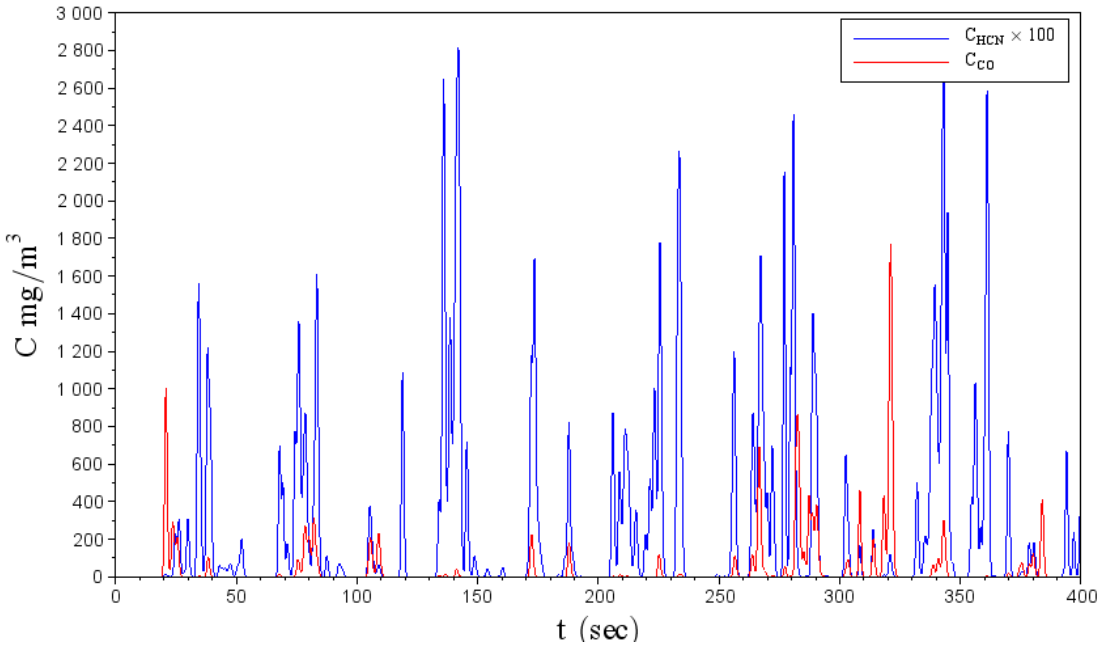


**Figure 40 Absolute concentrations from two sources (burning house and car).**

The absolute concentrations corresponding to Figure 39 are shown in Figure 40 for the specific emission rates estimated above for the two sources. At 100 m downwind both concentrations of CO and HCN exceed short-term exposure limits for tens of seconds at a time, sometimes at the same time at the sample point.

Thus this new tool gives the scope to assess the synergistic effects of simultaneous exposure to multiple chemical from multiple sources. Figure 40 shows that the exposure can occur in a mixed fashion:

1. Simultaneous peak exposure (example: at 265 seconds)
2. Independent exposure (example: house-plume peak at 20 seconds and car-plume peak at 35 seconds)

The frequency of independent exposures can be assessed with the cumulative distributions above, however the joint exposure requires the joint probability distribution which is not plotted.

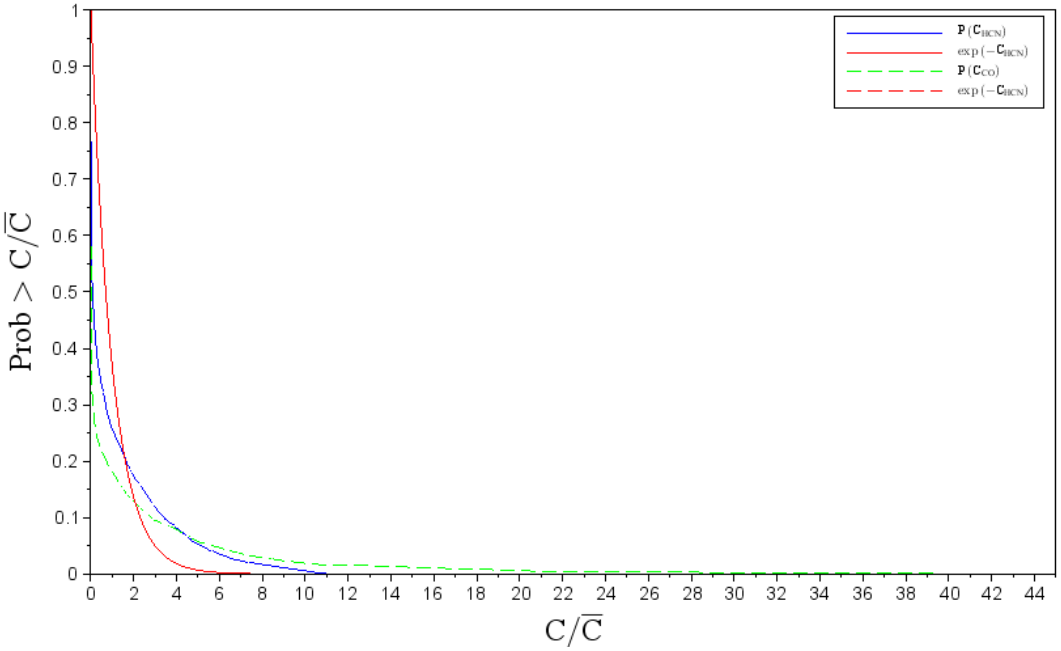


**Figure 41 Distributions of concentrations from two sources.**

The distributions are more highly intermittent than the exponential distribution with a heavy tail indicating large fluctuations of random concentrations. The distribution of the house plume fluctuations is more extreme because the sampling point sits at the edge of this plume, but is directly downwind of the car plume.

# 6 Exposure Assessment

Exposure assessment is the process of measuring or estimating the intensity, frequency and duration of human exposure to an agent present in the environment.

Exposures to air toxics in smoke are assessed against OES, presented as:

- peak or ceiling limits which should not be exceeded at any time,
- short-term exposure limits (STELs) (a 15-minute TWA exposure), or
- time-weighted average (TWA) exposure limits (average exposures over a normal 8-hour workshift).

Exposure standards are set to protect nearly all workers from adverse health effects or undue discomfort. They are not levels above which harm will definitely arise nor are they levels which are definitely safe. They are used to assess the quality of the work environment and indicate those areas where appropriate mitigation measures or control measures are required.

In this study, exposures were estimated using a new technique of dispersion modelling. The high time-resolution model provides short-term (in terms of seconds) modelled ground concentrations and thereby allows for assessment of peak exposure concentrations.

The most relevant standards include the STEL and the peak or ceiling limits. The estimated peak concentrations from the dispersion model are assessed against known peak limits presented in Table 5. For compounds that have no assigned STEL or peak limit, the following approach is taken. Maximum exposures should not exceed five times the TWA at any time and short-term exposures should not exceed three times the TWA for no more than 30 minutes in an 8-hour workshift.

The TWA depends on an 8-hour cumulative exposure, and while the modelled fire is programmed for just three hours, it is likely that multiple houses burn during an eight hour period so that the TWA will be a relevant assessment value.

**Table 5 Occupational exposure standards of major airborne contaminants present in smoke plumes**

| Substance | TWA (mg $m^{-3}$) | STEL (mg $m^{-3}$) | Peak limit (mg $m^{-3}$) |
|---|---|---|---|
| Carbon monoxide | 34.4 | 229 | 458 |
| Hydrogen cyanide | | | 11 |
| Hydrogen chloride | | | 7.5 |
| Nitrogen dioxide | 5.6 | 9.4 | |
| Benzene | 3.2 | | |
| Naphthalene | 52 | 79 | |
| Formaldehyde | 1.2 | 2.5 | 6 |
| Acrolein | 0.23 | 0.69 | |
| Particles | 3 | | |

A summary of the consequences of the dispersion calculations for the specific emissions for the typical house discussed above are collected in Table 6. The results simply use the mean concentrations (for the STEL limit) as described in equation (5), and estimate the peak concentrations from the top four in each time series to establish a peak maximum exposure (as described in section 4.1).

As a guide from the standards for CO, compounds that have a known STEL standard can infer a peak standard as twice the STEL value occurring at the fraction of 5% of the time or greater. These limits can be inferred from the cumulative probability density functions that produced from the simulated time series.

The variability of STEL exposures and allowable breaches depend on the variable meteorology, the finite duration of a particular house burn and the operation procedures. For example, it is possible to plan for exposure to a plume above a STEL limit, but below a peak limit, for an unprotected 15 minute 'mission' with an hour clean air recovery time. Four such missions can be undertaken in an eight-hour shift as an acceptable managed risk.

Unprotected exposure to plumes with concentrations above maximum peak limits have no known risk management strategy.

However, it can be noted that *fatal dose limits* for short term exposures can be many factors larger than the short maximum peak.

## 6.1 Downwind exposure to toxic smoke emissions from a typical burning house

A simple rural-urban environment has been modelled for a 3-hour slow-burn of a brick veneer house in winds ranging from 10 km $hr^{-1}$, 20 km $hr^{-1}$ and 30 km $hr^{-1}$ and conditions similar to the Canberra fires of 2003. The dispersion results are shown in Sections 4.2 to 4.5.

Table 6 displays the exposure estimates for key toxic chemicals released during the combustion of a typical house composed of a range of commonly used structural and/or furnishing materials. Both 15-minute averaged concentrations and peak concentrations recorded in that sample are shown, with bold figures showing dangerous peak values. The plumes are most hazardous closest to the burning house, but peak exposures can still be a risk far downwind. Risks appear to be lower still further than 150 m directly downwind from this burning house scenario at least for 15 minutes or less of exposure.

**Table 6 Modelled exposure estimates: 15-min averaged exposures (Avg) and maximum exposures (Peak). The STEL and peak limits are shown in brackets. Exceedances of OES are shown in red.**

| | Concentrations Downwind mg $m^{-3}$ | | | | | | | | |
|---|---|---|---|---|---|---|---|---|---|
| Distance Downwind (m) | 50 m | | | 100 m | | | 150 m | | |
| Wind speed (km $h^{-1}$) | 10 | 20 | 30 | 10 | 20 | 30 | 10 | 20 | 30 |
| Chemical | | | | | | | | | |
| $CO_{Avg}$ (229) | 655 | 464 | 475 | 179 | 125 | 126 | 87 | 60 | 60 |
| $CO_{Peak}$ (458) | 2620 | 1856 | 2850 | 465 | 338 | 504 | 174 | 132 | 180 |
| $HCl_{Avg}$ | 26.2 | 18.6 | 19 | 7.2 | 5.0 | 5.1 | 3.5 | 2.4 | 2.4 |
| $HCl_{Peak}$ (7.5) | 104.8 | 74.4 | 114 | 18.7 | 13.5 | 20.4 | 7.0 | 5.3 | 7.2 |
| $HCN_{Avg}$ | 37.4 | 26.5 | 27.2 | 10.3 | 7.2 | 7.2 | 5.0 | 3.4 | 3.4 |
| $HCN_{Peak}$ (11) | 149.6 | 106 | 163.2 | 26.8 | 19.4 | 28.8 | 10 | 7.5 | 10.2 |
| $PM_{Avg}$ (9[a]) | 318.2 | 87.3 | 42.4 | 225.5 | 61.0 | 29.2 | 231.1 | 61.6 | 29.1 |
| $PM_{Peak}$ (15[a]) | 1272.7 | 349.1 | 254.2 | 586.2 | 164.6 | 116.8 | 462.2 | 135.4 | 87.3 |
| $Benzene_{Avg}$ (9.6[a]) | 28.1 | 19.9 | 20.4 | 7.7 | 5.4 | 5.4 | 3.7 | 2.6 | 2.6 |

[a] As defined previously, STEL were taken as three-times the TWA and peak limits as five times the TWA.

The results indicate that for the scenario the plume within 50 m of the burning house is on average constantly exceeding the peak exposure limits and obviously in excess of STEL as well. There is no acceptable strategy for unprotected approach within the plume in that particular case.

Further downwind at 100 m, the average concentration is less than the thresholds for dangerous exposure, except for PM. For other chemicals at 100 m there are many peak concentrations exceeding allowable exposures, and the risk of exposure needs to be informed by a frequency estimate if, for example, considering a 15 minute exposure with a small number of allowable short term peak exceedances. The frequency can be estimated from the CDFs appropriate for each case.

Even at 150 m downwind, at least for higher wind speed so that material reaches the exposure point quickly, peak concentrations of HCl and HCN are close to their respective peak limits. The frequency is generally lower further downwind, so an informed strategy for unprotected operations this close downwind of a source could be considered.

Finally, other species like benzene are shown to exceed STEL limits, although species like this are less of a concern for acute affects like asphyxiation of being overcome by fumes, but net accumulation over longer times are important. The scenarios considered in this example, however, suggest limited allowable time for operations in the downwind zone in the plumes described, primarily because of risks to exposure to acutely toxic fumes. Protection from exposure to the acute toxic gases also confers protection from the other species (like benzene) that generally require longer exposure times for health effect responses.

## 6.2 Exposure risk assessment

For exposures to individual air toxics, there is unacceptable level of exposure risk if the hazard quotient, e.g. the ratio between the exposure concentration and the respective OES is greater than 1.

For the example shown above, hazardous exposures are primarily observed at close distance to the burning house (< 150 m). Further downwind, only particles are present at levels significantly exceeding exposure standards. This is consistent with studies looking at impacts from bushfire smoke that have confirmed that particles are consistently exceeding air quality guidelines during bushfire events (Reisen and Brown, 2006). Elevated levels of fine particles in the air can trigger acute health effects such as difficulty breathing, coughing, respiratory and eye irritation and exacerbate any cardiac and respiratory illnesses.

The calculated hazard quotients for HCl and HCN at 50 m from the burning structure range from 10 to 15, while CO peak concentrations lead to hazard quotients of approximately 5. Highest hazard quotients were calculated for PM concentrations ranging from 30 up to 80. These high hazard quotients are observed at lower wind speeds of 10 km $hr^{-1}$ at varying distances from the burning structure.

Furthermore, in a smoke plume, a number of air pollutants are present in varying concentrations. Some of these compounds may have additive health effects as they target the same organ. To assess potential health impacts for a mixture of pollutants targeting the same organ, e.g. irritation to eyes or respiratory tract, hazard indices are used.

The air pollutants will be grouped by primary target organs for acute health effects, e.g. eye irritation, respiratory effects, effects on the central nervous system and asphyxia. Examples for a range of air pollutants present in smoke are shown in Table 7.

A hazard index is the sum of hazard quotients of all air toxics with similar effects that a person is exposed to. Depending on whether short-term exposures (over a 15-minute period) or peak limits are assessed, either STELs or peak exposure limits are used as OES. Any hazard index exceeding unity represents an unacceptable level of exposure risk. Synergistic effects where one chemical enhances the toxicity of another chemical are much more difficult to assess.

In the case displayed above, we observed relatively few exceedances at 150 m downwind from the burning house. Individually the toxic compounds are within exposure limits. However both CO and HCN are asphyxiants and their additive effects need to be taken into account.

For the case displayed in Table 6, the hazard index for simultaneous exposure to CO and HCN equals 1.3 for windspeeds of 10km $hr^{-1}$ and 30 km $hr^{-1}$, thereby exceeding the safe exposure limit. Even though individually both compounds are within peak limits, they are likely to present a health hazard due to their additive effect.

Similarly HCl and HCN are respiratory irritants. The hazard index for HCl and HCN exceeds unity at 150 m downwind for windspeeds of 10 and 30 km $hr^{-1}$, even though individually peak limits were not exceeded.

The assessment of exposure risk enables to highlight air toxics that contribute predominantly to the hazard indices. Some compounds may be present at low concentrations, but due to their high toxicity, are likely to present a greater health risk. Similarly some compounds may be present at higher concentrations but due to their low toxicity present a lower health risk. Additionally, even though exposures to individual air toxics are within OES, exposures to a mixture of those air toxics may present an unacceptable level of exposure risk.

### Table 7 Compounds grouped by primary target organs for acute health effects and cancer

| COMPOUND | EYE IRRITATION | RESPIRATORY TRACT IRRITATION[1] | CENTRAL NERVOUS SYSTEM | ASPHYXIA | CARCINOGEN[2] |
|---|---|---|---|---|---|
| Carbon monoxide (CO) | | | x | x | |
| Hydrogen cyanide (HCN) | | x | | x | |
| Hydrogen chloride (HCl) | x | x | | | |
| Ammonia | x | x | | | |
| Nitric oxide (NO) | | x | | x | |
| Nitrogen dioxide ($NO_2$) | x | x[3] | | | |
| Sulphur dioxide ($SO_2$) | x | x | | | |
| Hydrogen sulphide ($H_2S$) | x | x | x | | |
| Alkanes | x | x | x | | |
| Benzene | | | | | Group 1 |
| Toluene | x | x | x | | |
| Ethylbenzene | x | x | x | | Group 2B |
| Xylene | x | x | x | | |
| Trimethylbenzene | x | x[3] | x | | |
| Styrene | x | x[3] | x | | Group 2B |
| Indene | x | x | | | |
| 1,3-Butadiene | | | | | Group 1 |
| Formaldehyde | x | x[3] | | | Group 1 |
| Acetaldehyde | x | x | | | Group 2B |
| Acrolein | x | x[3] | | | Group 3 |
| Crotonaldehyde | x | x[3] | | | Group 3 |
| Acetic acid | x | x | | | |
| Furfural | x | x | | | Group 3 |
| Phenol | x | x[3] | x | | |
| Cresol | x | x | | | |
| Naphthalene | x | | | | Group 2B |
| Benzo(a)pyrene | | | | | Group 1 |
| Isocyanates | | x[3] | | | Group 2B |
| Particles | x | x | | | Group 1 |

[1] Refers to the upper respiratory tract

[2] Classification according to the International Agency for Research on Cancer (IARC): Group1 Carcinogenic to humans, Group 2B Possibly carcinogenic to humans, Group 3 Not classifiable as to its carcinogenicity to humans

[3] Also lower respiratory tract irritation

# 7 Health Risks

Health effects can be acute or chronic. Acute or short-term health effects are real and immediate. For long-term health effects it is more difficult to prove a linkage between exposure and health outcomes. Many of the pollutants in smoke are linked to adverse acute or chronic health effects, including asphyxia, eye, nose, throat, lung or skin irritation, shortness of breath, exacerbation of existing respiratory or cardiovascular conditions, effects on the central nervous system and cancer (Alarie 2002).

The risk of an adverse effect on health is proportional to, $hazard \times exposure$ i.e. the more hazardous a substance (e.g. the lower the OES), the higher the risk. Likewise, for a given hazard the greater the exposure, the greater the health risk.

## 7.1 Acute health effects

### 7.1.1 ASPHYXIA

Asphyxia occurs when not enough oxygen is supplied to the tissues and organs in the body and under severe conditions can cause coma or death.

CO and HCN are both asphyxiants. They affect oxygen transport, availability and utilisation to tissues in the body. CO and HCN toxicity mainly targets organs with a high demand for oxygen, particularly the brain and heart (Piantadosi 1997). HCN is more dangerous than CO (Simeonova and Fishbein 2004).

Some of the symptoms include decreased exercise and work capacity, decreased vigilance, increased reaction time, and impaired ability to perform tasks. At higher concentrations it can lead to severe headaches, nausea, mental confusion and unconsciousness (WHO 1999).

CO can also increase the respiratory intake of other gases in the smoke by stimulating the respiratory centre in the brain.

### 7.1.2 IRRITATION AND IMPACTS ON RESPIRATORY TRACT

A wide range of gaseous compounds and particles can cause irritation of eyes, nose, throat and respiratory system and potentially lead to breathing difficulty and exacerbation of pre-existing respiratory conditions (Shusterman 2003; Miller 2013).

Particles produced from fires are primarily carbonaceous and smaller than 2.5 microns. The particles can easily reach the alveolar region of the lungs, where clearance is slow and the potential for adverse health effects is high. Fine particles increase airway resistance, cause irritation, coughing and difficulty breathing and aggravate asthma (Pope and Dockery 2006; Naeher et al. 2007). Acute exposures to high particle levels can trigger asthma attacks and may increase susceptibility to respiratory infections.

Other gases such as ammonia and HCl can cause intense and prolonged inflammatory reactions. Nitrogen dioxide is a highly acid irritant that can cause fluid accumulation and may cause respiratory failure. Sulphur dioxide is highly irritating to the eyes and respiratory tract (Shusterman 2003; Bessac and Jordt 2010; Miller 2013).

Isocyanates are powerful irritants to the mucous membranes of the eyes, gastrointestinal and respiratory tracts and can aggravate respiratory conditions, trigger severe asthma attacks in susceptible people, and cause shortness of breath, wheezing and chest tightness (Miller 2013).

A number of VOCs, including aliphatic and aromatic hydrocarbons, aldehydes, ketones and acids, are respiratory irritants that reduce cilia activity. This reduces the efficient removal of particles and microorganisms from the respiratory tract.

It is also suggested that inhalation of PAHs can cause airway inflammation.

### 7.1.3 IMPACTS ON CARDIOVASCULAR SYSTEM

Particles, CO and nitrogen dioxide can aggravate pre-existing heart conditions.

CO when inhaled competes with oxygen for binding sites on haemoglobin in the blood. It thereby reduces the oxygen carrying capacity of the blood. To compensate for the reduced oxygen delivery, the heart works harder and beats more frequently. Therefore people with underlying heart disease are at greater risk for CO ill effects (World Health Organization (WHO) 1999; Townsend and Maynard 2002).

Short-term exposures to elevated levels of fine particles can cause heart attacks and arrhythmias in people with heart disease.

### 7.1.4 IMPACTS ON CENTRAL NERVOUS SYSTEM

Most common symptoms include headaches, nausea, dizziness, fatigue, confusion and loss of coordination or judgement. Some of the compounds present in smoke that affect the central nervous system include CO, ethylbenzene, toluene, styrene, xylenes, alkanes, phenol and hydrogen sulphide. In general the symptoms disappear once exposure stops.

## 7.2 Carcinogens

Compounds emitted from fires that are carcinogenic to humans include benzene, formaldehyde and benzo(a)pyrene. Benzene has been linked to leukemia (IARC 1987); formaldehyde has been classified as a known human nasal carcinogen (National Industrial Chemicals Notification and Assessment Scheme 1996; IARC 2004). Recently, the International Agency for Research on Cancer (IARC) has also classified PM and outdoor air pollution as carcinogenic to humans (IARC 2013).

Other compounds such as acetaldehyde, ethylbenzene, naphthalene, styrene and isocyanates are possibly carcinogenic to humans.

## 7.3 Impact on health and protection measures

At close proximity to burning structures, exposures to CO and HCN can reach hazardous levels and cause a significant health risk. The only way to protect against the adverse health effects from exposures to high levels of CO and HCN is to wear self contained breathing apparatus (SCBA).

The exposure data also clearly shows that irritation to eyes and respiratory tract is a common health risk, with particle levels being particularly elevated. Protection can be achieved by wearing goggles and appropriate respiratory protection.

The elevated levels of PM estimated in downwind smoke plumes may present a potential health risk for people with pre-existing heart conditions and elderly people. The best protection would be to avoid smoke exposure.

A number of toxic chemicals emitted from burning structures can have an impact on the central nervous system (Table 7). Due to their additive effects, this can pose a significant health risk. Exposure to elevated concentrations of these chemicals can lead to fatigue, dizziness and impaired vigilance, and therefore can have significant impacts on the safety of firefighters, emergency crews and residents trying to defend their property.

# 8 Ambient Air Sampling During Experimental Room Burns

Ambient air sampling was conducted during a training exercise at the CFA Training Centre in Fiskville on 23 May 2013. The aim was to study the concentrations of a range of toxic air pollutants in smoke plumes from simulated room burns.

## 8.1 Methodology

The building where the training fires were conducted consisted of three separate rooms. Each room was set up with a range of furniture to simulate a living-room, a kid's bedroom and an office. The rooms were burnt sequentially.

The smoke plume emerging from the room fires was monitored downwind using two portable sampling boxes. Box A was initially installed in front of the building. Box B was installed on the ground directly behind the building. However, due to low smoke exposure, for the remaining two burns, Box A was moved to the rear approximately 15 m from the building. Figure 42 shows the layout of the experimental room burns.

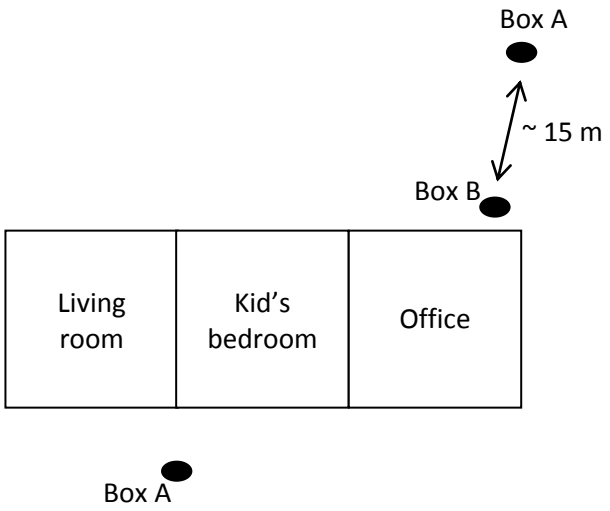


**Figure 42 Schematic layout of the experimental room burns.**

The sampling boxes contained a range of air monitoring equipment including (Figure 43):

- Q-Trak 8554 (TSI Inc., USA), an electronic data-logging device for continuous measurements of CO, carbon dioxide ($CO_2$), temperature and relative humidity. The Q-Trak was calibrated using a zero air calibration gas, a 100 ppm CO calibration gas and a 1000 ppm $CO_2$ calibration gas.
- an active sampling, data-logging, light-scattering real-time particle monitor Dust-Trak 8520 (TSI Inc., USA), operated with a $PM_{2.5}$ impactor for continuous measurements of fine particles.
- MicroVol-1100 (Ecotech Pty, Ltd, Knowfield, Australia) for collecting $PM_{2.5}$ on pre-weighed 47 mm fluoropore filters (Millipore, FALP04700, 1 μm pore size) and subsequent measurement of particle mass.

- 32 mm quartz filter followed by a pre-cleaned polyurethane foam (PUF) plug (ORBO1000 22 mm x 76 mm, Supelco) mounted in a pyrex glass holder directly behind the filter for measurements of PAHs.
- 2,4- dinitrophenylhydrazine (DNPH) impregnated cartridge (LpDNPH, Sigma-Aldrich) attached to an air sampling pump for collection and later analysis of carbonyls .
- PAS-500 Micro Air Sampler (Spectrex, USA) pump, fitted with a tube holder for Markes Tenax sorbent tubes for measurements of VOCs.


**Figure 43 Air sampling monitoring box**

## 8.2 Results

Sampling was conducted at the start of each burn until the burn was put out. For the office burn the sampling was started a few minutes after the burn was lit. The living room and kid's bedroom burns lasted on average 12-13 min. The office burn was slightly longer, with a sampling period of 20 min.

### 8.2.1 AMBIENT AIR SAMPLING

The results from the ambient air sampling are shown in Table 8.

Measured CO concentrations were within OES. The maximum CO concentration of 102 mg $m^{-3}$ was below the ceiling limit of 458 mg $m^{-3}$. Also, the average CO concentrations did not exceed the STEL of 229 mg $m^{-3}$. The highest average CO concentration was measured at 8.7 mg $m^{-3}$.

$PM_{2.5}$ concentrations were also below the proposed exposure standard of 3 mg $m^{-3}$, with highest average concentrations measured at 2.4 mg $m^{-3}$.

Similarly none of the measured carbonyls and VOCs exceeded OES.

**Table 8 Measured concentrations of a range of air toxics in plumes downwind from experimental room burns**

| Room | Living room | Living room | Kid's bedroom | Kid's bedroom | Office | Office | OES (mg/m$^3$) (TWA/STEL) | AQ standard (mg m$^{-3}$) |
|---|---|---|---|---|---|---|---|---|
| Box | A | B | A | B | A | B | | |
| Start time | 11:13 | 11:13 | 11:43 | 11:41 | 12:04 | 12:02 | | |
| End Time | 11:25 | 11:26 | 11:56 | 11:55 | 12:29 | 12:24 | | |
| CO ave (mg m$^{-3}$) | 0.16 | 8.66 | 4.21 | 1.94 | 1.23 | 3.84 | 34/229 | 10 (8-hr) |
| CO max (mg m$^{-3}$) | 1.60 | 87.0 | 33.0 | 12.6 | 33.9 | 101.9 | 458 | |
| $CO_2$ ave (mg m$^{-3}$) | 689 | 669 | 827 | 567 | 783 | 585 | | |
| $CO_2$ max (mg m$^{-3}$) | 858 | 1450 | 1010 | 878 | 999 | 1294 | | |
| $PM_{2.5}$ (mg m$^{-3}$) | 1.01 | 2.37 | 2.12 | 1.20 | 1.06 | 1.38 | 3 | 0.025 (24-hr) |
| Carbonyls (mg m$^{-3}$) | | | | | | | | |
| Formaldehyde | 0.006 | 0.078 | 0.054 | 0.022 | 0.035 | 0.062 | 1.2/2.5 | 0.1 (1-hr) |
| Acetaldehyde | 0.009 | 0.094 | 0.077 | 0.033 | 0.031 | 0.056 | 36/91 | |
| Acrolein | <MDL | 0.005 | 0.006 | 0.003 | 0.002 | 0.003 | 0.23/0.69 | |
| Acetone | <MDL | 0.030 | 0.023 | 0.010 | 0.010 | 0.017 | 1185/2375 | |
| Propionaldehyde | <MDL | 0.016 | 0.012 | 0.005 | 0.006 | 0.009 | | |
| Crotonaldehyde | <MDL | <MDL | 0.005 | 0.002 | 0.001 | 0.002 | 5.7 | |
| Methacrolein | <MDL | 0.007 | 0.006 | 0.003 | 0.002 | 0.005 | | |
| Methyl ethyl ketone | <MDL | 0.003 | <MDL | <MDL | <MDL | <MDL | 445/890 | |
| Butyraldehyde | 0.012 | 0.007 | 0.005 | 0.002 | 0.001 | 0.003 | | |
| Benzaldehyde | 0.001 | 0.006 | 0.007 | 0.004 | 0.002 | 0.003 | | |
| Glyoxal | <MDL | 0.021 | 0.034 | 0.028 | 0.024 | 0.038 | | |
| Valeraldehyde | <MDL | <MDL | <MDL | <MDL | <MDL | <MDL | 176 | |
| m-Tolualdehyde | <MDL | <MDL | <MDL | <MDL | <MDL | 0.001 | | |
| Methyl glyoxal | 0.004 | 0.048 | 0.065 | 0.050 | 0.038 | 0.055 | | |
| Hexaldehyde | <MDL | 0.001 | 0.001 | <MDL | <MDL | 0.0005 | | |
| VOCs (mg m$^{-3}$) | | | | | | | | |
| Benzene | 0.011 | 0.411 | 0.154 | 0.080 | 0.006 | 0.003 | 3.2 | 0.01 (annual) |
| Toluene | 0.005 | 0.058 | 0.029 | 0.014 | 0.006 | 0.001 | 191/574 | 15 (6-hours) |
| Ethylbenzene | 0.001 | 0.007 | 0.004 | 0.002 | 0.001 | 0.0001 | 434/543 | |
| Xylene | 0.001 | 0.006 | 0.004 | 0.002 | 0.002 | 0.0003 | 350/655 | 4.3 (30min) |
| Styrene | 0.007 | 0.066 | 0.027 | 0.015 | 0.003 | 0.0004 | 213/426 | |
| Indene | ND | 0.010 | 0.004 | 0.001 | ND | 0.0001 | 48 | |
| Naphthalene | 0.002 | 0.066 | 0.025 | 0.009 | 0.002 | 0.0006 | 52/79 | |
| Phenol | 0.049 | 0.526 | 0.309 | 0.115 | 0.055 | 0.020 | 4 | |

The time series of ambient CO, $CO_2$ and $PM_{2.5}$ concentrations are shown in Figure 44. The variability in concentrations was strongly influenced by the turbulent winds rather than the actual emissions. A major difference in CO and $PM_{2.5}$ concentrations was observed for the living room burn during which Box A was positioned in the front of the room and Box B towards the back of the room. The smoke plume was drifting over the building and impacted Box B, whereas smoke exposure to Box A was minimal.

During the burn of the kid's bedroom, CO and $PM_{2.5}$ concentrations were higher downwind (Box A), whereas higher CO and $PM_{2.5}$ concentrations were measured closer to the building during the office burn (Box B). This highlights that smoke dispersion can be very complex around buildings and can have a major effect on exposures to toxic gases and particles.

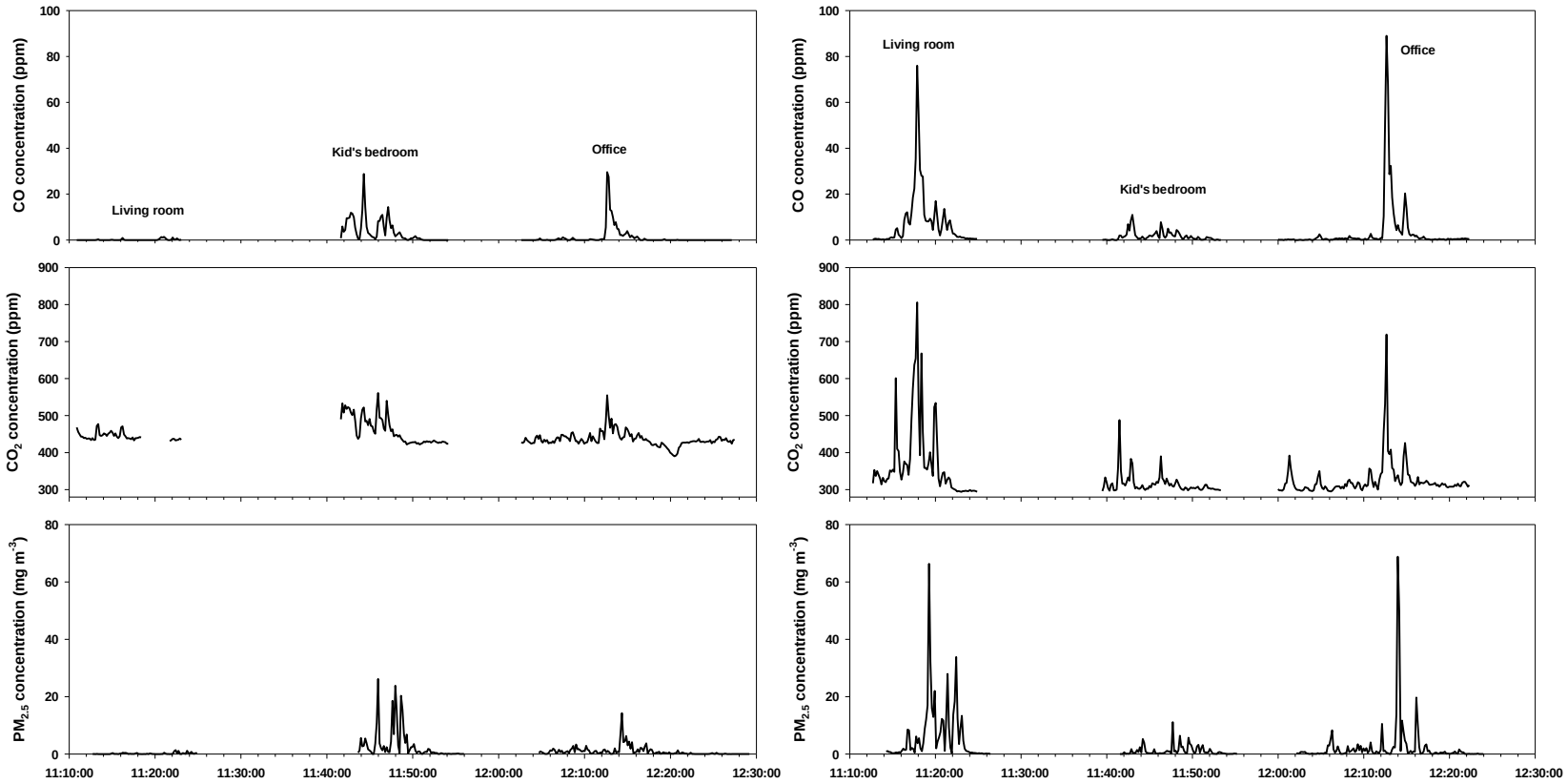


**Figure 44 Time series measurements of CO, $CO_2$ and $PM_{2.5}$ (non-corrected) sampled with Box A (left panels) and Box B (right panels)**

The highest contributions to ambient concentrations of carbonyls were attributed to formaldehyde and acetaldehyde, known and possible human carcinogens as well as glyoxal and methyl glyoxal. Benzene and toluene were significant contributors to VOC concentrations (Figure 45).

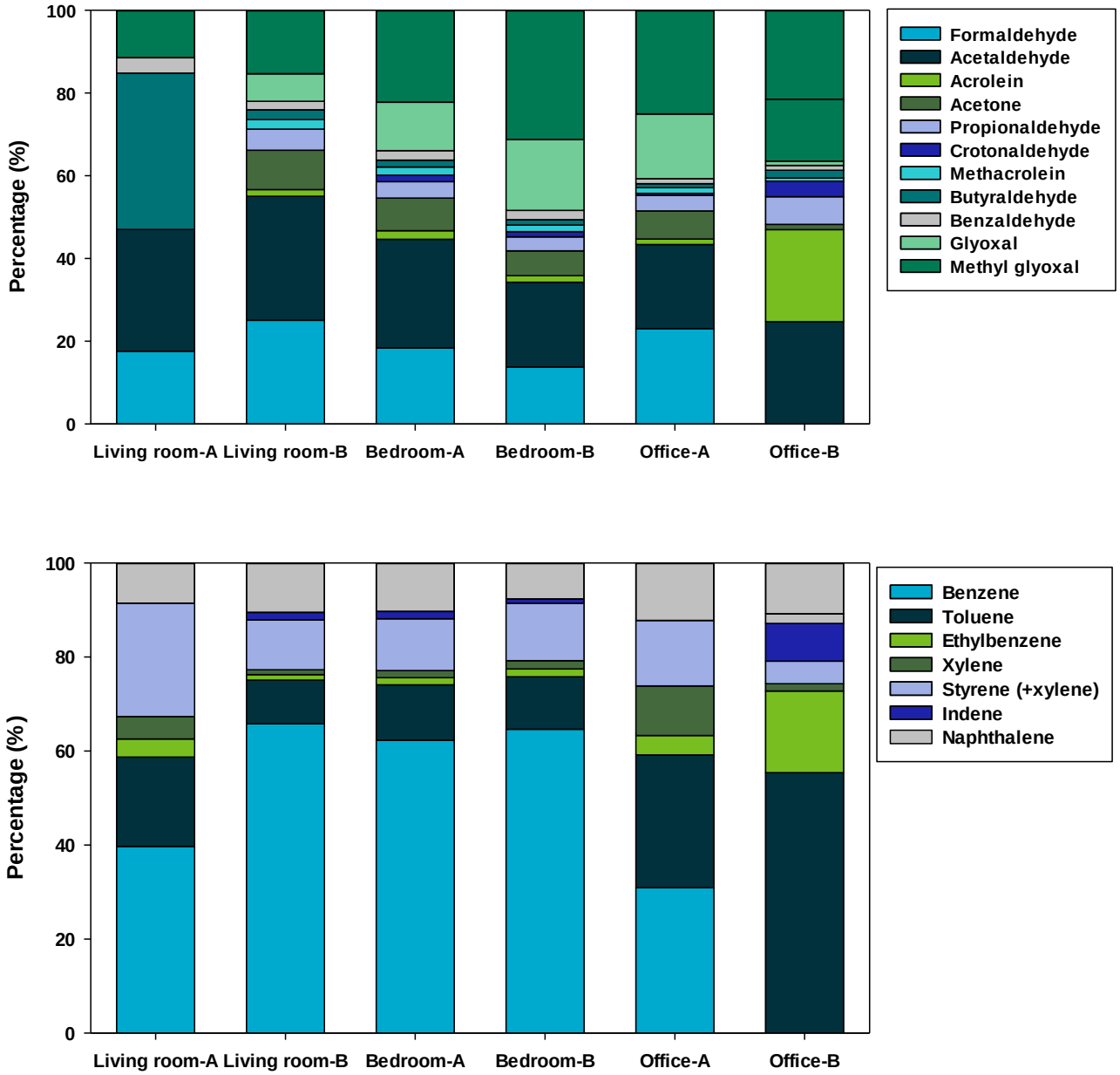


**Figure 45 Percent distribution of carbonyl compounds and selected VOCs**

Major VOCs can be identified from the GC chromatograms in Figure 46. For all three burns, similar peaks were observed and these included benzene, toluene, ethylbenzene, xylenes, styrene, naphthalene, benzoic acid, benzonitrile, α-methylstyrene, acetic acid, α -pinene, β-pinene, acetophenone and phenylethyne. While some of these VOCs have also been observed in bushfire smoke, others such as styrene, α -methylstyrene and benzonitrile are specific to burning structural and/or furnishing materials. Styrene has been primarily observed in emissions from burning wool/nylon carpet, polyester and polystyrene (Reisen and Borgas 2012), the latter being a dominant polymer in electronic appliances.

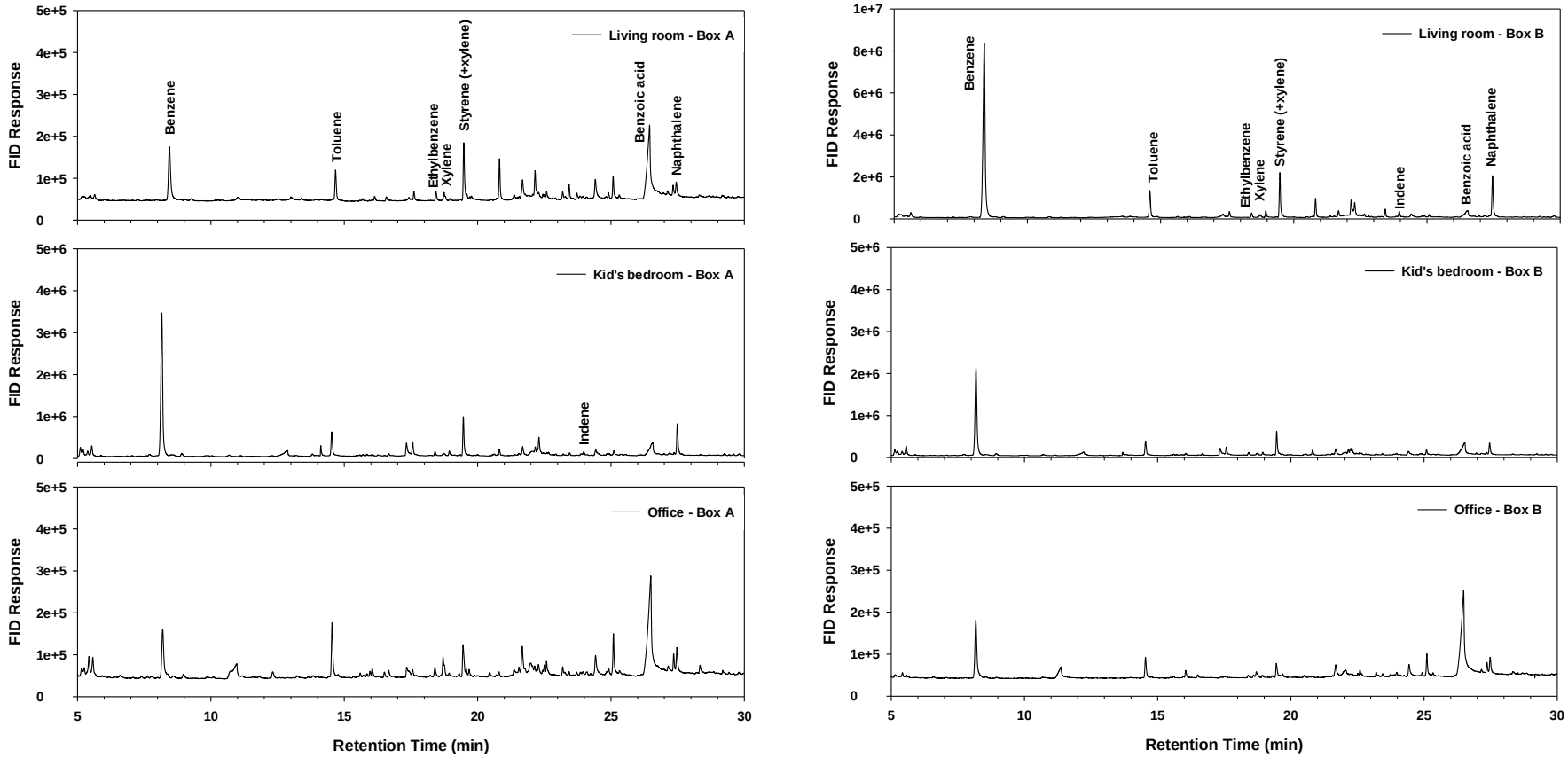


**Figure 46 FID chromatograms of VOC measurements during experimental room burns**

The results from the modelled scenario have highlighted some high concentrations in plumes 50-150 m downwind. These high levels could not be replicated during the experimental room burns.

The difference is that the room burns were individual rooms with only contents burning, and no structural materials being burnt. A typical room might have a combustible mass loading of approximately 1000 kg, whereas a house is likely to have a combustible mass loading of approximately 18000 kg.

Also the modelling captures the densest part of the smoke plume, whereas it was more difficult to capture the smoke using monitoring equipment located at ground level.

## 8.3 Inverse modelling

During room-contents burning tests in concrete buildings time-series measurements were made of particles, CO and $CO_2$. Runs of 14-20 minutes duration were typical and instruments were downwind but very close to the smoke outlets. Some sample measurements are shown in Figure 47 and Figure 49.

The winds during the measurements were largely unknown, but modest and the building structure complicates the dispersion description, however simply using the dispersion models with U=2 m $s^{-1}$, L=20 m, sig=0.5 m $s^{-1}$, x=20 m, y=10 m,Hs=3 m, (mean wind, wind correlation length scale, wind speed fluctuations, downwind displacement, lateral displacement and vertical height of the source), i.e. significant vertical and lateral offsets, light winds and large turbulence and length scale representative of the infrastructure givens a rough mimic of the observations as shown below in Figure 48 and Figure 50.

The comparison of CDFs is effectively an inverse modelling technique where the fluctuation structure is used to infer model parameters of the environment (turbulence and wind speed and upwind displacement to the source). This ad hoc technique can be formalised in more rigorous ways (including a metric for testing the similarity of the measured and modelled CDF), but the effort would generally need better data sets to make estimations more robust with less uncertainty.

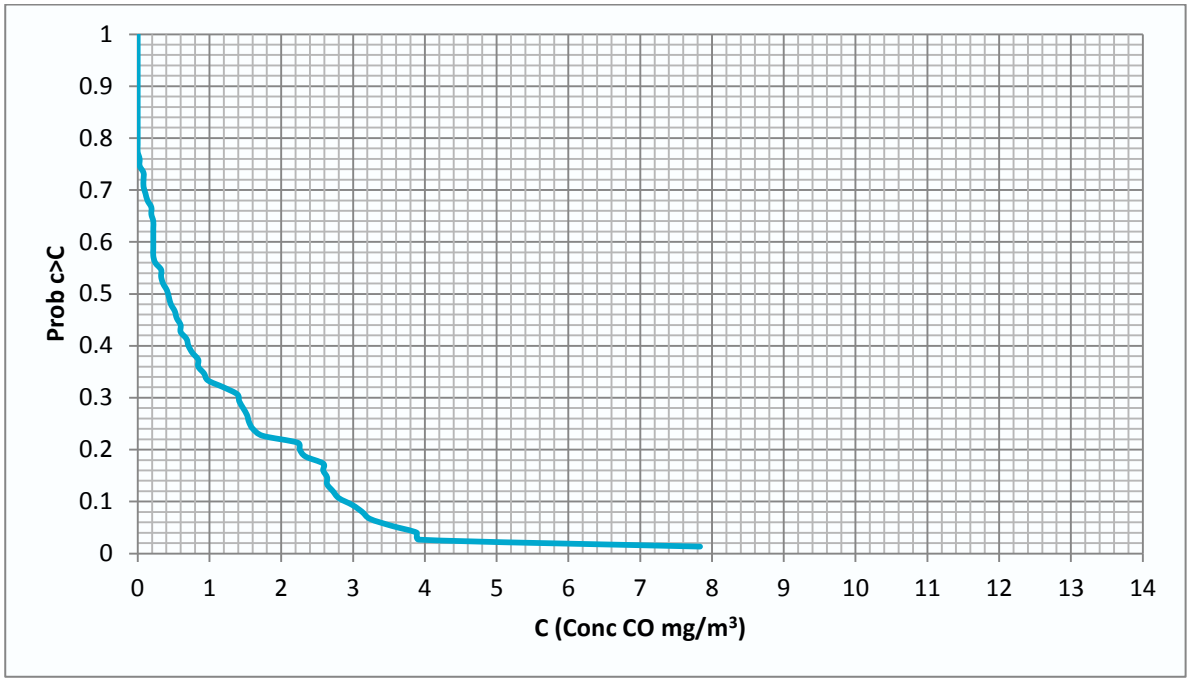


**Figure 47 CDF Observed Carbon Monoxide Concentration (x-axis CO mg $m^{-3}$, y axis Prob c>C)**

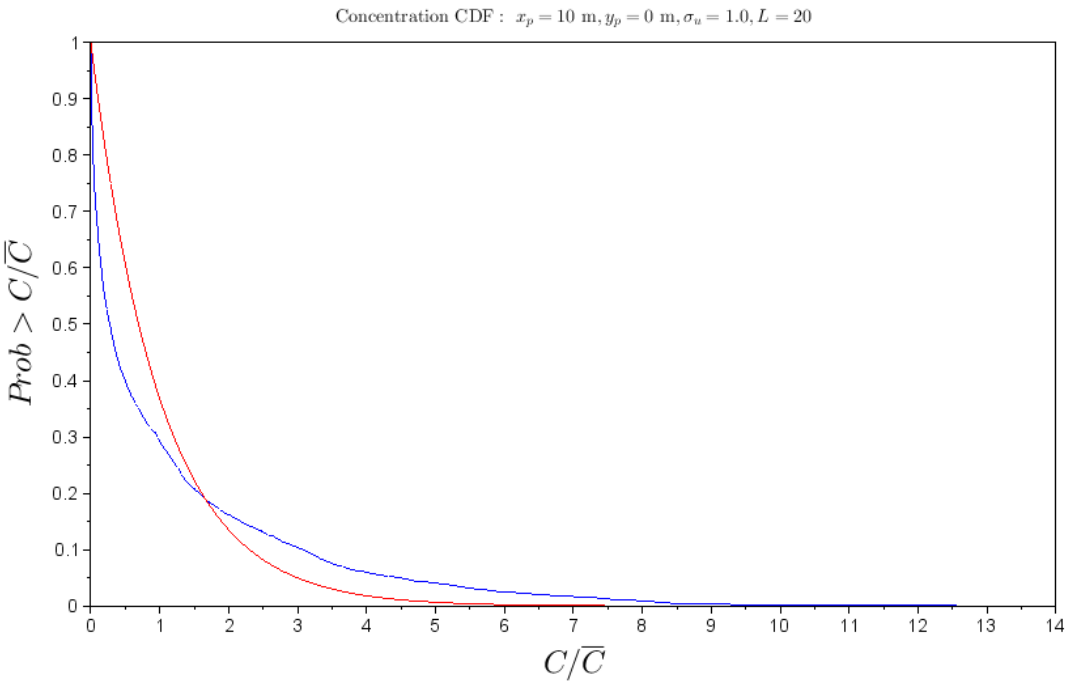


**Figure 48 Modelled CDF to mimic Fiskville observations**

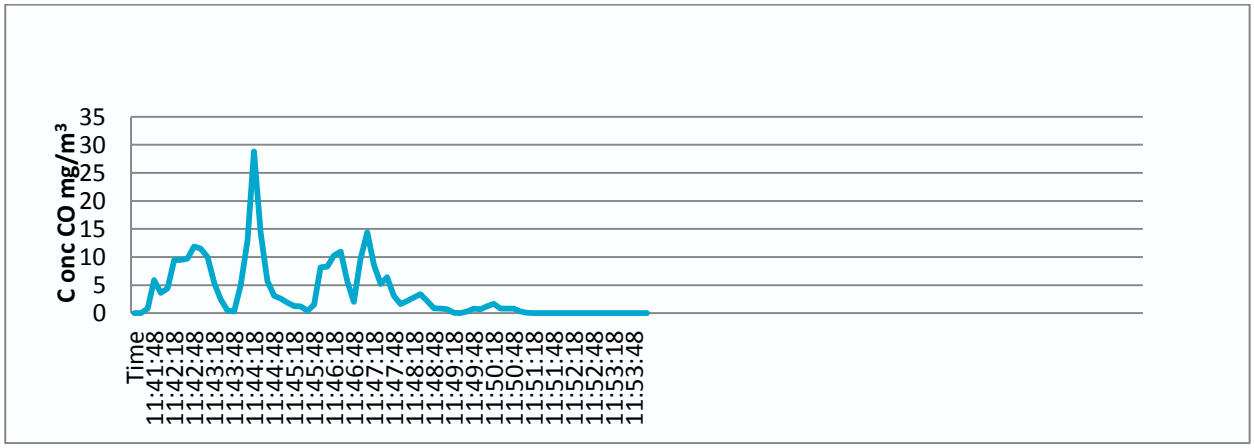


**Figure 49 Observed Carbon Monoxide Concentrations mg $m^{-3}$**

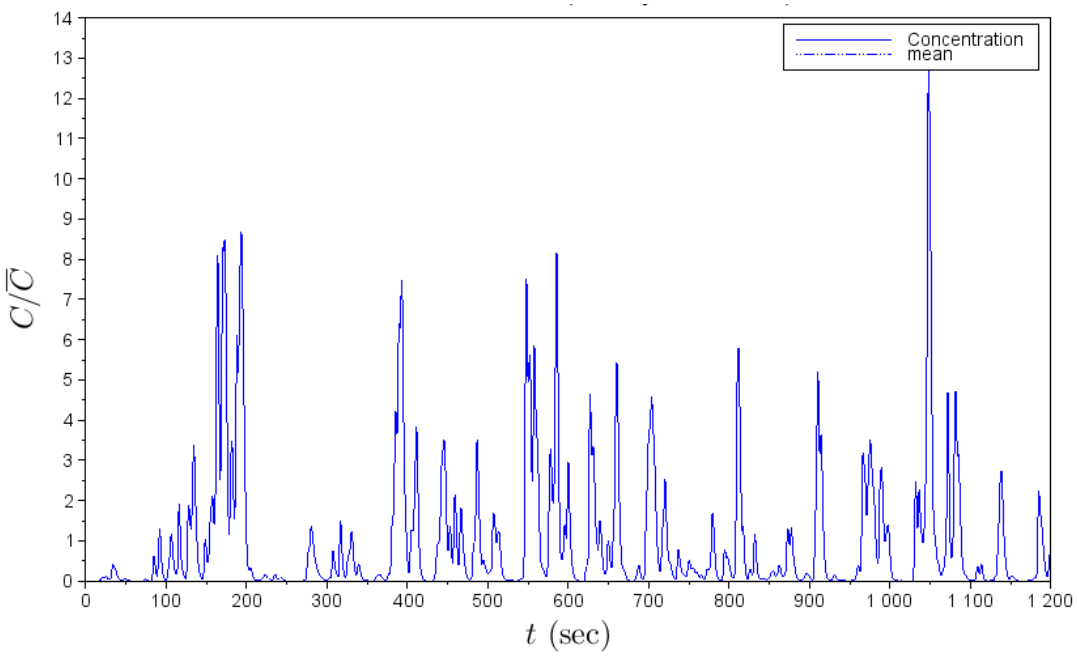


**Figure 50 Time series mimic of Fiskville observations**

This very brief and rough simulation is mostly suggestive. It indicates an inverse modelling technique where the input parameters of the flow are unknown and simply adjusted to get a better fit of the observed and simulated CDFs. The simulated time series is evidently more highly resolved than the measurements, but has some broad similarities with the observations beyond just the CDFs, mainly the overall patchiness and scale of the peaks.

Despite some caution in interpreting too much from this limited and non-ideal comparison, it nevertheless suggests potential for coupling such measurements with dispersion models for inverse modelling in the future.

# 9 Summary

Dispersion calculations are used to estimate exposure to toxic chemicals downwind of a typical burning house and in meteorological weather typical of bushfire conditions.

Emission estimates and a method of generating time series of concentrations allow us to examine short-term maximum exposures (conditions to always avoid) and 15-minute average conditions for STEL standards, which can be tolerated 4 times in an eight-hour shift with an hour recovery time between episodes. Knowledge of the dispersion, assuming knowledge of wind speed and direction, allows some operational plans for unprotected access to regions downwind of the house, either for fire fighting or search and rescue in exposed unburnt houses.

Models not considered here include multiple burning houses simultaneously, and multiple node complex fires internally within a single house. For the former, the present results can be used as independent plumes constructing a pattern of danger zones suburb by suburb.

More extensive calculation could impose more realistic node based fires, so that in any given 15-minute period we could have numerous spot fires distributed across the house. In different 15-minute blocks, a different set of nodes could operate, but the effect is mainly to distribute a plume across the house.

A very brief indicative study of observations of fire generated CO at a fire testing site is undertaken. The observations show highly variable fluctuations which can be mimicked with turbulent mixing with appropriate choices of positional offsets (vertical, lateral and downwind distance) and where the complexity of building wakes and uncertain flow is effectively lumped into random turbulent scaling. The cumulative distribution function sensitivity is roughly in agreement with the experimental scenario, suggesting that the method of matching distributions is a potentially useful technique for inferring fire states.

Finally, a case study of interacting plumes from multiple sources is considered: specifically a plume from burning plastics in a car and a plume from a nearby house offset by 10 m laterally and 2 m vertically. The time series shows points where large peak concentrations from both the car and house coincide at the sampling point, increasing the risk to exposure from toxic emissions in the burning rural-urban fringe.

# Appendix A Information sheet for house structure and household materials

**Combustible materials data sheet**

The RUI is characterised by a wide range of combustible materials from house structural and house furnishing components, outdoor furnishing components, vehicles, sheds and garages.

The type and amount of items in a house structure, house contents and surrounding outdoor environment can vary substantially. Below is a summary of data derived from available literature to provide estimates of the type and amount of combustible materials present at the RUI.

**Table 9 House structural components and estimated amount of combustible materials**

| Structure component | Combustible materials | Estimated amount (kg) |
|---|---|---|
| Foundation | Timber<br>PVC | 1,600<br>94 |
| Wall cladding | Weatherboard or plywood sheets<br>Plasterboard<br>Polystyrene, PVC | 2,650<br>4,500<br>2,000 |
| Frame | Timber | 11,000 |
| Insulation | Polyester, polystyrene, PUR, PIR | 300 |
| Flooring (130 $m^2$) | Wood, particle board, MDF<br>Carpet (wool, nylon) | 9,000<br>650 |
| Window frame | Wood or PVC | 140 |

Example for a brick single level home (amount of combustible materials):

- Timber frame 11,000 kg
- Polyester insulation 300 kg
- Particleboard flooring 4,500 kg
- Carpet flooring 300 kg

**Table 10 Estimated amount of materials in house contents**

| Major combustible material | Estimated amount (kg) |
|---|---|
| Wood | 1,520 |
| Wood-based products (particleboard, MDF) | 1,240 |
| Textile (wool, cotton, nylon, polyester) | 700 |
| Polystyrene | 325 |
| PUR foam | 190 |
| PVC | 245 |
| Polypropylene/polyethylene | 580 |
| Paper | 400 |

Items include furniture, appliances, electronic equipment and personal items and are based on a 3 bedroom house.

**Table 11 Composition and amount of combustible materials in items surrounding a house**

| Outdoor component | Combustible materials | Estimated amount (kg) |
|---|---|---|
| Fence | Timber<br>PVC | 350 |
| Decking | Timber | 350 |
| Patio set ( 5 piece) | Timber, PVC | 220 |
| Cushions | PUR foam | 6 |
| Water tank | Polyethylene | 140 |
| Garbage bin | Polyethylene | 50 |

Outside components include fences, decking, outdoor furniture, garbage bins, and water tanks. Similar to house contents the amount and type of these items can vary significantly.

# Appendix B Emissions data sheet

Emission yields are defined as the amount (in g) of toxic species emitted per amount (in kg) of material burnt. The emission yields are derived from small-scale laboratory fire tests conducted under well-controlled conditions.

**Table 12 Emission yields of key toxic chemicals released during the combustion of a range of commonly used structural and/or furnishing materials for flaming combustion**

| Toxic chemical | Emission yields in (g $kg^{-1}$) | | | | | | |
|---|---|---|---|---|---|---|---|
| | Wood | Wood-based products | PUR | Polyester | PE/PP | Polystyrene | PVC |
| CO | 7-9 | 4-48 | 11-40 | 20-40 | 10-30 | 10-50 | 20-200 |
| HCN | | <1 | 1.5-4.0 | ~1 | | | |
| HCl | | | | | | | 130-500 |
| Particles | 2-13 | 3.2-5.5 | 13-26 | 58 | 20-35 | 40-126 | 1 |
| Total hydrocarbons | | 10 | 2-5 | | 1-25 | | 5-10 |
| VOCs | | | | | | | 1 |
| PAHs | | | | | 10 | 4-12 | 0.5-8 |
| Benzene | 0.01-0.15 | 0.02-0.2 | 0.1-13 | 1.2-3.3 | | 1-10 | |
| Styrene | | | | 0.02-0.06 | | 19-24 | |
| Formaldehyde | 0.03-0.2 | 0.1-0.25 | 0.2-1.4 | 0.8-1.2 | | 0.4-1.5 | |
| Naphthalene | 0.03-0.1 | 0.003-0.1 | 0.02-0.4 | 0.04-0.16 | | 0.1-0.5 | |
| Isocyanates | 0.004-0.025 | 0.75 | 0.9-1.6 | | 0.003 | | |

**Table 13 Emission yields of key toxic chemicals released during the combustion of a range of commonly used structural and/or furnishing materials for smouldering combustion**

| Toxic chemical | Emission yields in (g $kg^{-1}$) | | | | | | |
|---|---|---|---|---|---|---|---|
| | Wood | Wood-based products | PUR | Nylon | PE/PP | Polystyrene | PVC |
| CO | 140 | 160 | 150 | 60-350 | 50-150 | 100-300 | 20-200 |
| HCN | | 4 | 9 | 4-70 | | | |
| HCl | | | | | | | 150-500 |
| Particles | | | | | 30 | 160 | 30 |
| THC | | 100 | | 18-300 | 30-600 | 90 | 10-45 |
| VOCs | | | | | 60-90 | | 25 |
| PAHs | | | | | 8-25 | 18-40 | 3-12 |
| Isocyanates | 0.005 | | | | | | |

# Appendix C Simple Plume Models

Simple plume models in complex winds are described in Borgas 2012, 2013.

The mathematical expression for the concentration of this plume at the sample point $(x, y, z)$

$$\langle C|H\rangle = \frac{Q}{(2\pi)^{3/2}} \int_{-\infty}^{t} \frac{1}{\sigma_x \sigma_y \sigma_z} \exp\left( -\tfrac{1}{2}\frac{(x - x_c(t'))^2}{\sigma_x^2(t')} - \tfrac{1}{2}\frac{(y - y_c(t'))^2}{\sigma_y^2(t')} - \tfrac{1}{2}\frac{(z - z_c(t'))^2}{\sigma_z^2(t')} \right) dt' \quad \text{(C1)}$$

where for example the downwind dispersion factors for a mean wind of $U$ are

$$x_c(t) = Ut + e^{-t/t_l}u', \quad \sigma_x^2 = 2\sigma_u^2 t_l^2 \left( t/t_l + e^{-t/t_l} - 1 - \tfrac{1}{2}\left(e^{-t/t_l} - 1\right)^2 \right) \quad \text{(C2)}$$

for the turbulence parameters of specific wind at the puff emission of $u'$ (say from figure 3), wind fluctuations $\sigma_u$ and a dispersion time scale of $t_l$, typically a few tens of seconds in the atmosphere. In fact the history in (1) is defined as $H = \{(u', v', w') | t' \in [0, T]\}$ for a long simulation in time $T$.

Because the winds at the source are so variable this puff plume model generates highly intermittent concentrations downwind. An example of complex winds is given in Figure 51.

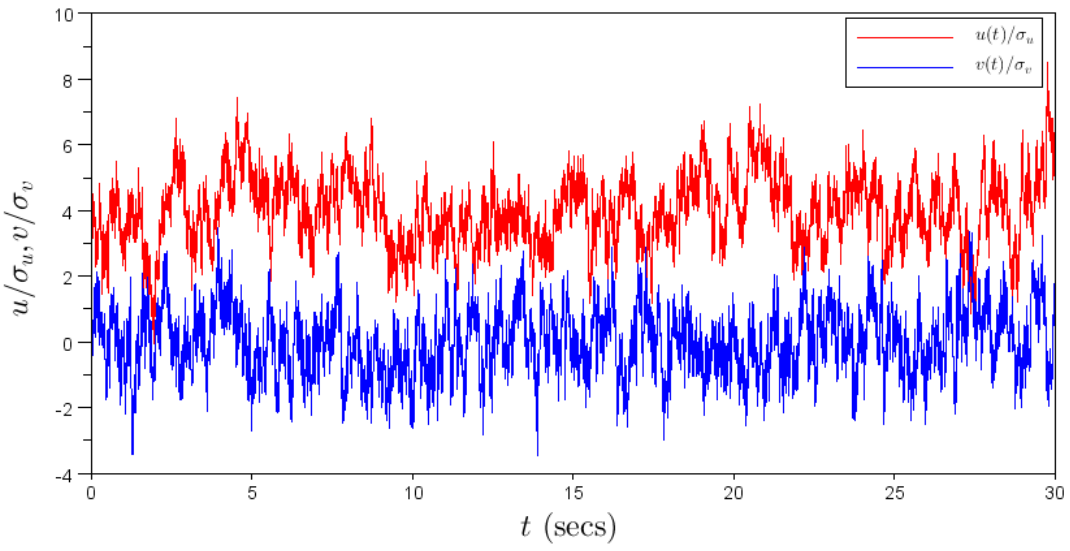


**Figure 51 Fluctuating winds in a turbulent flow**

## C.1 Plume Rise and Ground-Level Concentrations

To account for ground effects and possible buoyant plume rise of the plumes it is appropriate to consider the slight plume generalisation, while still in putting the source wind history (now imposed at an effective plume-rise height. The formula (by reflecting in the zero-flux surface $z=0$) is

$$\langle C|H\rangle = \frac{Q}{(2\pi)^{3/2}} \int_{-\infty}^{t} \frac{1}{\sigma_x \sigma_y \sigma_z} \left( \exp\left( -\tfrac{1}{2}\frac{(x-x_c(t'))^2}{\sigma_x^2(t')} - \tfrac{1}{2}\frac{(y-y_c(t'))^2}{\sigma_y^2(t')} - \tfrac{1}{2}\frac{(z-z_c(t'))^2}{\sigma_z^2(t')} \right) + \exp\left( -\tfrac{1}{2}\frac{(x-x_c(t'))^2}{\sigma_x^2(t')} - \tfrac{1}{2}\frac{(y-y_c(t'))^2}{\sigma_y^2(t')} - \tfrac{1}{2}\frac{(z+z_c(t'))^2}{\sigma_z^2(t')} \right) \right) dt' \quad \text{(C3)}$$

and with the plume rise $H$ imposed (as an empirical or observed input) in the puff centroid equation

$$z_c(t) = H + e^{-t/t_l} w', \quad \text{(C4)}$$

for each of the puffs sequentially released.

An example plume is illustrated in Figure 52.

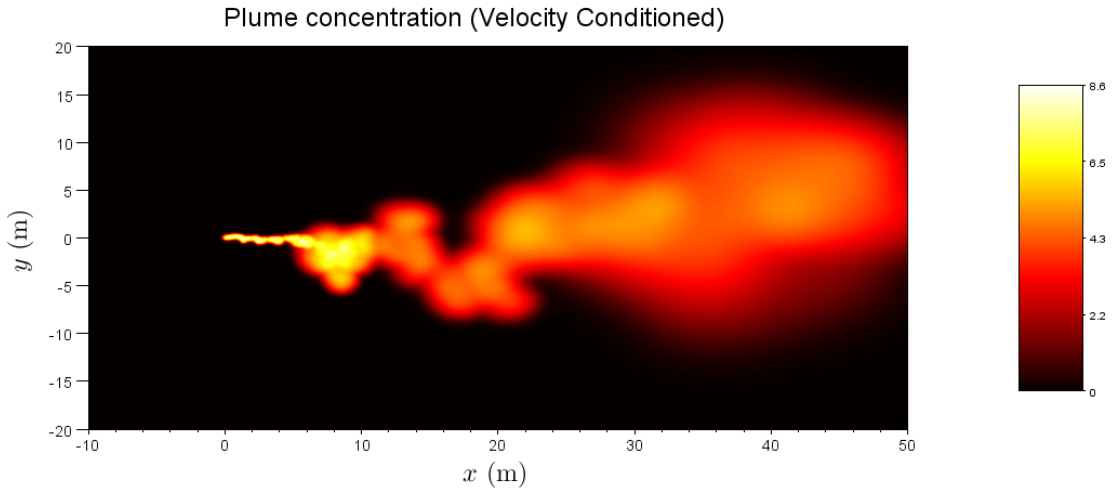


**Figure 52 Example computed plume (log concentration)**

# References


"Automobile". The World Book Encyclopedia (1996). Chicago: World Book

Alarie, Y. (2002). "Toxicity of fire smoke." Critical Reviews in Toxicology **32**(4): 259-289.

Austin, C. C., D. Wang, D. J. Ecobichon and G. Dussault (2001b). "Characterization of volatile organic compounds in smoke at municipal structural fires." Journal of Toxicology and Environmental Health-Part A **63**(6): 437-458.

Beringer, J. (2000). "Community fire safety at the urban/rural interface: The bushfire risk." Fire Safety Journal **35**(1): 1-23.

Bessac, B. F. and S.-E. Jordt (2010). "Sensory Detection and Responses to Toxic Gases: Mechanisms, Health Effects, and Countermeasures." Proceedings of the American Thoracic Society **7**(4): 269-277.

Blanchi, R., C. Lucas, J. Leonard and K. Finkele (2010). "Meteorological conditions and wildfire-related house loss in Australia." International Journal of Wildland Fire **19**(7): 914-926.

Bolstad-Johnson, D. M., J. L. Burgess, C. D. Crutchfield, S. Storment, R. Gerkin and Wilson, Jr. (2000). "Characterization of firefighter exposures during fire overhaul." Aihaj **61**(5): 636-641.

Borgas, M. S. (2012). Smoke and VOC Dispersion Integration in the burnt rural-urban interface., Report to Bushfire CRC.

Borgas, M. S. (2013). "Complex Diffusion by Continuous Movements." Submitted to Physics of Fluids.

Brandt-Rauf, P. W., L. F. J. Fallon, T. Tarantini, C. Idema and L. Andrews (1988). "Health hazards of fire fighters: exposure assessment." British Journal of Industrial Medicine **45**: 606-612.

DeBell, L. J., R. W. Talbot, J. E. Dibb, J. W. Munger, E. V. Fischer and S. E. Frolking (2004). "A major regional air pollution event in the northeastern United States caused by extensive forest fires in Quebec, Canada." Journal of Geophysical Research-Atmospheres **109**(D19): -.

Dutkiewicz, V. A., L. Husain, U. K. Roychowdhury and K. L. Demerjian (2011). "Impact of Canadian wildfire smoke on air quality at two rural sites in NY State." Atmospheric Environment **45**(12): 2028-2033.

Emmanuel, S. C. (2000). "Impact to lung health of haze from forest fires: the Singapore experience." Respirology **5**: 175-182.

Frankenberg, E., D. McKee and D. Thomas (2005). "Health consequences of forest fires in Indonesia." Demography **42**(1): 109-129.

Gill, A. M. and S. L. Stephens (2009). "Scientific and social challenges for the management of fire-prone wildland-urban interfaces." Environmental Research Letters **4**(3).

IARC (1987). Overall evaluations of carcinogenicity: an updating of IARC Monographs volumes 1 to 42. . IARC Monogr Eval Carcinog Risks Hum Suppl. **7:** 1-440.

IARC (2004). IARC classifies formaldehyde as carcinogenic to humans. Press Release N° 153. International Agency for Research on Cancer.

IARC (2013). IARC: Outdoor air pollution a leading environmental cause of cancer deaths. Press Release N° 221.

Jankovic, J., W. Jones, J. Burkhart and G. Noonan (1991). "Environmental study of firefighters." Annals of Occupational Hygiene **35**(6): 581-602.

Kunzli, N., E. Avol, J. Wu, W. J. Gauderman, E. Rappaport, J. Millstein, J. Bennion, R. McConnell, F. D. Gilliland, K. Berhane, F. Lurmann, A. Winer and J. M. Peters (2006). "Health effects of the 2003 Southern

California wildfires on children." American Journal of Respiratory and Critical Care Medicine **174**(11): 1221-1228.

Miller, S. N. (2013). Acute Toxicity of Respiratory Irritant Exposures. The Toxicant Induction of Irritant Asthma, Rhinitis, and Related Conditions. W. J. Meggs, Springer.

Naeher, L. P., M. Brauer, M. Lipsett, J. T. Zelikoff, C. D. Simpson, J. Q. Koenig and K. R. Smith (2007). "Woodsmoke health effects: A review." Inhalation Toxicology **19**(1): 67-106.

National Industrial Chemicals Notification and Assessment Scheme (1996). Formaldehyde, Priority Existing Chemical Assessment Report No. 28. Department of Health and Ageing.

Persson, B. and M. Simonson (1998). "Fire emissions into the atmosphere." Fire Technology **34**(3): 266-279.

Phuleria, H. C., P. M. Fine, Y. F. Zhu and C. Sioutas (2005). "Air quality impacts of the October 2003 Southern California wildfires." Journal of Geophysical Research-Atmospheres **110**(D7): -.

Piantadosi, C. A. (1997). Toxicity of carbon monoxide: hemoglobin vs. histotoxic mechanisms. Carbon monoxide. D. G. Penny. London, CRC Press**:** 163-186.

Pope, C. A. and D. W. Dockery (2006). "Health effects of fine particulate air pollution: Lines that connect." Journal of the Air & Waste Management Association **56**(6): 709-742.

Reisen, F. (2011). Toxic emissions from fires at the rural urban interface - Desktop study, Report to Bushfire CRC.

Reisen, F. (2011a). Inventory of major materials present in and around houses and their combustion emission products, Report to Bushfire CRC.

Reisen, F. and M. S. Borgas (2012). Exposures to toxic emissions from fires at the rural-urban interface, Report to bushfire CRC.

Reisen, F. and S. K. Brown (2009). "Australian firefighters' exposure to air toxics during bushfire burns of autumn 2005 and 2006." Environment International **35**(2): 342-352.

Reisen, F., D. Hansen and C. P. Meyer (2011). "Exposure to bushfire smoke during prescribed burns and wildfires: Firefighters' exposure risks and options." Environment International **37**(2): 314-321.

Reisen, F. and C. P. Meyer (2009). Smoke exposure management on the fire ground: a reference guide., East Melbourne, VIC: Bushfire CRC. 72p.

Robbins, A. P., I. C. Page and R. A. Jaques (2010). House Fire GHG Emissions Estimation Tool - A Preliminary Framework. BRANZ Study Report 217, BRANZ, Judgeford, New Zealand.

Shelter-in-Place Report (2011). Issued by the Metropolitan Fire and Emergency Services Board, Authorised by MFB, CFA, DH, OESC and ChemCentre 35.

Shusterman, D. (2003). "Toxicology of nasal irritants." Current Allergy and Asthma Reports **3**(3): 258-265.

Simeonova, F. P. and L. Fishbein (2004). Hydrogen cyanide and cyanides: Human health aspects. Concise International Chemical Assessment Document 61. World Health Organization. Geneva.

Simonson, M., H. Tuovinen and V. Emanuelsson (2000). Formation of Hydrogen Cyanide in Fires: A Literature and Experimental Investigation. BRANDFORSK Project 510-991, SP Swedish National Testing and Research Institute, SP Fire Technology.

Townsend, C. L. and R. L. Maynard (2002). "Effects on health of prolonged exposure to low concentrations of carbon monoxide." Occupational and Environmental Medicine **59**(10): 708-711.

Vedal, S. and S. J. Dutton (2006). "Wildfire air pollution and daily mortality in a large urban area." Environmental Research **102**(1): 29-35.

Wegesser, T. C., K. E. Pinkerton and J. A. Last (2009). "California Wildfires of 2008: Coarse and Fine Particulate Matter Toxicity." Environmental Health Perspectives **117**(6): 893-897.

Weil, J. C., R. I. Sykes and A. Venkatram (1992). "Evaluating air-quality models: review and outlook." Journal of Applied Meteorology **31**: 1121-1145.

World Health Organization (WHO) (1999). Environmental Health Criteria 213: Carbon Monoxide. Geneva.

Wu, J., A. M. Winer and R. J. Delfino (2006). "Exposure assessment of particulate matter air pollution before, during, and after the 2003 Southern California wildfires." Atmospheric Environment **40**(18): 3333-3348.

CONTACT US

**t** 1300 363 400
+61 3 9545 2176
**e** enquiries@csiro.au
**w** www.csiro.au

YOUR CSIRO

Australia is founding its future on science and innovation. Its national science agency, CSIRO, is a powerhouse of ideas, technologies and skills for building prosperity, growth, health and sustainability. It serves governments, industries, business and communities across the nation.

FOR FURTHER INFORMATION

**Marine & Atmospheric Research**
Fabienne Reisen
**t** +61 3 9239 4435
**e** fabienne.reisen@csiro.au
**w** www.csiro.au/cmar

**Marine & Atmospheric Research**
Michael Borgas
**t** +61 3 9239 4543
**e** michael.borgas@csiro.au
**w** www.csiro.au/cmar

# For Further Information

**Marine & Atmospheric Research**
Fabienne Reisen
**t** +61 3 9239 4435
**e** fabienne.reisen@csiro.au

Michael Borgas
**t** +61 3 9239 4543
**e** michael.borgas@csiro.au
**w** www.csiro.au/cmar